Norwegian University of Life Sciences

Master's Thesis 2022/23 60 ECTS
Faculty of Chemistry, Biotechnology and Food Science

Characterization of the two novel *Lactiplantibacillus pentosus* strains KW1 and KW2, and exploration of their ability to surface display a Mycobacterium tuberculosis hybrid antigen

Jelena Rončević
MTech, Chemical Engineering and Biotechnology

Acknowledgments

The work conducted in this thesis was performed at the Faculty of Chemistry, Biotechnology and Food Science at the Norwegian University of Life Sciences (NMBU), and supervised by researcher Geir Mathiesen and Ph.D. candidate Kamilla Wiull.

First, I would like to thank my main supervisor Geir Mathiesen, for his great guidance and endless support. His expertise in the field has been invaluable in my work and helped me stay motivated throughout the process. A huge thanks to Kamilla Wiull for always making the time to answer all my questions and for her exceptional guidance, especially with the laboratory work. Overall, I feel incredibly grateful to have had the opportunity to work with both of you, and I could not have asked for better supervisors.

Thanks to Professor Vincent Eijsink and Professor Gustav Vaaje-Kolstad for their helpful and inspirational suggestions during the laboratory meetings. I would also like to thank everyone in the PEP group for creating such a friendly and inspiring working environment. I felt like a part of the team from day one!

Special thanks to Todor Cvetanović and Nemanja Kutlešić for helping me translate the abstract to Serbian and to my friends Martina Idžanović and Sigrid Helena Bue for thesis proofreading.

Lastly, I would like to thank my family, friends, and roommates for their support as well as for believing in me throughout this whole process.

Aas, Norway
May 2023

Jelena Rončević

Abstract

Many lactic acid bacteria are natural inhabitants of the human gut and are considered safe for human consumption. Food-grade lactic acid bacteria from the genus *Lactiplantibacillus* are generally tolerant to highly acidic environments, allowing them to survive and colonize the human gastrointestinal tract. Furthermore, certain species can have vaccine adjuvant effects through direct interactions with the human immune system. Thus, *Lactiplantibacilli* are promising candidates for the delivery of antigens to mucosal surfaces.

The aim of this study was to characterize the two novel *Lactiplantibacillus pentosus* strains, KW1 and KW2, isolated from table olives; and explore their capability to surface display a *Mycobacterium tuberculosis*-derived hybrid antigen. The *L. pentosus* strains were evaluated by analyzing cell morphology and growth analysis. The microscopy analysis showed that *L. pentosus* KW1 and KW2 were morphologically similar and rod-shaped. The optimum growth temperatures were found to be in a range from 33 to 39 °C. In addition, the present study conducted a functional analysis of the inducible gene expression system (pSIP) to evaluate its applicability for use in *L. pentosus*. It was shown that the pSIP system is strictly regulated in KW1 and KW2, where the protein production of mCherry, used as a reporter protein, increased more than 20-fold upon full induction. The protein production of mCherry was found to be highest at 37 °C and *L. pentosus* KW1 was the most efficient producer.

Eight recombinant bacteria were constructed for surface exposure of the H56 hybrid tuberculosis antigen. Four different anchors derived from the genome of KW1 and KW2 were selected, and translationally fused to the antigen, generating the eight recombinant strains. The selected anchors were: (1) an N-terminal transmembrane (NTTM) anchor that non-covalently attaches the antigen to the cell membrane, (2) a lipoprotein anchor to covalently attach the antigen to the cell membrane, (3) a LysM anchor for non-covalently anchoring of the antigen to the cell wall, and (4) an LPxTG peptidoglycan anchor to covalently attach H56 to the cell wall. The recombinant strains showed only a slight reduction in growth, except for strains harboring NTTM-anchored antigens. Western blot analysis confirmed antigen production for seven out of eight recombinant strains. Furthermore, flow cytometry analysis detected exposed antigens on the surface for all recombinant strains except for the KW2_LPxTG anchor. The strongest fluorescent shift was observed in *L. pentosus* KW1, especially with lipoprotein and LysM-anchored antigens.

The successful secretion and surface exposure of the tuberculosis antigen show that these recombinant bacteria are promising candidates for antigen delivery. The analyses demonstrated that *L. pentosus* KW1 seems to be the most promising strain for further development as a vaccine delivery vehicle.

Sammendrag

Mange melkesyrebakterier er naturlige innbyggere i mennesketarmen og er trygge å spise. Matvaregodkjente melkesyrebakterier fra slekten *Lactiplantibacillus* tåler generelt svært surt miljø, noe som gjør at de kan overleve og kolonisere gastrointestinalkanalen. Videre kan visse arter ha vaksineadjuvante effekter ved direkte interaksjoner med immunsystemet. Dermed er *Lactiplantibacilli* lovende kandidater for levering av antigener til slimhinner.

Målet med denne studien var å karakterisere de to nye stammene av *Lactiplantibacillus pentosus*, KW1 og KW2, isolert fra oliven, og utforske deres evne til å feste et hybridantigen avledet fra *Mycobacterium tuberculosis* på overflaten. *L. pentosus*-stammene ble evaluert ved å analysere cellemorfologien og vekstanalyse. Mikroskopi-analysen viste at *L. pentosus* KW1 og KW2 var morfologisk like og stavformede. De optimale veksttemperaturene ble funnet til å være mellom 33 til 39 °C. I tillegg ble det utført en funksjonell analyse av det induserbare genuttrykkssystemet (pSIP) for å vurdere dets anvendelighet for bruk i *L. pentosus*. Det ble vist at pSIP-systemet er strengt regulert i KW1 og KW2, der produksjonen av mCherry-proteinet, brukt som et rapporteringsprotein, økte mer enn 20 ganger ved full induksjon. Produksjon av mCherry var høyest ved 37 °C, og *L. pentosus* KW1 var den mest effektive produsenten.

Åtte rekombinante bakterier ble konstruert for å uttrykke H56-hybridtuberkuloseantigenet på overflaten. Fire forskjellige ankre ble hentet fra genomet til KW1 og KW2, og translasjonelt fusjert til antigenet, som genererte åtte rekombinante stammer. Ankrene som ble valgt er: (1) en N-terminal transmembran (NTTM)-anker som ikke-kovalent binder antigenet til cellemembranen, (2) et lipoproteinanker for kovalent binding av antigenet til cellemembranen, (3) et LysM-anker for ikke-kovalent binding av antigenet til celleveggen, og (4) et LPxTG peptidoglykananker for kovalent binding av H56 til celleveggen. De rekombinante stammene viste bare en liten reduksjon i vekst, bortsett fra stammer som hadde NTTM-ankrede antigener. Western blot-analyse bekreftet antigenproduksjonen for syv av åtte rekombinante stammer. Flowcytometri-analyse detekterte eksponerte antigener på overflaten for alle rekombinante stammer, bortsett fra KW2 LPxTG-ankeret. Den sterkeste fluorescerende forskyvningen ble observert i *L. pentosus* KW1, spesielt med lipoprotein- og LysM-ankrede antigener.

Den vellykkede sekresjonen og overflateeksponeringen av tuberkuloseantigenet viser at disse rekombinante bakteriene er lovende kandidater for levering av antigener. Analysene viser at *L. pentosus* KW1 ser ut til å være mest lovende stammen for utvikling av vaksine leveringsvektor.

Sažetak

Mnoge bakterije mlečne kiseline su prirodni stanovnici ljudskih creva i smatraju se bezbednim za ljudsku upotrebu. Mlečnokiselinske bakterije roda *Lactiplantibacillus* namenjene za prehrambenu upotrebu su generalno tolerantne na izuzetno kiselo okruženje. Ove karakteristike im omogućavaju da prežive i nasele ljudski gastrointestinalni trakt. Pored toga, određene vrste mlečnokiselinskih bakterija poboljšavaju imunski odgovor kroz dodatne ćelijske interakcije sa ćelijama imunskog sistema. Stoga, *Lactiplantibacilli* su obećavajući kandidati za dostavu antigena preko sluzokože.

Cilj ovog istraživanja bio je da se opišu dva nova soja *Lactiplantibacillus pentosus*, KW1 i KW2, koja su izolovana iz maslina, kao i da se ispita njihova sposobnost za izlaganje hibridnog antigena dobijenog iz *Mycobacterium tuberculosis* na površini. Sojevi *L. pentosus* su okarakterisani ćelijskom morfologijom i analizom rasta. Mikroskopija je pokazala da su *L. pentosus* KW1 i KW2 morfološki slični i štapićastog oblika. Optimalne temperature za rast su u opsegu od 33 do 39°C. Dodatno, u ovom istraživanju je izvršena i funkcionalna analiza inducibilnog sistema za ekspresiju gena (pSIP) kako bi se procenila njegova primenljivost za upotrebu u *L. pentosus*. Pokazano je da je pSIP sistem strogo regulisan kod sojeva KW1 i KW2, pri čemu se proizvodnja mCherry, korišćenog kao reporterskog proteina, povećala više od 20 puta usled potpune indukcije. Proizvodnja mCherry proteina je bila najviša pri 37°C, a *L. pentosus* KW1 je bio najefikasniji proizvođač ovog proteina.

Konstruisano je osam rekombinantnih bakterija za površinsko izlaganje hibridnog tuberkuloznog antigena H56. Iz genoma KW1 i KW2 su odabrana četiri različita sidra koja će se translaciono vezati za antigen, generišući osam rekombinantnih sojeva. Kao sidra su odabrani: (1) transmembransko sidro (NTTM) na N-terminusu koje nekovalentno vezuje antigen za ćelijsku membranu, (2) lipoproteinsko sidro koje kovalentno vezuje antigen za ćelijsku membranu, (3) LysM sidro za nekovalentno vezivanje antigena za ćelijski zid i (4) LPxTG peptidoglikansko sidro za kovalentno vezivanje H56 antigena za ćelijski zid. Rekombinantni sojevi su pokazali samo blago smanjenje rasta, osim sojeva koji sadrže antigen usidren za transmembransko NTTM sidro. Uz pomoć western blota, potvrđena je ekspresija antigena kod sedam od osam rekombinantnih sojeva. Dalje, protočnom citometrijom su detektovani izloženi antigeni na površini kod svih rekombinantnih sojeva, osim kod KW2 soja i LPxTG sidra. Najveći pomeraj fluorescentnog signala u odnosu na negativnu kontrolu je primećen kod L. pentosus KW1, posebno kod lipoproteina- i LysM-usidrenih antigena.

Uspešna ekspresija tuberkuloznog antigena i njegovo izlaganje na površini ćelija pokazuju da su ove rekombinantne bakterije obećavajući kandidati za dostavu antigena. Može se zaključiti da *L. pentosus* KW1 izgleda kao najperspektivniji soj za dalji razvoj sistema za dostavu antigena.

Abbreviations

aa Amino acids.

BCG Bacillus Calmette-Guérin.

BHI Brain Heart Infusion.

bp Base pair.

BSA Bovine serum albumin.

CWA cell wall anchor.

EPS Exopolysaccharides.

FITC Fluorescein isothiocyanate.

GIT Gastrointestinal tract.

GRAS Generally recognized as safe.

HRP Horseradish peroxidase.

LAB Lactic acid bacteria.

LAB-EPS Exopolysaccharides produced by lactic acid bacteria.

MRS deMan, Rogosa, Sharpe.

NTTM N-terminal transmembrane.

PBS Phosphate Buffered Saline.

PCR Polymerase Chain Reaction.

rpm Revolutions per minute.

SDS-PAGE Sodium dodecyl-sulfate polyacrylamide gel electrophoresis.

SP signal peptide.

TB Tuberculosis.

TBS Tris Buffered Saline.

WB Western blot.

Contents

1 Introduction

Lactic acid bacteria (LAB) have been used in dairy production and food fermentation for centuries, considered safe for human consumption. Certain species are known as probiotics and have been linked to health benefits. Due to their safe consumption, high tolerance to acidity, surviving harsh conditions, and ease of handling, LAB have gained interest for applications beyond traditional food production and preservation. They have successfully been engineered as mucosal vaccines and delivery vectors of therapeutic proteins. Several studies have shown the potential of using LAB as a vaccine carrier of mucosal vaccines (e.g. Fredriksen et al., 2010; Kuczkowska et al., 2019a; Wiull et al., 2022). This thesis focuses on characterizing two newly isolated strains of *Lactiplantibacillus pentosus* and explores their potential as delivery vectors of *Mycobacterium tuberculosis* antigens. *M. tuberculosis* is the second leading infectious killer in the world. The only available vaccine on the market, the BCG vaccine, doesn't provide good protection to fight tuberculosis worldwide. Additionally, there is an increase in the occurrence of multi-drug resistant bacteria, which makes an urgent need for a new and more effective vaccine.

1.1 Lactic acid bacteria

Lactic acid bacteria (LAB) are gram-positive bacteria that ferment carbohydrates into lactic acid as the primary end-product of the metabolism. Many LAB are food-grade bacteria and have the generally recognized as safe (GRAS) status given by The United States Food and Drug Administration (FDA). Several species, especially from the genus *Lactiplantibacillus*, inhabit the human gastrointestinal tract (GIT) and vaginal cavities. Several LAB strains have been commercialized and are today commonly sold at pharmacies as probiotics (Daniel et al., 2011). World Health Organisation (WHO) defines probiotics as "live microorganisms which when consumed in adequate amounts as part of food confer a health benefit on the host" (FAO/WHO, 2001). LAB have probiotic effects because of the production of lactic acid, which lowers the pH of the environment and inhibit the growth of other microorganisms. Additionally, some LAB produce bacteriocins, thus have antimicrobial activity (Kiousi et al., 2023).

The group of lactic acid bacteria includes many species from several genera of the *Lactobacillaceae* family, but mainly from, what previously was classified as, the genus *Lactobacillus*. A study from (Zheng et al., 2020) divides *Lactobacillus* into 23 new genera based on sequencing of 16S ribosome. The bacteria previously classified as *Lactobacillus* now belong to the genus *Lactiplantibacillus*. The members of the new genus *Lactiplantibacillus* are gram-positive, non-motile, and non-sporulating rods, like most LAB bacteria (Zheng et al., 2020).

1.1.1 *Lactiplantibacillus pentosus*

Lactiplantibacillus pentosus, previously known as *Lactobacillus pentosus*, was defined as a new species for the first time in a study by Zanoni et al. (1987). It has long been difficult to distinguish *L. pentosus* from its close relative, *Lactiplantibacillus plantarum*. After genome sequencing became the standard method for taxonomical classification, some *L. plantarum* strains have been reclassified as *L. pentosus* (Hurtado et al., 2012).

L. pentosus are gram-positive, as other LAB, nonmotile bacilli or coccobacilli that appear individually, in pairs, or in short chains. They are facultatively anaerobic and grow at a wide temperature range: from 10°C to 45°C (Zanoni et al., 1987). *L. pentosus* is usually found in fermented plant-based food, such as olives, mustard pickles, and soybeans, but also in dairy products. It has also been isolated from human vaginal flora and stool samples, indicating that *L. pentosus* might be a part of the GIT bacterial flora (Zheng et al., 2020). Several *L. pentosus* strains have previously been isolated from table olives and characterized as potential probiotic strains (e.g. Blana et al., 2014; Gu et al., 2023; Hurtado et al., 2012; Montoro et al., 2016; Romero-Gil et al., 2013). It has been shown that *L. pentosus*, in correlation with the yeast species *Candida diddensiae* and *Candida boidinii*, are mainly responsible for the natural fermentation of olives (Hurtado et al., 2008). Furthermore, some strains have an additional layer around the cell, mainly composed of exopolysaccharides (EPS). The EPS layer facilitates bacterial attachment to the mucosal surface of the host. This feature enables them to colonize the host's surface and prevents them from immediately being removed. LAB-produced EPS has therefore been linked with an immunomodulatory effect (Hidalgo-Cantabrana et al., 2012; Yang et al., 2023; Xu et al., 2022).

1.2 Inducible gene expression system

Gene of interest must be integrated into the bacterial DNA genome to be expressed and to produce the desired protein. Beside genomic (chromosome) DNA, the bacterial genome often contains additional circular DNA called plasmids. The easiest way to genetically engineer bacterial genomes is to integrate the desired gene into a plasmid and transform it into bacteria. To accomplish this, two main gene expression systems can be used: constitutive and inducible. In the constitutive expression system, the target gene is continuously transcribed.

Inducible gene expression systems enable highly-controlled gene expression because the genes are expressed only when an inducer protein is added to the bacterial culture. One example is the nisin-controlled expression (NICE) system, originally constructed for *Lactococcus* bacteria, widely used LAB. The NICE system has been shown to be unsuitable for use in *L. plantarum* because of a high protein production rate, also non-induced (Sørvig et al., 2003). Therefore, there was a need for a better-regulated gene expression system for use in *L. plantarum*. The new and well-regulated inducible gene expression system was developed (Sørvig et al., 2003, 2005).

1.2.1 The pSIP inducible gene expression system

The pSIP system is a one-plasmid system, with the machinery needed for replication and controlled gene expression of a target gene in several LAB (Sørvig et al., 2003, 2005). The vectors are easy to modify through restriction enzyme digestion and cloning because of incorporated restriction sites. The system consists of the genes encoding for a histidine protein kinase (*sppK*), a response regulator protein (*sppR*), and the inducible promotor (P*sppA*) (figure 1.1). The native function of these genes is to produce the bacteriocin sakacin P. Overproduction of these proteins is activated by a peptide pheromone SppIP (Sørvig et al., 2003). The *sppIP* gene, encoding for the inducer peptide, is deleted from the spp operon to get complete control of protein induction. Therefore, the inducer peptide (SppIP) activates the system when extracellularly added.

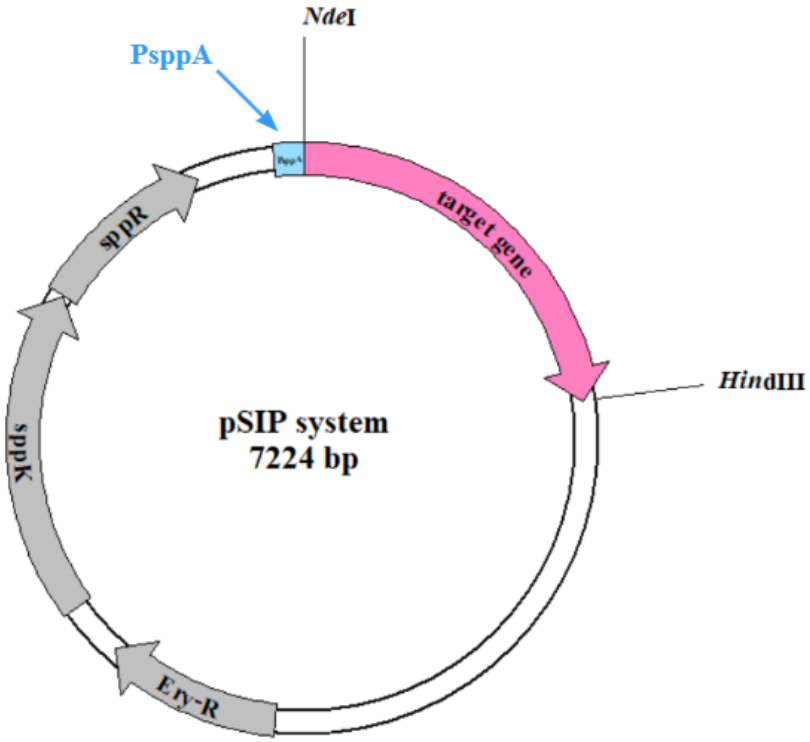

Figure 1.1: The pSIP expression system. The figure represents a standard plasmid, illustrating the circular DNA with two lines. The histidine protein kinase (*sppK*) gene, the response regulator (*sppR*) gene, and the gene encoding for erythromycin resistance (Ery-R) are marked with *grey* arrows. P_{sppA} promoter is marked in *light blue*. The hypothetical target gene is indicated in *pink*. Two restriction enzymes, *Nde*I and *Hind*III, are shown. This plasmid plot is made using pDraw32 1.1.148 (Acaclone) software.

Since the development of the pSIP vectors, the system has successfully been used for the overexpression of various proteins. The system has been used to secrete enzymes included in the degradation of cellulose, indicating that this might find application in biofuel production (Moraïs et al., 2013). Furthermore, hydrolytic enzymes have effectively been secreted using the pSIP system. Also, it was found that the system is functional without the erythromycin resistance gene, which makes it suitable for application in the food industry. The same study

tested three signal peptides and found that protein production was highest using the production strain's native signal peptide (Sak-Ubol et al., 2016). In addition, cell surface anchoring of several heterologous proteins on *L. plantarum* has been studied in the last years (Fredriksen et al., 2012; Kuczkowska et al., 2017, 2019a).

1.3 Protein secretion in gram-positive bacteria

Gram-positive bacteria have a cell membrane and a thick cell wall, mostly made of peptidoglycan. In comparison, gram-negative bacteria have a thinner peptidoglycan layer and an additional outer membrane (Silhavy et al., 2010). About 30% of all proteins synthesized in the cell are transported outside of the cell or attached to the membrane, where they have important functions such as adhesion to the extracellular surface, interaction with the host, extracellular DNA uptake, and quorum sensing, to mention some (Anné et al., 2017). Gram-positive bacteria can secrete the proteins via seven known mechanisms (Kleerebezem et al., 2010):

1. Secretion (Sec) pathway
2. Twin-arginine translocation (Tat) pathway
3. Flagella export apparatus (FEA) pathway
4. Fimbrilin-protein exporter (FPE) pathway
5. Holin pathway
6. Peptide-efflux ABC-transporters pathway
7. WXG100 secretion system (Wss)

The Sec pathway (1.) transports unfolded proteins with a characteristic N-terminal containing signal peptide (see below for more details). The Sec pathway is utilized for the secretion of the proteins expressed through the pSIP system (section 1.2.1), as discussed below. In contrast to the Sec pathway, the Tat pathway (2.) is used for the transport of folded proteins. These proteins utilize similar signal peptides as proteins transported via the Sec pathway, but the sequences are more conserved. The FEA pathway (3.) is found in both gram-positive and gram-negative bacteria and is used for secretion of the proteins that are building blocks of flagella (Anné et al., 2017; Kleerebezem et al., 2010). The FPE pathway (4.) is believed to play a role in the transport of precursors associated with developing the competence pathway and facilitating DNA uptake from the extracellular environment through the cell membrane. The Hollin pathway (5.) transports enzymes associated with the cell lysis of bacterial own cells. Hollins are small proteins, usually integrated into the cell membrane. The ABC transporters (6.) are responsible for export of proteins with antimicrobial activity, e.g. bacteriocins (Kleerebezem et al., 2010). The Wss system (7.) was first discovered in *M. tuberculosis*, and is involved in transport of ESAT-6 homologs, also called WXG100 proteins (Anné et al., 2017). These proteins are

essential for how bacteria interact with the immune system, as will be discussed later. The only mechanisms that have been applied for biotechnology use are the secretion (Sec) pathway and the twin-arginine translocation (Tat) pathway (Anné et al., 2017).

1.3.1 The major secretion pathway (Sec)

The Sec pathway also called the general secretion pathway, is the main secretion pathway in gram-positive bacteria. Secreted proteins are either integrated into the cell membrane or transported out of the cell. Proteins transported through the Sec pathway have a characteristic three-part N-terminus called a signal peptide (SP). The structure of the signal peptide is mainly composed of three parts: (1) a positively charged N-terminus, (2) a hydrophobic (H) region, and (3) a polar C domain, often with a signal peptidase cleavage site as illustrated in figure 1.2. Signal peptides are normally short, with about 20 to 30 amino acid residues. The signal peptide guides the premature protein to the signal peptidase (SPase), a membrane-attached enzyme that cleaves the signal peptide outside the cell membrane. Cleaving the signal peptide yields the mature protein (Anné et al., 2017; Driessen & Nouwen, 2008; Tsirigotaki et al., 2017).

Figure 1.2: Schematic overview of a standard protein secreted through the Sec pathway. The figure illustrates two main components of premature protein: signal peptide (*light pink*) and the part which becomes the mature protein sequence (*pink*) after cleaving the SP. Three main components of the signal peptide are indicated each with its own box (*light pink*).

Secretion of the proteins includes targeting the premature protein to the Sec translocase, transporting the protein through the SecYEG channel, and cleaving the signal peptide by SPase (Tsirigotaki et al., 2017). The Sec translocase is a protein complex incorporated into the cell membrane, which mediates protein transport from the cytosol across the cell membrane. The main components of Sec translocase are the SecYEG channel and SecA, an ATP-dependent motor protein. ATP hydrolysis at SecA and proton motive force push the preprotein through the SecYEG channel (figure 1.3) (Anné et al., 2017; Tsirigotaki et al., 2017).

First, preprotein must be recognized and transferred to the Sec translocase in order to be translocated over the cell membrane through the passage of the SecYEG channel. Premature proteins can be directed to Sec translocase machinery in several ways, as illustrated in figure 1.3. During or right after the translocation of premature proteins across the membrane, the signal peptide is cleaved by a SPase. Signal peptide sequences are not highly conserved but often have Ala-X-Ala as a cleavage site (Anné et al., 2017; Driessen & Nouwen, 2008). The presence and

localization of the signal peptide cleavage site can be predicted via software. The most used software for predicting signal peptides based on the amino acid sequence is SignalP (Nielsen, 2017).

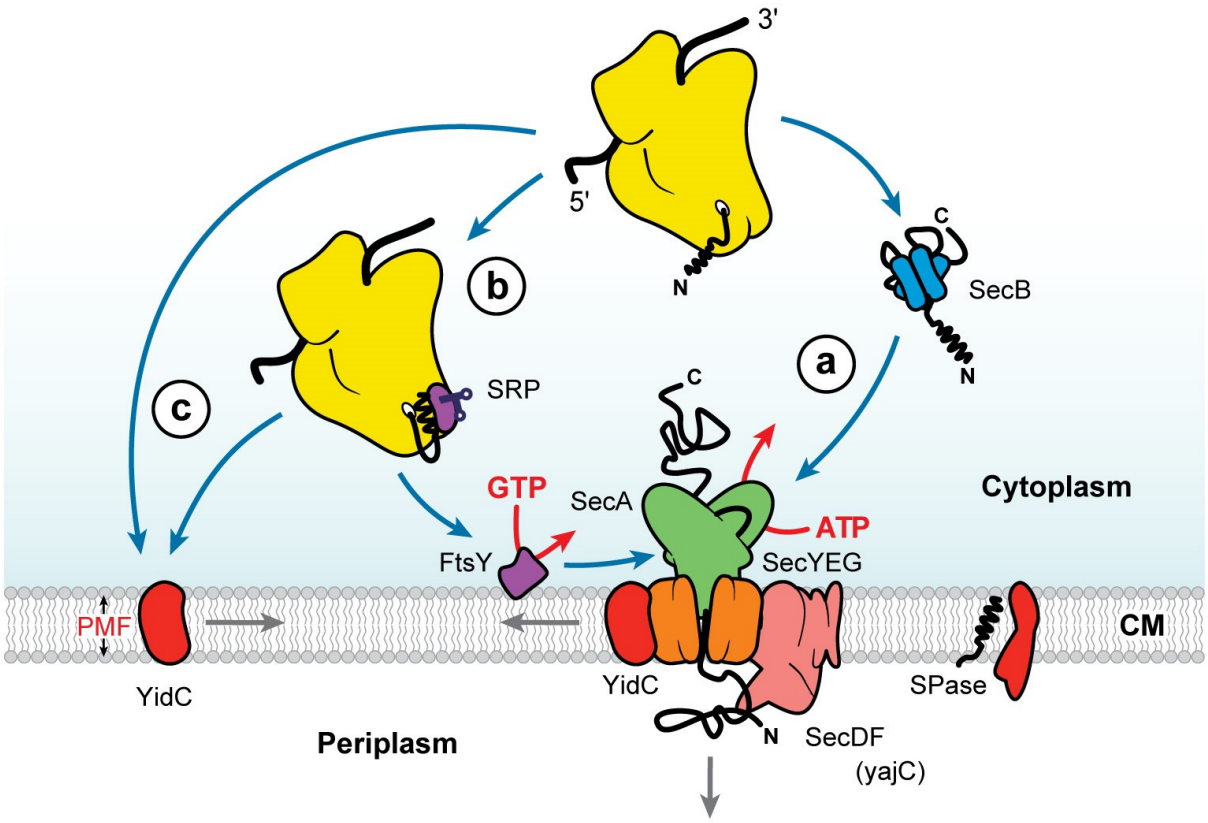

Figure 1.3: Schematic overview of Sec pathway. The Sec translocase membrane complex consists of a motor domain SecA (*green*), a protein-conducting channel SecYEG (*orange*), and the accessory proteins SecDF and yajC, shown in *pink* and *red*. Secretory proteins can be guided to the Sec translocase via several routes: (a) with the assistance of chaperone protein, SecB, (b) via ribonucleoprotein signal recognition particle (SRP), or (c) via membrane protein, YidC (*red*), that facilitates the incorporation of membrane proteins. SPase (*red*) cleaves the signal peptide after translocation, yielding a mature protein. The figure is taken from Driessen & Nouwen (2008). Copyrights provided by Copyright Clearance Center, Inc with license number: 5545270852613

1.4 Anchoring of proteins in lactic acid bacteria

Bacteria synthesize all their proteins inside the cell, some proteins have important functions outside the cell. Therefore bacteria need to secrete and anchor these proteins on the surface. In gram-positive bacteria, proteins are anchored either to the cell membrane or cell wall via covalent or non-covalent binding. The four main methods for surface attachment of the proteins to the surface of gram-positive bacteria are: (a) N-terminal transmembrane anchor (NTTM), (b) Lipoprotein anchor, (c) LysM domain, and (d) LPxTG peptidoglycan anchor (figure 1.4) (Anné et al., 2017; Michon et al., 2016; Tsirigotaki et al., 2017).

1.4.1 N-terminal transmembrane proteins

Proteins secreted via the Sec pathway usually have signal peptides that facilitate transport across the cell membrane, as described in section 1.3.1. However, some proteins secreted through this pathway do not have signal peptide cleavage sites. Instead, the signal peptide function as an N-terminal transmembrane (NTTM) helix that remains embedded in the cell membrane, resulting in the attachment of the protein to the cell membrane (figure 1.4(a)) (Michon et al., 2016).

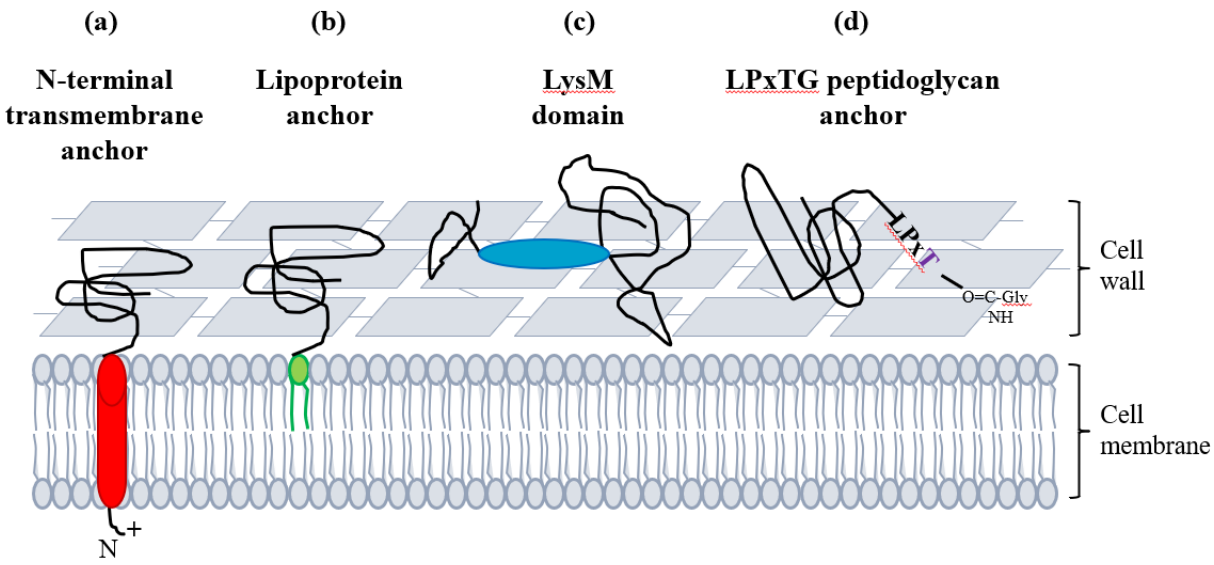

Figure 1.4: Schematic overview of the strategies for surface display of heterologous proteins in *Lactiplantibacilli*. The proteins can be non-covalently bound to the cell membrane via (a) N-terminal transmembrane anchor; covalently bound to the cell membrane via (b) lipoprotein anchor; non-covalently bound to the cell wall via (c) LysM domain motif; or covalently anchored to the cell wall with (d) LPxTG peptidoglycan anchor. The figure was provided by Geir Mathiesen and later modified.

1.4.2 Lipoproteins

A lipoprotein is a typical protein secreted via the Sec pathway. It is synthesized in the cytosol as a preprotein, containing the three-part signal peptide with signal peptide cleavage site (figure 1.2). The signal peptide consists of a positively charged N-terminal part, followed by a hydrophobic region and a lipobox at the C-terminal end of the signal peptide. Lipoboxes always contain a cysteine at the terminus. After secretion, an enzyme, diacylglycerol transferase, catalyzes the reaction between a sulfhydryl group of the cysteine and phospholipids of the cell membrane. Cysteine is then covalently bound to the cell membrane through a thioether linkage. Another enzyme, SPaseII, removes the signal peptide, and cysteine becomes the N-terminal end of the mature lipoprotein (figure 1.4(b)) (Michon et al., 2016; Babu et al., 2006).

1.4.3 LysM proteins

LysM motifs are usually between 44 and 65 residues in length, located either at the N- or C-terminus of the protein. It is less common to find LysM domains in the middle of the protein sequence. The LysM domains bind to the peptidoglycan and chitin of the cell wall, resulting in non-covalently attachment of the protein to the cell wall. One protein can have several LysM domains, separated with linker sequences. These linkers make surface-anchored proteins more mobile and flexible (figure 1.4(c)) (Michon et al., 2016).

1.4.4 LPxTG-motif proteins

These proteins consist of an N-terminal signal peptide, followed by the central part of the protein, and LPxTG-motif near the C-terminus. Signal peptides contain SPaseI cleavage sites. During the secretion, the LPxTG motif act as a sortase cleavage site. Sortase cleaves between threonine and glycine in the LPxTG motif, forming covalent binding between the threonine and the peptidoglycan and resulting in the surface attachment of the protein. The composition of LPxTG motifs can vary between different bacterial strains (figure 1.4(d)) (Michon et al., 2016).

1.5 Use of anchor motifs for surface display of target proteins

Bacterial native secretory machinery can be manipulated for the secretion of proteins of interest. Heterologous protein production has gained great interest, especially with gram-positive bacteria as expression hosts. The advantage of gram-positive bacteria is their monoderm cell structure, which allows for the direct secretion of the proteins into their surroundings (Anné et al., 2017; Silhavy et al., 2010). Because of their safety consumption, GRAS status, probiotic and immunomodulatory effects, survival through the GIT, and well-developed genetic manipulating tools, lactic acid bacteria seems like perfect delivery vectors of heterologous proteins to the mucosal surface (Anné et al., 2017; Michon et al., 2016).

A general strategy to achieve surface anchoring on lactic acid bacteria is to select an anchor motif from the native bacterial genes and replace the rest of the sequence with the sequence of target protein, as shown in figure 1.5. A linker sequence can be added between the anchor motif and protein of interest to increase flexibility and generate more exposed protein (Fredriksen et al., 2012; Michon et al., 2016).

To utilize an NTTM as an anchor of heterologous proteins, the N-terminal transmembrane helix is selected from the native protein. A linker sequence can be added after the helix, and the target protein is translationally fused to the linker region, as illustrated in figure 1.5. The length of the linker sequence influences the position of the target protein. If the linker region is too short, the protein may be embedded too deep in the cell wall and be inaccessible for host response (Michon et al., 2016).

Figure 1.5: The strategy of anchor design shown on an example of N-transmembrane anchored proteins. The figure shows the expression cassette of the selected anchor motif (red), fused with a linker sequence (blue), before fusion to the protein of interest (yellow). Similar strategy can be used for construction of LysM- and lipoprotein-anchored heterologous proteins.

A similar strategy as for NTTM can be used for covalent anchoring to the cell membrane using lipoproteins. Any protein of interest can be displayed at the surface by fusion of the target protein sequence right after the cysteine of a signal peptide in lipoprotein. The selected anchor length can be longer than just the signal peptide in order to make the target protein more exposed, or the target protein can be fused directly to the signal peptide to achieve more embedded protein (Michon et al., 2016). To anchor proteins of interest using LysM proteins, the signal peptide and LysM motif need to be selected from the original protein and fused to the target sequence.

In order to achieve anchoring with LPxTG peptidoglycan anchor, a slightly different strategy is needed. In this case, the protein of interest is placed between the signal peptide and anchor motif containing the LPxTG motif, meaning that only the central part of the native protein is replaced. This results in covalently bound, LPxTG-anchored heterologous proteins.

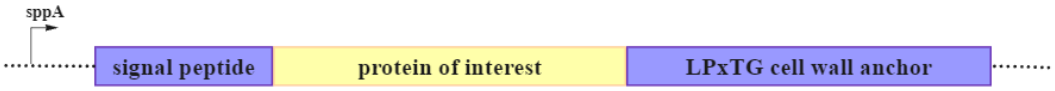

Figure 1.6: The schematic overview of the expression cassette for covalent anchoring of heterologous proteins to the cell wall through LPxTG anchor. The purple boxes represent parts of the sequence derived from the native gene. Predicted signal peptide (first purple box) fused to a protein of interest (yellow) and cell wall part of the anchor containing LPxTG motif (second purple box).

A study by Fredriksen et al. (2012) has studied the display of a virulence factor, invasine, on the surface of *L. plantarum* using four anchor types (described above). Surface anchoring was achieved in all recombinant strains, but the immune responses were influenced by the choice of anchor motif, and that lipoprotein anchored invasin was best. Also, the study highlighted that anchored proteins are not necessarily evenly distributed over the cell surface. The NTTM anchor is probably the least studied strategy for the surface display of target proteins. However, a few studies have proved an immune response based on NTTM anchoring (Fredriksen et al., 2012; Kuczkowska et al., 2015; Liu et al., 2020). The established hypothesis for lower immune responses gained from NTTM-anchored proteins (compared to lipoprotein- and cell-wall anchored) was that NTTM might be too protected in the cell membrane and not able to interact with the antibodies (Kuczkowska et al., 2015; Fredriksen et al., 2012). However, a recent study

by Liu et al. (2020) has shown that N-terminally anchored proteins induce an immune response in mice and that lactic acid bacteria can be used as delivery vectors. Lipoprotein anchor is well studied and seems to be the most effective anchoring strategy (Fredriksen et al., 2012; Wiull et al., 2022). Protein length and orientation of the protein may have an influence on display efficiency (Michon et al., 2016). Also, Mathiesen et al. (2020) has proved that growth rates of recombinant *Lactiplantibacilli* vary based on anchor type but also among different strains. It was shown that the growth of LPxTG cell-wall anchor protein was the most reduced and that lipoprotein and LysM anchored antigen give the most exposure at the surface.

1.6 Bacteria as live vectors for antigen delivery

Already over 30 years ago, it was suggested that the surface display of heterologous proteins could have the potential as live vaccines through non-pathogenic bacteria (Charbit et al., 1986). Since then, this research topic has been studied in more detail and several display systems have been developed, especially for gram-positive bacteria (Michon et al., 2016).

Early-developed vaccines have normally used weakened pathogens to cause an immune response in the host, but not an infection. These vaccines have a risk to cause an active infection, especially in people with a weak immune system. Therefore it is beneficial to develop safer strategies for vaccine design. Because of their safe consumption and GRAS status, lactic acid bacteria gained attention as potential vaccine delivery vectors (Seegers, 2002).

Infections often transmit through mucosal surfaces. Vaccines are normally administrated by injection, which normally gives weak mucosal immunity. Because of that, mucosal immunity has gained more attention in vaccine design. An oral LAB-based vaccine would be easier to administrate, transport, and make accessible to a broader population. A drawback with oral vaccines is that it is difficult to administrate accurate doses, as the immunity is dependent on uptake from GIT (Ramirez et al., 2017).

Kuczkowska et al. (2019b) has proved that using LAB as hosts for surface expression of *M. tuberculosis* antigens causes an immune response in human dendritic cells. Wiull et al. (2022) has tested the same antigens in mice with promising results.

1.7 Tuberculosis

Mycobacterium tuberculosis is the bacteria that causes tuberculosis (TB). The disease usually affects the lungs. The most characteristic symptoms are severe coughing, fever, and chest pains. Over a century ago, the Bacillus-Calmette Guérin (BCG) vaccine was developed and broadly administered (Fogel, 2015). However, over 10 million people still get infected with tuberculosis every year. For the first time after many years of a decrease in the number of cases, new data shows a 4.5% increase from 2020 to 2021. The same trend is observed for the mortality rate.

Geographically, most of the new TB cases are reported in South-East Asia, Africa, and the Western Pacific. Over 1.4 million people die from TB every year, implying that tuberculosis is one of the world's most mortal infectious diseases (WHO, 2022).

M. tuberculosis is transmitted by close contact with an infected person, through the inhalation of aerosol particles containing live bacteria. The majority of people will get a good immune response and be able to stop *M. tuberculosis* from developing an active infection. Instead, the bacteria will become dormant and cause an asymptomatic infection (Sia & Rengarajan, 2019; Fogel, 2015). A third of the world's population is estimated to have a latent TB infection (WHO, 2022). People with a latent infection can develop active TB many years after the primary infection and continue to transmit the disease. Especially exposed to TB infection are people with HIV, complex medical conditions, other underlying diseases, the elderly, and immunosuppressed people (Kanabalan et al., 2021).

The treatment for TB has been effective since the discovery and development of antibiotics. However, the occurrence of drug-resistant and multi-drug-resistant *M. tuberculosis* (MDR-TB) makes treatment more challenging. More sensitive and rapid diagnostic tests are needed. Currently, available diagnostic tests require a high concentration of bacteria in the samples. It could take up to 6 weeks to get the results, which prolongate the beginning of the therapy (Kanabalan et al., 2021). The long-term consequence of TB infection is an increased risk of developing lung damage and dysfunction, including airflow obstruction, restrictive ventilatory defects, and impaired gas exchange (Ravimohan et al., 2018).

Because of challenges in both the diagnosis and treatment of TB, the best strategy is to prevent infections. The BCG vaccine has been used since 1921. It contains an inactive form of *Mycobacterium bovis*. The efficiency of the BCG vaccine is inconsistent. The protection is best in children but limited in adults (Fogel, 2015). Therefore, a new and better vaccine is needed.

1.7.1 *Mycobacterium tuberculosis* antigens

Pathogens invade the host organism by evading the host immune system so that an immune response doesn't occur. Proteins that provoke an immune response in the host are defined as antigens (Foley, 2015). *M. tuberculosis* encodes over 300 known antigens, investigated in a review study from Meier et al. (2018).

H1 hybrid antigens have been used in several studies (Kuczkowska et al., 2017, 2019a; Wiull et al., 2022). The H1 antigen consists of two antigens, Ag85B and ESAT-6, translationally fused together. The Ag85B antigen is regarded to have high immunogenicity. The ESAT-6 is important in the initial phase of infection, and it is considered the central target for T cells (Kuczkowska et al., 2017; Aagaard et al., 2011). Fusing Rv2660c to H1 makes a new hybrid antigen, called H56 (Ag85B, ESAT-6, and Rv2660c). The Rv2660c is expressed at the same level in both early and late phases of the infection (Aagaard et al., 2011).

The study by Aagaard et al. (2011) tested immune responses in mice of both H1 and H56 vaccines, and their individual antigens (Ag85B, ESAT-6, and Rv2660c). Although Rv2660c failed to cause an immune response alone, the H56 vaccine was more effective than H1 in the late phase of the infection. In addition, the H56 vaccine was up to ten times more effective in reducing the bacterial number, compared to H1. This indicated that the addition of Rv2660c may boost the immune response. In this study, the H56 antigen is used.

1.8 Aim of this study

This thesis is part of a larger research project with a long-term goal of developing a mucosal vaccine against tuberculosis, using LAB as delivery vectors. Previously, *L. plantarum* has successfully been engineered to surface display TB antigens (Kuczkowska et al., 2017, 2019a; Wiull et al., 2022). LAB-based vaccine candidates have generated good immune responses in mice, which encouraged the future development of LAB-based vaccines. Because of trade rights and no restrictions for further use of the strains, the group wanted to isolate its own LAB strain. Prior to the present study, two bacterial strains from the genus *L. pentosus* have been isolated from table olives and whole-genome sequenced.

This thesis aimed to contribute to vaccine development through (1) characterization of novel *L. pentosus* KW1 and KW2 strains and (2) validating their ability to surface display the H56 antigen derived from *M. tuberculosis*. *L. pentosus* KW1 and *L. pentosus* KW2 were characterized based on finding the optimal growth temperature and the optimal temperature for heterologous protein production. The functionality of the inducible pSIP expression system was tested by transformation and protein expression of mCherry as a reporter protein. An *in silico* analysis of anchor proteins derived from KW1 and KW2 was performed using four types of anchor proteins derived from each strain. Anchors were translationally fused to hybrid tuberculosis antigen H56, giving rise to eight recombinant strains.
The recombinant *L. pentosus* strains were studied through growth curve analysis, western blot, and flow cytometry. Planned workflow is visualized through figure 1.7. The recombinant strains were compared to *L. plantarum* to examine if they could be better candidates for vaccine development.

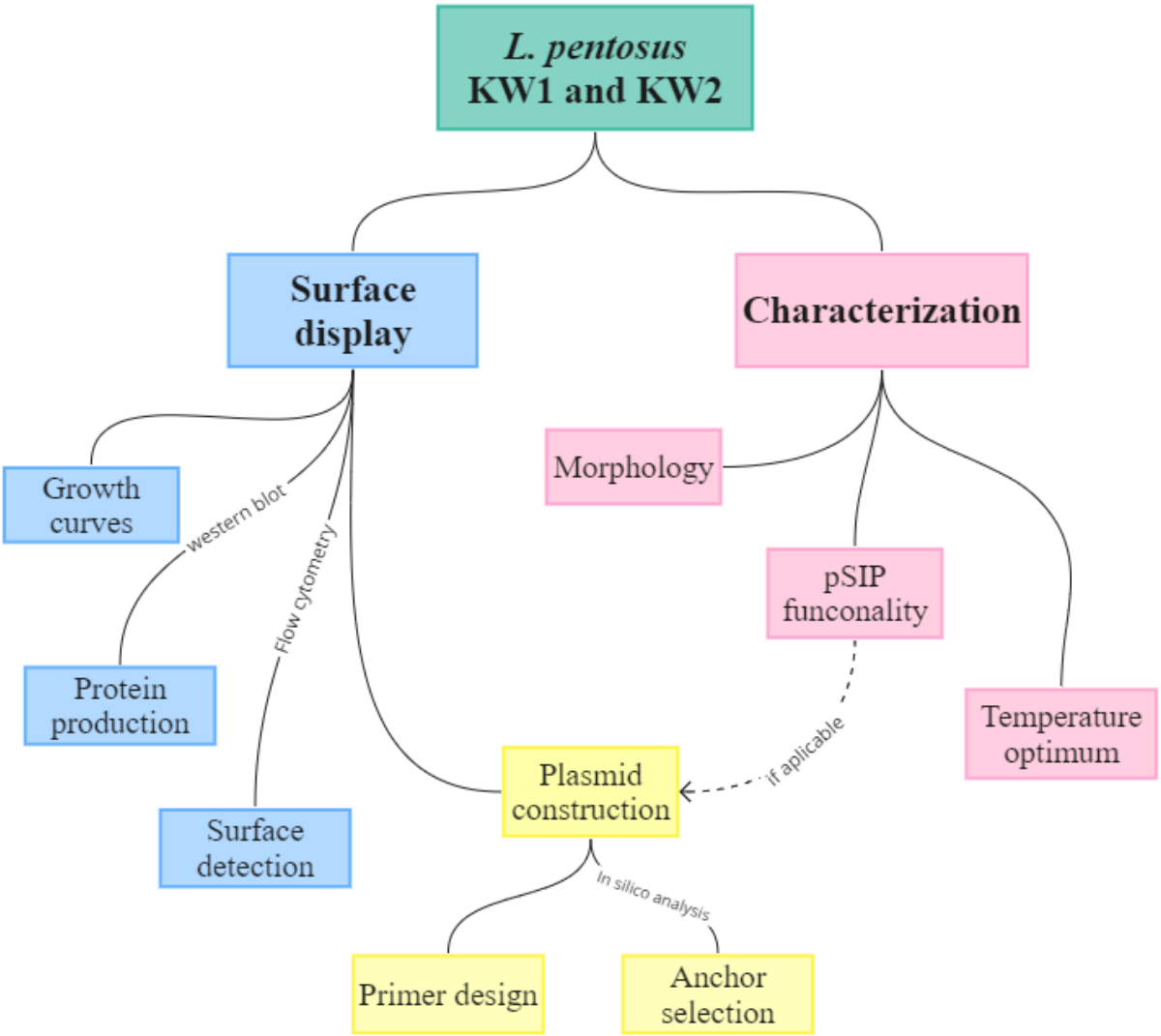

Figure 1.7: Diagrammatic illustration of planned workflow for this study. The flowchart visualizes the two main goals of this thesis: (1) characterization of novel *L. pentosus* strains and (2) exploring their ability to surface display TB antigens. The strains will be characterized through analysis of their morphology and temperature optimums for growth and protein production. Exploring the potential for surface display of the antigens includes several steps, where the key analysis is shown in the figure.

2 Materials and methods

2.1 Agars and media

Brain-Heart Infusion (BHI) media

Materials:
Brain-Heart Infusion (BHI) (Oxoid, Hampshire, England)
MiliQ water
Procedure:
37g BHI was added to 1 L MiliQ water, dissolved, and sterilized in CertoClav (OneMed, Goeteborg, Sweden) at 121°C for 17 minutes.

BHI agar plates

Materials:
Brain-Heart Infusion (BHI) (Oxoid)
MiliQ water
Agar powder (Oxoid)
Procedure:

1. 37g BHI and 1.5% agar powder was added to 1 L MiliQ water, mixed, and sterilized in CertoClav (OneMed, Goeteborg, Sweden) at 121°C for 17 minutes.
2. Media was mixed and chilled to roughly 60°C, before 200 µg/mL erythromycin was added to the media.
3. The media was distributed to petri dishes, and kept at 4°C after solidification.

De Man, Rogosa, Sharpe (MRS) media

Materials:
De Man, Rogosa, Sharpe (MRS) (Oxoid)
MiliQ water
Procedure:
52g MRS was dissolved in 1 L MiliQ water, and sterilized in CertoClav (OneMed) at 115°C for 15 minutes.

MRS agar

Materials:
De Man, Rogosa, Sharpe (MRS) (Oxoid)
MiliQ water

Agar powder (Oxoid)

Procedure:

1. 52g MRS was mixed with 1.5% agar powder and 1 L MiliQ water and sterilized in CertoClav (OneMed, Goeteborg, Sweden) at 121°C for 15 minutes.
2. Media was mixed and chilled to around 60°C, before eventually the addition of 10 µg/mL erythromycin.
3. The media was distributed to petri dishes and kept at 4°C after solidification.

MRSSM-media

Materials:

5.2g MRS (Oxoid)

17.1 g sucrose (VWR, Radnor, PA, USA)

2.0 g $MgCl_2x6H_2O$ (Merck, Darmstadt, Germany)

dH_2O to 100 mL

Procedure:

The components listed above were mixed, dissolved, and sterile-filtered through a filter (0.2 µm pore size). Media was distributed to microcentrifuge tubes and kept at -20°C.

2.2 Buffers and solutions

Phosphate Buffered Saline (PBS) 10X

Materials:

8 g NaCl (Merck)

0.2 g Kcl (Merck)

1.44 g Na_2HPO_4 (Merck)

0.24 g KH_2PO_4 (Merck)

dH_2O to 1 L

Procedure:

The components listed above were mixed and dissolved. Ph was adjusted to 7.4, and the solution was sterile-filtered and stored at room temperature.

Tris Buffered Saline (TBS) 10X

Materials:

150 mM NaCl (Merck)

10 mM Tris-HCl (Amresco, Solon, OH, USA)

Procedure:

Buffer was sterile filtered and stored at room temperature.

Tris Glycine SDS (TGS)

Materials:
Tris Glycine SDS (TGS) (Bio-Rad, Hercules, CA, USA)
Procedure:
Prepared from the supplier.

TTBS

Materials:
TBS buffer
0.1% (w/v) Tween-20 (Sigma Aldrich, St. Louis, MO, USA)
Procedure:
Freshly mixed right before use.

2.3 Databases and software

Database or software	**Purpose**	**Source**
BLAST	*In silico* analysis	https://blast.ncbi.nlm.nih.gov/Blast.cgi
ImageJ	Image analysis	https://fiji.sc/
pDRAW32	Plasmid visualization	https://www.acaclone.com/
Phobius	*In silico* analysis	https://phobius.sbc.su.se/
SignalP	*In silico* analysis	https://services.healthtech.dtu.dk/services/SignalP-6.0/
TMHMM	*In silico* analysis	https://services.healthtech.dtu.dk/services/TMHMM-2.0/
Website	**Purpose**	**Source**
Biorender	Figure design	https://www.biorender.com/
Canva	Figure design	https://www.canva.com/
Miro	Figure design	https://miro.com/app/

2.4 Primers

Table 2.1 lists all primers used in this study. The primers were used to PCR amplify anchor motifs from the genome of *L. pentosus* KW1 and KW2 and for sequencing (sections 2.10 and 2.15). The In-Fusion® HD Cloning Kit User Manual was followed for the construction of In-Fusion

primers (section 2.13.1).

Table 2.1: Primers used in this study. Restriction enzyme sites are bolded in the sequence.

Primer name	DNA sequence*	Application	Restriction enzyme
Cyt-H56_F	GGAGTATGATT**CATATG**TTTAGTCGTCCAGGTTTGCCAG	Forward In-Fusion primer used for PCR amplification of H56 antigen.	*Nde*I
Cyt-H56_R	C G T G C T G T A A T T T G **AAGCTT** T T A T G G C C G T T GTGGCGTA	Reverse In-Fusion primer used for PCR amplification of H56 antigen.	*Hind*III
KW1_Lipo-0478_F	GGAGTATGATT**CATATG**CGTTTTAAATCATTATTCATCCTACC	Forward In-Fusion primer used for amplification of lipoprotein anchor dervied from *L. pentosus* KW1	*Nde*I
KW1_Lipo-0478_R	GACGACTAAA**GTCGAC**CGCCGCAATCGTGCCCTTAGCGGCTTGACTCGT	Reverse In-Fusion primer used for amplification of lipoprotein anchor dervied from *L. pentosus* KW1	*Sal*I
KW1_NTTM-0418_F	GGAGTATGATT**CATATG**CGAGTTCAACGTAGAAGGC	Forward In-Fusion primer used for amplification of NTTM anchor dervied from *L. pentosus* KW1	*Nde*I
KW1_NTTM-0418_R	GACGACTAAA**GTCGAC**CGCCGCAATCGTGCCCAGCGCGTAGACTGGAACGT	Reverse In-Fusion primer used for amplification of NTTM anchor dervied from *L. pentosus* KW1	*Sal*I
KW1_LysM-1485_F	GGAGTATGATT**CATATG**AAAAAAATTATTAACCACAATCTTAACAACT	Forward In-Fusion primer used for amplification of LysM anchor dervied from *L. pentosus* KW1	*Nde*I
KW1_LysM-1485_R	GACGACTAAA**GTCGAC**ATATAATGCCCAGGCTTGCA	Reverse In-Fusion primer used for amplification of LysM anchor dervied from *L. pentosus* KW1	*Sal*I
KW1_SP-1420_F	GGAGTATGATT**CATATG**ACAAAGGCACTAAAAGTTGCA	Forward In-Fusion primer used for amplification of signal peptide dervied from *L. pentosus* KW1	*Nde*I
KW1_SP-1420_R	TTGGATAAAA **GTCGAC**GATGGCCGCACTGGCAGCG	Reverse In-Fusion primer used for amplification of signal peptide dervied from *L. pentosus* KW1	*Sal*I

Table 2.1: Primers used in this study. Restriction enzyme sites are bolded in the sequence.

Primer name	DNA sequence*	Application	Restriction enzyme
KW1_CWA-1420_F	TCAGTTCCAC**ACGCGT**GCT AACGCCGATATTGAA	Forward In-Fusion primer used for amplification of cell wall anchor dervied from *L. pentosus* KW1	*Mlu*I
KW1_CWA-1420_R	CTGTAATTTG**AAGCTT**TTA ATCAGTCGTGTGACGT	Reverse In-Fusion primer used for amplification of cell wall anchor dervied from *L. pentosus* KW1	*Hind*III
KW2_NTTM-2724_F	GGAGTATGATTCATATGCA AAATAATGGTTTTTGGGC	Forward In-Fusion primer used for amplification of NTTM anchor motif dervied from *L. pentosus* KW2	*Nde*I
KW2_NTTM-2724_R	GACGACTAAA**GTCGAC**CGC CGCAATCGTGCCCACCGCA TTTTGCAAGTT	Reverse In-Fusion primer used for amplification of NTTM anchor motif dervied from *L. pentosus* KW2	*Sal*I
KW2_LysM-1392_F	GGAGTATGATT**CATATG**AA AATCAAACACCTCTTATTA TCC	Forward In-Fusion primer used for amplification of LysM anchor motif dervied from *L. pentosus* KW2	*Nde*I
KW2_LysM-1392_R	GACGACTAAA**GTCGAC**GTA CCAACCGTTAGCTTGCCA	Reverse In-Fusion primer used for amplification of LysM anchor motif dervied from *L. pentosus* KW2	*Sal*I
KW2_SP-1650_F	GGAGTATGATT**CATATG**CG AAAAAAGCGAATAGGT	Forward In-Fusion primer used for amplification of signal peptide dervied from *L. pentosus* KW2	*Nde*I
KW2_SP-1650_R	TTGGATAAAA**GTCGAC**TTC CTTGGCATGCGCCGT	Reverse In-Fusion primer used for amplification of signal peptide dervied from *L. pentosus* KW2	*Sal*I
KW2_CWA-1650_F	TCAGTTCCAC**ACGCGT**GGC AAACCAAGCGAACCA	Forward In-Fusion primer used for amplification of cell wall anchor dervied from *L. pentosus* KW2	*Mlu*I
KW2_CWA-1650_R	CTGTAATTTG**AAGCTT**TTA GCCGTGCCGACGCCG	Reverse In-Fusion primer used for amplification of cell wall anchor dervied from *L. pentosus* KW2	*Hind*III

Table 2.1: Primers used in this study. Restriction enzyme sites are bolded in the sequence.

Primer name	DNA sequence*	Application	Restriction enzyme
Sek_F	GGCTTTTATAATATGAGAT AATGCCGAC	Forward sequencing primer, used for sequencing of all pSIP plasmids.	
Sek_R	CCTTATGGGATTTATCTTCC TTATTCTC	Reverse sequencing primer, used for sequencing of all pSIP plasmids.	

2.5 Bacterial strains and cultivation conditions

An overview of the bacterial strains and antibiotic concentrations used in this study is given in table 2.2. *Lactiplantibacillus* strains were cultivated in deMan, Rogosa, Sharpe (MRS) media (Oxoid) (either liquid or 1.5% agar plates) in static conditions at 37°C. Erythromycin (Merck) was added to cultures of recombined strains. *Escherichia coli* strains were grown in Brain Heart Infusion (BHI) media (Oxoid), either liquid or 1.5% agar plates, with the addition of 10 µg/mL erythromycin (Merck). These strains were incubated at 37°C, with shaking at 200-225 rpm. Both MRS and BHI media were prepared according to the package description and autoclaved at 115°C and 121°C for 20 minutes, respectively.

Table 2.2: Bacterial strains used in this study

Bacterial strain	Source
Escherichia coli-Stellar^{TM} Competent Cells	Takara Bio USA, Inc, San Jose, CA
Lactiplantibacillus pentosus KW1	PEP strain collection
Lactiplantibacillus pentosus KW2	PEP strain collection
Lactiplantibacillus plantarum WCFS1	Kleerebezem et al., 2003

2.6 Storage of bacteria

Glycerol stocks were prepared by mixing 300 µL sterile 87 % glycerol (Merck, Darmstadt, Germany) and 1000 µL of the bacterial overnight culture in a cryovial tube (Sarstedt, Trollasen, Norway). The tube was inverted a few times, appropriately marked, and placed in a freezer at -80°C for long-term storage.

Later cultivation of bacteria from glycerol stock was performed by scooping a tiny amount of the

frozen bacteria suspension from the tube with a toothpick under sterile conditions and dropping it in 10 mL growth media supplemented with the appropriate antibiotic concentration or without antibiotics for wild type strains.

2.7 Plasmid isolation

NucleoSpin® Plasmid Kit (MACHEREY-NAGEL, Düren, Germany) was used to isolate plasmid DNA from liquid bacterial cultures. The isolated DNA was used for cloning, restriction enzyme digestion, PCR, or sequencing.

Protocol 5.1 for isolating high-copy plasmids was followed as described by the manufacturer except that sterilized water was used instead of Elution Buffer AE.

2.8 DNA quantification

DNA quantification was performed using Qubit™ Fluorometer (Invitrogen, Waltham, MA, USA) and dsDNA BR Assay Kit. Calibration of the instrument was done occasionally.

The protocol given by the manufacturer was followed.

2.9 DNA digestion with restriction enzymes

Restriction enzymes digest double-stranded DNA at enzyme-specific recognition sites. Digestion with restriction enzymes was used to prepare plasmid DNA for further use in cloning. In order to get two fragments of DNA, either insert or backbone, the plasmids were cut at two different recognition sites, using two restriction enzymes in one reaction. When the same enzymes are used to digest both insert and vector, both fragments get the same overhang which makes them suitable for ligation. The usage of two enzymes at once requires a buffer that is compatible with both enzymes. NEBcloner® restriction enzyme calculator was used to find a compatible buffer.

Materials:

All components required for restriction enzyme digestion are listed in table 2.3.

Procedure:

1. The components listed in table 2.3 were mixed at room temperature in a microcentrifuge tube.
2. The mixture was incubated in a 37°C water bath for 1.5 to 2 hours before it was loaded on an agarose gel for separation.

Table 2.3: Components for the digestion of DNA using two restriction enzymes.

Component	Volume [µL]
Restriction enzyme 1	2.5
Restriction enzyme 2	2.5
Compatible buffer	5
DNA	up to 1 µg (variable)
dH_2O	to 50

Table 2.4: Restriction enzymes and buffers used in this study.

Enzyme or buffer	Supplier
*Nde*I	NEB
*Sal*I-HF®	NEB
*Mlu*I-HF®	NEB
*Hind*III	NEB
CutSmart (10X)	NEB
r.2.1 (10X)	NEB

2.10 Polymerase chain reaction (PCR)

PCR is a well-known method used for DNA amplification. The DNA fragments of interest are amplified using specific primers and heat-stable DNA polymerase. The PCR includes the following steps: denaturation (94-98°C), annealing (50-72°C), and elongation (72°C), repeated for 25-30 cycles. The annealing temperature depends on the primers, while the elongation step depends on the length of the DNA fragment.

2.10.1 PCR using Q5® High-Fidelity Polymerase

Q5® High-Fidelity Polymerase (Q5) (New England Biolabs [NEB], Inc. Ipswich, MA) was used to amplify fragments from genomic DNA or plasmid template. Q5® master mix (NEB) contains all components (DNA polymerase, NTPs, buffer) needed for the synthesis of new DNA fragments. Consequently, only template DNA, water, and primers should be added.

Materials:

All components needed for the PCR reaction are given in table 2.5.

Procedure:

1. The components that are given in table 2.5 were mixed in 0.2 mL PCR tubes (Axygen®, Inc. Union City, CA) on ice.
2. The tubes were placed in a PCR machine and the program in table 2.6 was started.

Table 2.5: Components for one PCR reaction using Q5® High-Fidelity Polymerase

Component	Volume [µL]
Q5® Hot Start High-Fidelity 2X Master Mix (NEB)	25
Forward Primer [10 µM]	2.5
Reverse Primer [10 µM]	2.5
DNA template	x*
dH_2O	to 50

* normally 0.5-1 µL (up to 1 µg)

Table 2.6: PCR program using Q5® High-Fidelity Polymerase

Step	Temperature [°C]	Time	Cycles
Initial denaturation	98	30 s	1
Denaturation	98	10 s	25-35
Annealing	50-72*	30 s	
Elongation	72	20-30 s/kb**	
Final elongation	72	2 min	1
Hold	4	∞	

* The temperature was chosen based on which primers were used.

** Depending on the length of the DNA sequence to be amplified, the duration of the elongation step was adjusted.

2.10.2 Colony PCR using RedTaq DNA Polymerase

PCR using RedTaq DNA Polymerase Master Mix (VWR) was used to screen colonies after transformation. This was done to verify the successful transformation.

Materials:

All components needed for the PCR reaction are given in table 2.7.

Procedure:

1. One colony was picked up with a sterile toothpick and stroked inside a PCR tube.
2. The remaining components given in table 2.7 were transferred to the same 0.2 mL PCR tubes (Axygen®) on ice.
3. The tubes were placed in a PCR machine and the program was adjusted as given in table 2.8.

Table 2.7: Components for the digestion of DNA using two restriction enzymes

Component	Volume [µL]
Taq 2X Master Mix (VWR)	25
Forward Primer [10 µM]	1
Reverse Primer [10 µM]	1
DNA template	one colony
dH_2O	to 50

Table 2.8: PCR program using RedTaq Polymerase

Step	Temperature [°C]	Time	Cycles
Initial denaturation	95	2 min	1
Denaturation	95	20-30 s	25-35
Annealing	50-65*	30 s	
Elongation	72	1 min/kb**	
Final elongation	72	5 min	1
Hold	4	∞	

* The temperature was chosen based on which primers were used.

** Depending on the length of the DNA sequence to be amplified, the duration of the annealing step was adjusted.

2.11 Agarose gel electrophoresis

The principle of this method is the separation of DNA fragments by size by applying an electric current. DNA is negatively charged and will move toward the positive pole of the gel. Since the charge of DNA is equally distributed, separation depends only on fragment size. The smaller DNA fragments move faster through a matrix of polysaccharides such as in an agarose gel. The sizes of the fragments are estimated by applying a DNA ladder of known fragment sizes in one well of the gel and comparing it with samples. The concentration of agarose in all gels was 1.2%.

Materials:

1 x TAE Buffer

SeaKem® LE Agarose (Lonza, Basel, Switzerland)

peqGREEN (peqLab)

DNA Gel Loading Dye 6X (NEB)

Quick-Load® Purple 1 kb DNA Ladder (NEB)

GelDoc EZ imager (Bio-Rad)

Procedure:

1. 0.6 g SeaKem® LE Agarose (Lonza) was dissolved in 50 mL 1 x TAE Buffer by heating the mixture in a microwave for one minute at 700 W.
2. The mixture was cooled down to approximately 60°C before 1 µL peqGREEN (peqLab, Wilmington, USA) was added to make fragments visible under UV light. The prepared mixture was poured into a gel tray with eight combs.
3. After 20 to 30 minutes, when the gel was solid and the comb was removed. The gel was transferred to an electrophoresis chamber and covered with 1 x TAE Buffer.
4. The loading dye was added to the samples before these were loaded into the wells.
5. The gel was run at 90 V for 30-80 minutes, depending on the expected sizes of the fragments.
6. GelDoc EZ imager (Bio-Rad) was used to analyze and document pictures of the gels.
   (a) If some of the isolated DNA fragments were to be used later, the bonds of interest were excised from the gel with a scalpel under UV light. The gel pieces were kept in a microcentrifuge tube and stored at -20°C or used immediately.

2.12 Extraction and purification of DNA fragments from agarose gels

The NucleoSpin® Gel and PCR Clean-up Kit (MACHEREY-NAGEL) was used to purify PCR products or to extract DNA fragments excised from the agarose gel, following the protocol 5.1 or 5.2, respectively.

2.13 Cloning

2.13.1 In-Fusion® Cloning

The In-Fusion® HD Cloning Kit User Manual (Takara Bio) was followed for cloning of target fragments into backbone vectors. The basis of In-Fusion cloning is a unique In-Fusion enzyme that joins DNA fragments by recognizing 15 bp overlaps at their ends. The primers are designed to have 15 bp complementarity with linearized vector sequences. Therefore, the PCR reaction of the insert sequence will generate overhangs at the ends of the insert fragment. In-Fusion enzymes recognize these overhangs and bring insert DNA together with backbone DNA.

In this study, protocols for designing specific PCR primers (table 2.1), cloning the fragments into vector DNA (figure 2.1), and transforming them into *E. coli* used as a subcloning host (see section 2.14).

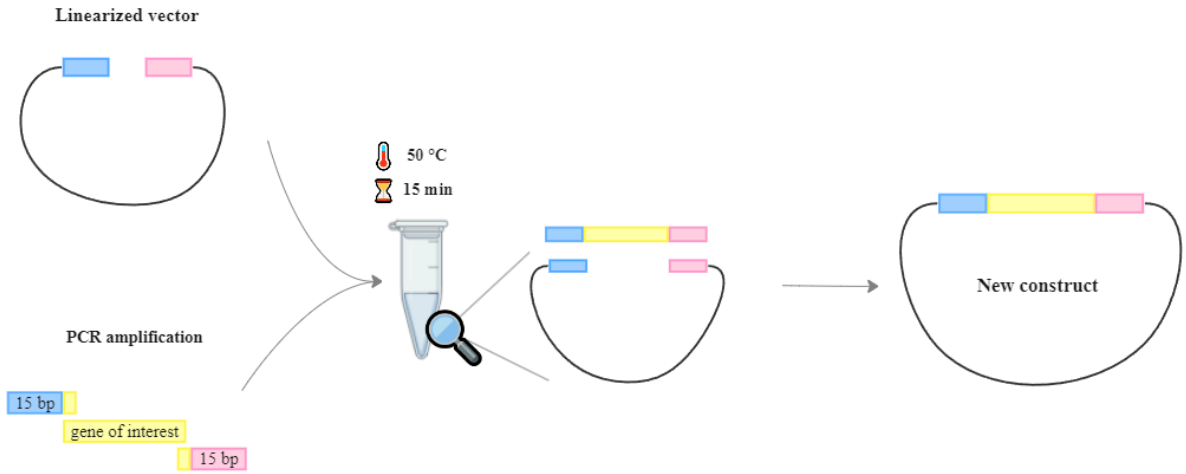

Figure 2.1: In-Fusion cloning. The strategy for In-Fusion cloning is to digest the vector with restriction enzymes and amplify target DNA fragments (*yellow*) using In-Fusion primers, with 15 bp homologous overhangs (*blue* and *pink*) to the vector. PCR amplified fragments, linearized vectors, and reaction mix (table 2.9) are mixed and incubated at 50°C for 15 minutes. The new construct should be generated and transferred into a host. The figure inspired by the In-Fusion® HD Cloning Kit User Manual.

Materials:

Components needed for an In-Fusion Cloning reaction are given in table 2.9.

Procedure:

Table 2.9: Components for the digestion of DNA using two restriction enzymes.

Component	Volume [µL]
5X In-Fusion HD Enzyme Premix	2
Linearized vector (backbone DNA)	x
Purified PCR fragment (insert DNA)	x
dH_2O	to 10

1. In-Fusion molar ratio calculator (takarabio.com/in-fusion-molar-ratio-calculator) was used to calculate the amount of DNA needed for insert to vector 2:1 ratio. Typically a vector concentration of up to 100 ng and a concentration of the insert of up to 50 ng were used.
2. The components listed in table 2.9 were mixed in a microcentrifuge tube at room temperature.
3. The reaction mix was incubated for 15 minutes at 50°C.
4. Then the mixture was placed on ice and transformed into *E. coli* (described in section 2.14).

2.13.2 Quick Ligation

Ligation is used to connect two DNA fragments digested with the same restriction enzyme pair. During this process, a ligase enzyme covalently links the two DNA fragments with complementary ends together. This method is an alternative to In-Fusion cloning, described above.

Materials:

All components needed are given in table 2.10.

Table 2.10: Components for the digestion of DNA using two restriction enzymes.

Component	Volume
Quick Ligase Reaction Buffer (2X)	10 µL
Linearized vector (backbone DNA)	50 ng
Purified PCR fragment (insert DNA)	x ng
dH_2O	to 20
Quick Ligase	1 µL

Procedure:

1. NEBioCalculator was used to calculate insert to vector 3:1 ratio needed in the reaction.
2. The components given in table 2.10 were mixed in a microcentrifuge tube.
3. The sample was incubated for five minutes at room temperature (25°C).
4. The tube was transferred to ice before further use or stored at -20°C for later use.

2.14 Transformation of *E.coli*

The In-Fusion or Quick ligation reaction mixture was transformed into chemically competent *E. coli* cells. Two *E. coli* strains were used: (1.) Stellar™ Competent Cells (Takara Bio) for In-Fusion reaction mix and (2.) OneShot™ TOP10 Chemically Competent *E. coli* (Invitrogen) for Quick Ligation reaction mix. The transformation procedure given by the respective manufacturer was followed.

2.15 Sequencing of plasmids

In order to verify successful plasmid construction, the plasmid DNA was sent for sequencing. In a microcentrifuge tube, purified plasmid (400-500 ng) was mixed with 2.5 µL primer (10 µM) and sterile water for a total volume of 11 µL. The tube was barcoded and sent to Eurofins Genomics (Bayern, Germany) for analysis. After sequencing, the results were analyzed with

CLC DNA Main Workbench 7.

2.16 Electrocompetent *Lactiplantibacillus pentosus*

The electroporation method uses a high-voltage electric current to shock cells and makes them competent for DNA uptake (Aukrust et al., 1995). The electrocompetent *L. pentosus* KW1 and KW2 were made using the protocol originally developed for *Lactiplantibacillus plantarum*, described by Aukrust et al. (1995).

Materials:
MRS
MRS + 1 % glycine
30% PEG_{1450} (made fresh)
MRSSM (MRS + 0.5 M sucrose + 0.1 M $MgCl_2$)
Ice
Allegra X-30R Centrifuge (Beckman Coulter, Brea, CA, USA)
Procedure:

1. *L. pentosus* KW1 and KW2 from glycerol stocks were cultured overnight in 10 mL MRS at 37°C.
2. 1 mL of the overnight culture was used to make a serial dilution (10^{-1} - 10^{-10}) in MRS + 1% glycine. The cultures were incubated overnight at 37°C.
3. The next day, 1 mL from a culture with an OD_{600} of 2.5±0.5 was further diluted in 20 mL MRS + 1 % glycine (can be scaled up). The culture was then grown for approximately 2-3 hours until it reached the logarithmic phase (OD_{600} of 0.7±0.07) and placed on ice for 10 min.
4. The culture was centrifuged for 5000 x g for 5 min at 4°C, and the supernatant was discarded.
5. The pellet was resuspended in 5 mL ice-cold fresh 30 % PEG_{1450} before an additional 20 mL of 30 % PEG_{1450} was added. The tube was inverted gently and placed on ice for 10 min.
6. The cells were collected by centrifugation at 5000 x g for 5 min at 4°C.
7. The pellet was resuspended in 400 µL 30 % PEG_{1450} and 40 µL aliquots were pipetted into pre-freezed microcentrifuge tubes and stored at -80°C.

2.17 Transformation of electrocompetent *L. pentosus*

Materials:
GenePulser® II (Bio-Rad)
Electrocompetent *L. pentosus* KW1 and KW2
0.2 cm Electroporation cuvette (Gene Pulser®)
MRSSM-media
MRS agar plates with erythromycin (Merck)
Purified plasmid
Procedure:

1. Previously made electrocompetent *L. pentosus* KW1 and/or KW2 (section 2.16) were placed on ice for a few minutes, until thawed. Purified plasmid (5 µL) was added to one aliquot of the electrocompetent cells. The mixture was transferred to an electroporation cuvette.
2. The electroporator was set to appropriate settings (1.5 kV, 25 µF, 400 Ω), and the cuvette was placed in the machine and exposed to an electrical pulse.
3. 450 µL MRSSM media was immediately added to the cuvette. The mix was transferred to a new microcentrifuge tube, and incubated at 37°C for 2 hours at static conditions.
4. The transformation mix (100 µL) was spread on MRS / 10 µg/mL Ery agar plates and incubated overnight at 37 °C.

2.18 Cultivation and harvesting of recombinant *L. pentosus*

The *L. pentosus* KW1 and KW2 strains were cultivated and harvested as described here, were further analyzed through growth and protein production optimums, growth curve analysis, western blot and flow cytometry analysis (see section 2.20)
Materials:
Inducer peptide: SppIP (CASLO, Copenhagen, Denmark)
1x Phosphate Buffered Saline (PBS)
MRS (Oxoid)
Erythromycin (Merck)
Ultrospec 10 Cell Density Meter (Amersham Biosciences, Amersham, UK)
Allegra X-30R Centrifuge (Beckman Coulter)
Procedure:

1. Recombinant *L. pentosus* KW1 and KW2 strains were grown in MRS medium supplemented with erythromycin (Merck) to a final concentration of 10 µg/mL at 37°C.
2. The overnight cultures were diluted in 50 mL preheated (37°C) MRS, to an OD_{600} of

0.14-0.15. Erythromycin (Merck) was added to a concentration of 10 µg/mL.

3. The cultures were incubated at 37°C until they reached an OD_{600} of 0.28-0.33, and 25 ng/mL SppIP (inducer peptide) was added to each culture to induce protein production. The induced cultures were then incubated for three hours at 37°C.
4. Subsequently, the cultures were harvested by centrifugation at 4°C and 4700 rpm for 5 minutes.
   (a) The volume transferred to microcentrifuge tubes of each culture was normalized based on the measured OD_{600} ($\frac{500\ \mu L}{OD_{600}}$), and further analyzed with flow cytometry (section 2.25)
5. The pellet was washed with 10 mL cold PBS and centrifuged again at 4°C and 4700 rpm for 5 minutes.
6. The supernatant was removed and the pellet was stored at -20°C until further analysis through western blot (section 2.24).

2.19 Growth and production optimum

The optimal temperatures for growth of the novel *L. pentosus* KW1 and KW2 strains were analyzed by measuring the optical density at 600 nm (OD_{600}) after incubating the wild type strains for three hours at different temperatures. The overnight cultures of wild type *L. pentosus* KW1 and KW2 were prepared for analysis similar to what was described in section 2.18(steps 1-3). The cultures were diluted to 0.14-0.15 OD_{600} in preheated MRS media. The cultures were grown at 37°C until OD_{600} reached 0.28 to 0.33. This was considered as the initial point. The cultures were then transferred to sterile 96-well microtiter plates and incubated for three hours at 30°C, 33°C, 35°C, 37°C, 39°C, 42°C. The analysis was done with three biological parallels per temperature, measured as technical triplets, gaining a minimum of nine values for each strain at each temperature. To check for variations in absorbance and that separate parallels are comparable, measurements at 37°C were used as a reference point. They were done in six parallels since not all measurements were taken simultaneously.

The optimal temperatures for recombinant protein production of *L. pentosus* KW1 and KW2 were analyzed similarly to growth optimum analysis. The cultures of wild type strains and KW1 and KW2 strains harboring pSIP_mCherry (Wiull et al., 2022) were prepared in the same way, as described above for the growth optimums. Production optimums were analyzed by measuring OD_{600} and fluorescence signal (587/620nm) simultaneously. Non-induced strains were used as negative controls of the pSIP system. The first measurement was performed right after the induction of protein production (t=0) and after three hours of incubating at 30°C, 33°C, 35°C, 37°C, 39°C and 42°C.

2.20 Growth curve analysis

The growth rates of *L. pentosus* KW1 and KW2 wild types, as well as recombinant strains, were examined by growth curve analysis. *L. pentosus* strains were grown in MRS medium overnight, diluted to an OD_{600} around 0.15. At this point, 10 µg/mL erythromycin was added to the recombinant cultures. The cultures were further incubated until OD_{600} reached approximately 0.3. Then, the SppIP inducer was added to recombinant cultures. Non-induced recombinant cultures were taken as a negative control of induction.

Materials:

Sterile 96-Well Microplates (Thermo Fisher Scientific)
Microplate Sealing Film (Thermo Fisher Scientific)
Multiskan™ FC Microplate Photometer (Thermo Fisher Scientific)

Procedure:

1. The cultures were prepared as described in section 2.18 (steps 1-3), except that wild-type strains, were cultivated without the addition of antibiotics.
2. Immediately after induction, 200 µL of the culture was pipetted to a sterile 96-well microtiter plate in three technical replicates.
3. The microtiter plate was sealed with transparent film and placed in a Multiscan™ FC Microplate Photometer, and the absorbance was measured every 15 minutes at OD_{595} for 24 hours.

2.21 Fluorescence microscopy

Fluorescence microscopy was performed to study the cell morphology of the novel *L. pentosus* KW1 and KW2 strains. The strains were compared to well-studied *L. plantarum*. The volumes of *L. pentosus* cultures taken to analysis were doubled (0.8 µL) for KW1 and KW2 strains because only a few cells were observed when the original protocol (0.4 µL) was followed.

Materials:

SeaKem® LE Agarose (Lonza)
1xPBS
Overnight cultures
Zeiss LSM 700 Confocal Microscope

Procedure:

1. 0.12 g agarose was mixed with 10 mL 1xPBS to make a 1.2% agarose.
2. The mixture was heated in a microwave with intervals of 5-10 seconds until homogenization of the mixture.
3. 600 µL freshly prepared 1.2% agarose was added to the objective glass.

4. After approximately one minute, another objective glass was placed above the objective glass with agarose and pressed down to distribute the agarose evenly.
5. After 30-60 seconds, the objective glass was slid off, and 0.4 µL from the overnight cultures was placed into each circle on the objective glass. The microscopy preparate was covered on the top and ready for microscopy.

2.22 Preparation of cell-free protein extracts

This protocol was used to make cell-free protein extracts that were further analyzed through western blot analysis, as described below (section 2.24).

Materials:

FastPrep® tube (Thermo Fisher Scientific, Waltham, MA, USA)
Glass beads (Sigma Aldrich)
FastPrep® - 24 Tissues and Cell homogenizer (Thermo Fisher Scientific)
PBS

Procedure:

1. The pellets of bacteria cultivated and harvested bacteria as described in section 2.18 were re-suspended in 1 mL PBS and transferred to a FastPrep® tube with approximately 0.5 g glass beads for cell lysis.
2. The FastPrep® tubes were shaken in FastPrep® - 24 Tissues and Cell homogenizer at 6.5 m/s for 45 seconds. This step was repeated 3 times with incubation for 5 minutes on ice between the runs.
3. The tubes were centrifuged at 16 000 x g at 4°C for one minute. Supernatants were transferred to new microcentrifuge tubes.
4. Step 3 was repeated.
5. The protein extracts were used directly (section 2.24) or stored at -20°C.

2.23 Protein concentration of cell-free protein extract

Protein concentrations of cell-free protein extracts prepared as described above were quantified using Qubit™ Fluorometer (Invitrogen) and Qubit™ Protein Assay Kit. The instrument was calibrated before measurement. The protocol given by the supplier was followed.

2.24 Western blot

Western blotting, also called immunoblotting or protein blotting, is a standard method used to detect proteins in the sample (Kurien & Scofield, 2015). The method includes several steps described in the following subsections: separation of proteins with SDS-PAGE gel electrophore-

sis (section 2.24.1), followed by transfer (blotting) of the proteins from the gel to an adsorbent membrane (section 2.24.2), antibody hybridization (section 2.24.3), and detection of the proteins with chemiluminescence (section 2.24.4).

2.24.1 Gel electrophoresis of proteins

Sodium dodecyl-sulfate polyacrylamide gel electrophoresis (SDS-PAGE) is a common method for separating denatured proteins by molecular weight. The protein samples are denatured after mixing with lithium dodecyl-sulfate (LDS), dithiothreitol (DTT), and heating (>70°C). LDS is an anionic detergent that unfolds proteins by breaking non-covalent bindings, while DTT is a reducing agent that breaks covalent disulfide bridges. LDS binds to the proteins, which makes them negatively charged. When running the gel, the proteins will move through the gel matrix toward the positively charged electrode. Since the charge of the proteins is evenly distributed, the bands are separated by molecular mass. The sizes of the bands are estimated by applying a protein standard with known molecular weights in one of the wells of the gel.

Materials:

NuPAGE® LDS Sample Buffer (4X) (Invitrogen)
NuPAGE® Reducing Agent (10X) (Invitrogen)
NuPAGE® Novex Bis-Tris gel (Bio-Rad)
MagicMark® XP Western Protein Standard (Invitrogen)

Procedure:

1. In a microcentrifuge tube, 7.5 µL NuPAGE® LDS Sample Buffer (4X), 3 µL NuPAGE® Reducing Agent (10X), and 20 µL protein extract prepared as described in section 2.22 were mixed.
2. The samples were incubated at 100°C for 10 minutes.
3. A 15 wells NuPAGE® Novex Bis-Tris gel was mounted in an electrophoresis chamber. Tris-glycine-SDS (TGS) buffer was added to the chamber.
4. MagicMark® XP Western Protein Standard and the protein samples (1-4 µg) were loaded onto the gel. The gel was run for 30 minutes at 200 V.
5. Picture of the gel was taken with GelDoc EZ imager (Bio-Rad).

2.24.2 Blotting with iBlot™ Dry Blot System

The proteins were transferred from the gel to a nitrocellulose membrane in a process called blotting, using the iBlot™ Dry Blot System (Invitrogen). The transfer system consists of a so-called *sandwich* made of a copper anode, stack bottom, blotting membrane, and protein gel, followed by stack top and copper cathode, as described in more detail below and illustrated in figure 2.2.

Procedure:

1. The iBlot^{TM} Anode Stack, Bottom (Invitrogen) was opened and placed in the iBlot^{TM} Gel Transfer Device (Invitrogen). The bottom stack contains a copper anode and the blotting membrane.
2. The gel was placed directly on the blotting membrane.
3. A piece of iBlot^{TM} filter paper (Invitrogen) was moistened with Milli-Q®water and placed on the gel. Air bubbles were removed with a Blotting Roller.
4. The iBlot^{TM} Cathode Stack, Top (Invitrogen), containing a copper cathode, was placed on the top. The Blotting Roller was used once more time to remove eventual air bobbles.
5. A iBlot^{TM} Disposable sponge (Invitrogen) was placed in the iBlot^{TM} Transfer Device and the lid was closed.
6. The blotting process was performed using the P3 program on the machine.

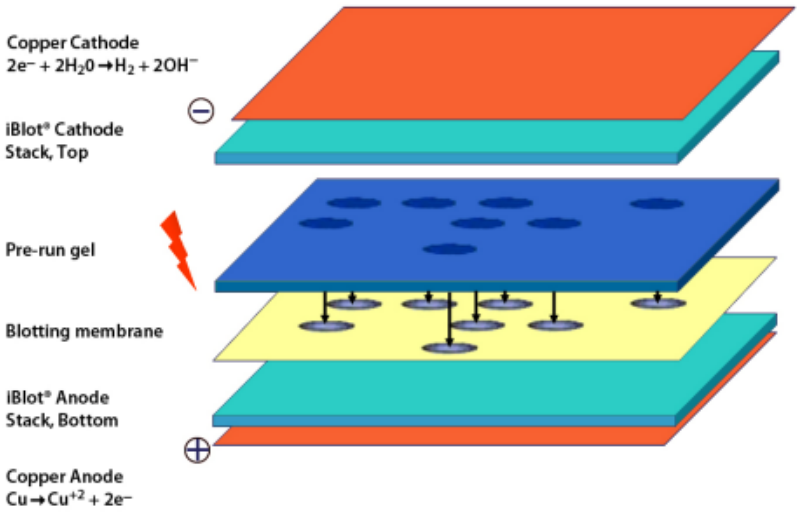

Figure 2.2: Components of iBlot^{TM} transfer stack. The transfer stack consists of copper anode and cathode, with so-called "sandwich" in between. The anode stack bottom (*turquoise*) is in direct contact with the copper anode (*orange*), followed by a proper blotting membrane (yellow), protein gel (from SDS-PAGE) (*blue*), and top stack (*turquoise*) with direct contact with copper cathode (*orange*). The figure was taken from (iBlot^{TM}Dry Blot System Manual)

2.24.3 Immunodetection using SNAP i.d.® 2.0 Protein Detection System

The immunodetection of the tuberculosis antigen was carried out using SNAP i.d.® immunodetection system (Millipore), following the manufacturer's instruction as indicated below (see the procedure). The system uses a vacuum to run solutions through the membrane. Non-specific binding of the antibody is inhibited by adding BSA to a blocking solution. The primary antibody used in this study is antigen-specific. The secondary antibody binds to the primary antibody. The secondary antibody, conjugated with horseradish peroxidase (HRP), in the presence of a

chemiluminescent agent, emits light, as illustrated in figure 2.3.

Materials:
SNAP i.d.® 2.0 Protein Detection System
Washing solution: TTBS (TBS + 0.1% v/v Tween-20)
Blocking solution: TTBS + 3% BSA
Primary antibody: ESAT6 Rabbit polyclonal (bs-13107R) (1:500)
Secondary antibody: HRP-Rabbit Anti-Mouse IgG (A9917) (1:20000)

Procedure:

1. After blotting (section 2.24.2), the membrane was transferred to the blot holder. The membrane was placed with the protein side facing downwards, and a filter paper pre-soaked in MilliQ water was placed on top. The blot roller was used to remove air bobbles.
2. The blot holder was placed in a cassette of the SNAP i.d.® immunodetection device with the protein side pointing up.
3. The blocking solution (30 mL) was poured into the cassette in portions of approximately 10 mL. The vacuum was turned on until all the liquid went through the membrane.
4. 5 µL of the primary antibody (1:500) was added to 5 mL of blocking solution. The mixture was vortexed for a few seconds before the solution was poured into the cassette. After 10 minutes of incubation, the vacuum was turned on until the solution went through the membrane.
5. The membrane was then washed three times with 30 mL TTBS while the vacuum was continuously turned on. When all of the washing solution had gone through, the vacuum was turned off.
6. 5 mL of the blocking solution was mixed with 0.33 µL of the secondary antibody (1: 20 000) and vortexed for a few seconds. The solution was poured into the cassette and incubated for 10 minutes. The vacuum was on until all of the solution went through.
7. The membrane was washed four times as described in step 5.
8. The membrane was disassembled from the blot holder and the antigens were visualized using the SuperSignal™ kit (Thermo Fisher Scientific) (section 2.24.4).

2.24.4 Detection of proteins with chemiluminescence

Materials:
SuperSignal™ West Pico Chemiluminescent Substrate:
Luminol/Enhancer
Stable Peroxide Buffer

Procedure:

1. 5 mL of SuperSignal™ Luminol/Enhancer and 5 mL of SuperSignal™ Stable Peroxide Buffer were mixed in a plastic container and covered with aluminum foil to limit light exposure.
2. The membrane from the last step in section 2.24.3 was transferred to the container and incubated for five minutes without exposure to the light.
3. Visualization of the proteins on the membrane was carried out using Azure c400 (Azure Biosystems).

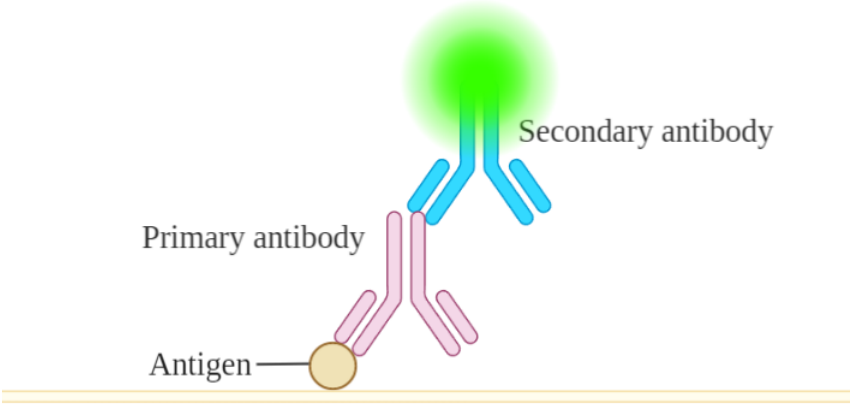

Figure 2.3: Illustration of antigen detection. The figure illustrates the hybridization of the specific primary antibody (*pink*) to the antigen (*yellow*). This is followed by the binding of the secondary antibody (*blue*) to the primary antibody (*pink*), which results in fluorescent emission, as indicated in *green*. The figure was created using Biorender

2.25 Flow cytometry analysis

The principle of flow cytometry is based on living cells flowing one by one through the laser beam. Every cell scatters the light in a specific manner. These signals are recognized by detectors, converted to electronic signals, and visualized as dot plots of individual cells McKinnon, 2018.

Antigens are detected on the bacteria's surface through flow cytometry by treating live cells with antibodies and their hybridization to the antigen. The primary antibody is specific to ESAT-6 of the H56 antigen. The secondary antibody carries a FITC molecule that binds to the primary antibody, giving rise to a detectable fluorescent signal, similar to the illustration in figure 2.3. The strength of the fluorescent signal depends on the quantity of conjugated secondary antibodies bound to the primary antibody. The greater shift along the x-axis from the negative control, the better signal is, indicating that the antigen is most exposed (McKinnon, 2018).

In this study flow cytometry is used to investigate the surface display of hybrid tuberculosis antigen, H56 on the surface of eight recombinant strains of *L. pentosus* KW1 and KW2.

Materials:

PBS

Washing solution: PBS + 2% BSA

Primary antibody: ESAT6 Mouse monoclonal (ab26246)

Secondary antibody: Anti-Mouse IgG-FITC (Sigma Aldrich)

Procedure:

1. Bacterial cultures were cultivated and harvested as described in section 2.18(steps 1 to 4(a)).
2. The cultures were centrifuged at 8 000 x g for 3 minutes to harvest cells. The supernatant was discarded.
3. In a microcentrifuge tube, 50 µL (PBS + 2 % BSA) per sample was mixed with 0.15 µL/sample of the primary antibody. 50 µL of this mixture was added to each sample and the pellet was resuspended.
4. The samples were incubated for 30 minutes at room temperature.
5. The cells were spun down by centrifugation at 8 000 x g for one minute.
6. The pellets were washed three times with 600 µL of the washing solution at the time.
7. Each sample was resuspended with 50 µL washing solution containing 0.3 µL of the secondary antibody per sample. The samples were packed in aluminum foil and incubated for 30 minutes at room temperature.
8. The samples were centrifuged at 8 000 x g for one minute and washed four times, as described in step 6.
9. The cells were resuspended in PBS (1 mL).
10. The samples were further diluted with PBS in a 1:10 ratio, before them were analyzed using MacsQuant® Analyser and MacsQuantify™ software.

3 Results

L. pentosus KW1 and KW2 were newly isolated from table olives and were whole-genome sequenced. In this thesis, these strains were characterized through several experiments. Optimal temperature conditions for growth and protein production were analyzed. Morphology was determined through fluorescence microscopy and further analyzed with image analysis software.

L. pentosus KW1 and KW2 were modified to produce and surface display hybrid tuberculosis antigens on their surface, using four different strategies. Eight pSIP plasmids were constructed and transformed into *E. coli* (table 2.2), used as the subcloning host before transforming the plasmids into *L. pentosus* strains. To investigate the production and secretion of the antigens, growth curve analysis, western blot analysis, and flow cytometry were performed on the recombinant *L. pentosus* KW1 and KW2.

3.1 Optimum temperatures for growth

Since *L. pentosus* KW1 and KW2 were newly isolated strains, it was desirable to test which temperature is optimal for their growth before doing any further analysis. The optimum temperatures for the growth of KW1 and KW2 strains were analyzed based on growth rates of wild types after three hours of incubation at different temperatures (figure 3.1). There was very little

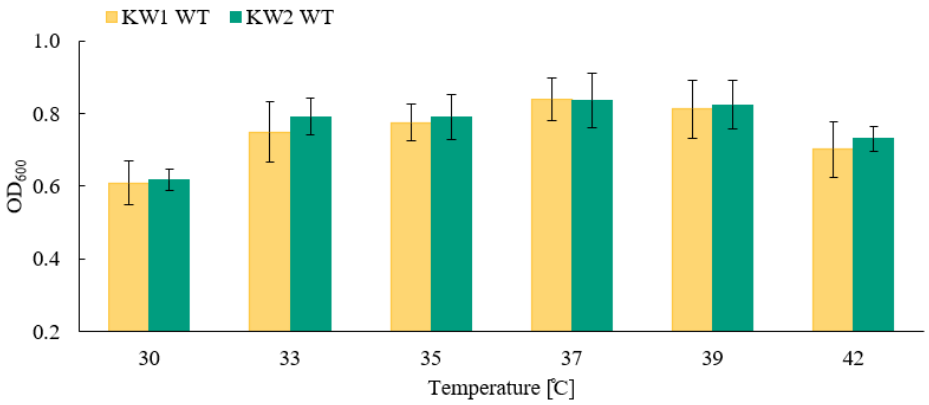

Figure 3.1: Growth optimum of *L. pentosus* KW1 and KW2. The figure shows the growth rate of wild type *L. pentosus* KW1 (yellow) and wild type *L. pentosus* KW2 (green) measured at OD_{600} after three hours of incubation at 30°C, 33°C, 35°C, 37°C, 39°C and 42°C. The black flated lines show the standard deviation between the measurements of the biological and technical replicates.

difference in growth rates between wild type *L. pentosus* KW1 and KW2, considering that both strains grow equally well (figure 3.1). The strains show a slight reduction in growth at terminal temperatures (30 and 42°C), considering that the optimum temperature for the growth of *L. pentosus* KW1 and KW2 is between 33°C and 39°C. Figure 3.1 indicates that the growth of wild type *L. pentosus* strains was slightly higher at 37°C, compared to other temperatures. Because of this and for practical reasons, further analyses of *L. pentosus* strains were done at 37°C.

Growth curve analysis

Growth curve analysis of wild type *L. pentosus* KW1 and KW2 was performed over 16 hours at 37°C (figure 3.2). The growth curves were laying on top of each other, and it was impossible to observe any difference between the strains. Also, the figure 3.2 indicates that *L. pentosus* KW1 and KW2 have a short lag phase of approximately 20 to 30 minutes from the initial measuring point before they achieve the exponential phase. Both strains were growing exponentially until approximately five hours from the first measurement. The KW1 and KW2 strains were in the stationary phase for the rest of this analysis.

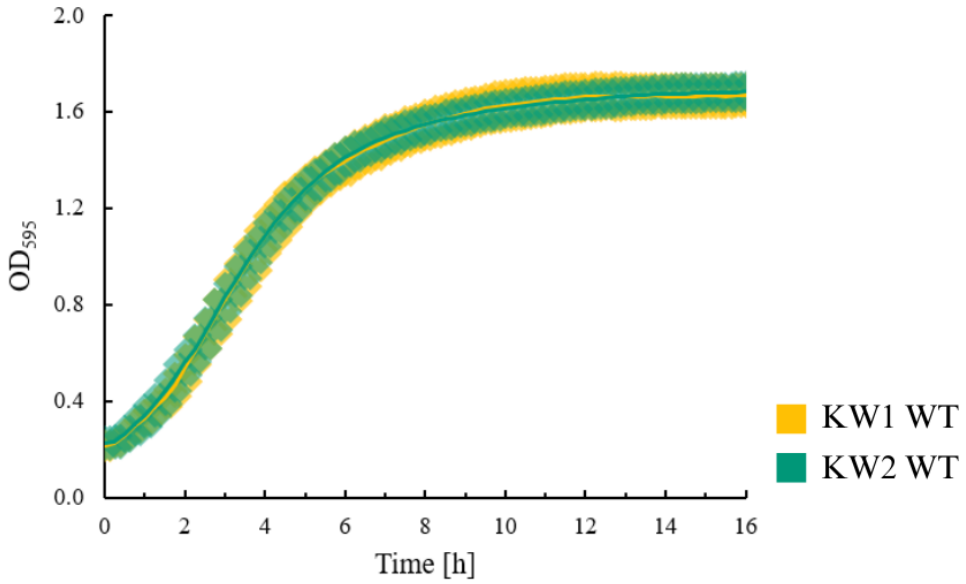

Figure 3.2: Growth curve analysis of wild type *L. pentosus* KW1 (*yellow*) and KW2 (*green*). Growth rates were measured at OD_{595} over 16 hours. The analysis was done with three biological parallels in technical triplets. Standard deviations between the measurements are shown with the transparent squares in *yellow* for KW1 and *green* for KW2.

3.2 The optimum temperature for protein production

The inducible pSIP gene expression system was originally developed for use in *L. plantarum* and *Latilactobacillus sakei* (Sørvig et al., 2003, 2005). Before further experiments, the suitability of the pSIP system for use in *L. pentosus* KW1 and KW2 was validated. This was done using mCherry as a reporter protein in the pSIP system (pSIP_mCherry, Wiull et al. (2022), table 3.2) under the control of the inducible sppA promotor. Plasmid harboring mCherry (pSIP_mCherry) was transformed into *L. pentosus* KW1 and KW2. The production of mCherry was determined by measuring the fluorescence signal (587/620nm) of wild type *L. pentosus* KW1 and KW2 (negative controls) and *L. pentosus* KW1 and KW2 carrying pSIP_mCherry plasmid with and without the addition of SppIP inducer to the cultures. The fluorescence signal was measured in relative fluorescence units (RFU) at the induction point (data not shown) and after three hours of incubation at temperatures in a range from 30°C to 42°C (figure 3.3). Protein production per

bacterial cell was compared by dividing the mean RFU with mean OD_{600} values (section 3.1) and plotted against temperature (°C), visualized in figure 3.3.

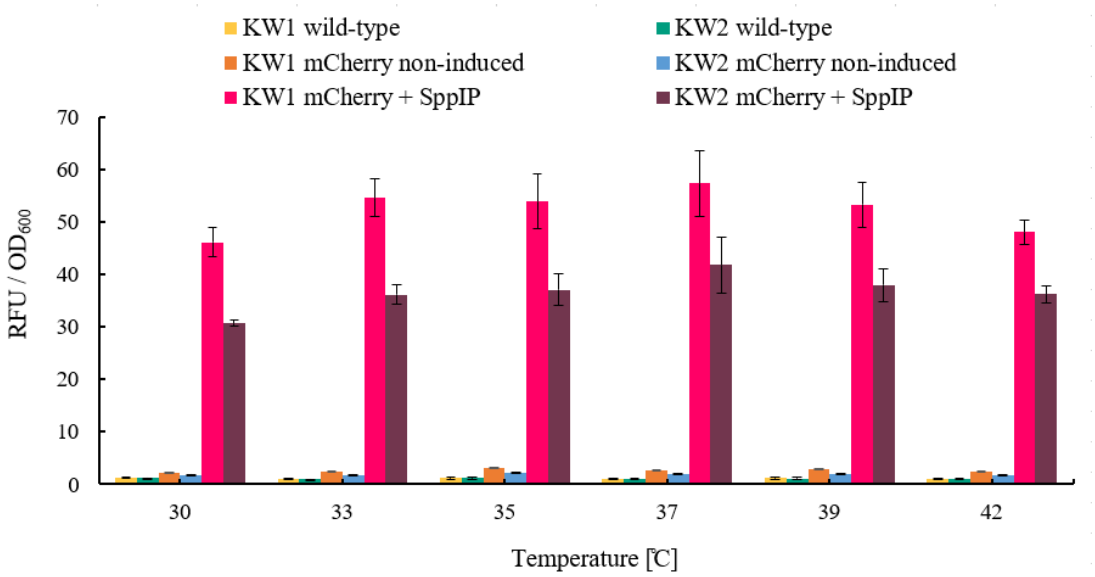

Figure 3.3: Temperature optimum for protein production in *L. pentosus* KW1 and KW2. Protein production per cell was calculated by the measured relative fluorescent unit (RFU) divided with the measured absorbance signal (OD_{600}). Production of mCherry protein was measured after three hours of incubation at 30°C, 33°C, 35°C, 37°C, 39°C and 42°C. The data gained from wild type *L. pentosus* KW1 are represented in *dark yellow*, wild type *L. pentosus* KW2 in *green*, non-induced *L. pentosus* KW1 in *orange*, non-induced *L. pentosus* KW2 in *blue*, induced *L. pentosus* KW1 in *pink* and induced *L. pentosus* KW2 in *purple* color. Error bars show the standard deviation between three biological replicates. Each biological parallel was analyzed in technical triplets.

The figure 3.3 shows that the signal acquired from *L. pentosus* KW1 was higher than KW2 at all temperatures, indicating that KW1 produced more protein. The protein production of both strains was slightly higher at 37°C compared to other analyzed temperatures. For the purpose of this project, it was considered that both growth and protein production optimums were at 37°C, but more research is needed to confirm this.

RFU/OD_{600} values at 37°C of wild type *L. pentosus* KW1 and KW2 were 1.06 and 1.05, respectively, while non-induced *L. pentosus* strains carrying the pSIP_mCherry were 2.63 and 2.02, respectively. This indicates that leakage (protein production of non-induced strains) was slightly higher in KW1_mCharry but still very low compared to induced KW1 and KW2 strains (57.3 and 41.75, table 3.1). Based on these measurements, induction factors were calculated to examine the difference between the wild type strains and non-induced mCherry strains; and between induced *L. pentosus* strains (table 3.1). The induction factor represents the increase of mCherry production upon induction. Although it seemed like protein production was much higher in *L. pentosus* KW1 (figure 3.3), table 3.1 shows that the induction factors of *L. pentosus* KW1 and KW2 were 20 and 19, respectively. This result implies that induced KW1 and KW2 harboring the pSIP_mCherry produced 20 and 19 times more protein than non-induced strains, respectively.

Table 3.1: Induction factors of mCherry protein production in *L. pentosus* KW1 and KW2. Increase of mCherry production upon induction per bacterial cell calculated by division of average relative fluorescent unit (RFU) with the optical density (OD_{600}.

Strain	Characteristics	Fluorescence (RFU/OD_{600})*		Induction factor
		Uninduced	Induced**	
KW1_WT	Wild type *L. pentosus* KW1	1.06	~ 1.06	~ 1
KW1_mCherry	*L. pentosus* KW1 carrying the pSIP_mCherry plasmid	2.63	57.31	22
KW2_WT	Wild type *L. pentosus* KW2	1.05	~ 1.05	~ 1
KW2_mCherry	*L. pentosus* KW2 carrying the pSIP_mCherry plasmid	2.02	41.75	21

* Average values of at least three parallels measured at 37°C

**The values of induced wild types were assumed to be the same as those of non-induced wild type strains.

Both recombinant *L. pentosus* KW1 and KW2 produced mCherry protein in high concentrations only when the SppIP inducer was added to the cultures. Therefore these analyses (figure 3.3 and table 3.1) strongly indicated that the pSIP system could be used for the overproduction of desired proteins in *L. pentosus* KW1 and KW2.

3.3 Morphology of *L. pentosus* KW1 and KW2

The morphology of *L. pentosus* KW1 and KW2 was studied by fluorescence microscopy and compared to the morphology of the closely related species *L. plantarum* WCFS1. The microscope images were analyzed with the ImageJ software (https://imagej.nih.gov/ij/download.html). Six cultures were prepared for microscopy: *L. pentosus* KW1 and KW2, and *L. plantarum* WCFS1, all with pEV and induced pSIP_mCherry (Wiull et al. (2022), table 3.2), as shown in figure 3.4.

In the red fluorescing bacteria (figure 3.4B, D, and F), the expression of mCherry were induced. Interestingly, a larger fraction of the *L. pentosus* KW1 cells were not visibly red compared to *L. pentosus* KW2 and *L. plantarum* WCFS1, implying that these did not produce mCherry. Strains carrying the empty vector (figure 3.4A, C, and E) did not give any fluorescent signal, as expected.

The microscope images (figure 3.4) indicate that the *L. pentosus* strains were found as single cells, in pairs or in short chains. KW1 and KW2 seem longer and narrower than the *L. plantarum* strain. The microscopy images were further analyzed with ImageJ software, as shown in figure 3.5. The figure shows that the length of *L. pentosus* was approximately 3.8 µm, while *L. plantarum* was around 3 µm (figure 3.5). Also, it indicates the most variation in the shape of *L. pentosus* KW1 because the line of predicted shape is the widest on figure 3.5. However, the number of

bacteria included in the analysis was insufficient to completely define the cell morphology of L. pentosus strains. An additional microscopy analysis with more bacteria should be performed to conclude the final shape and cell size.

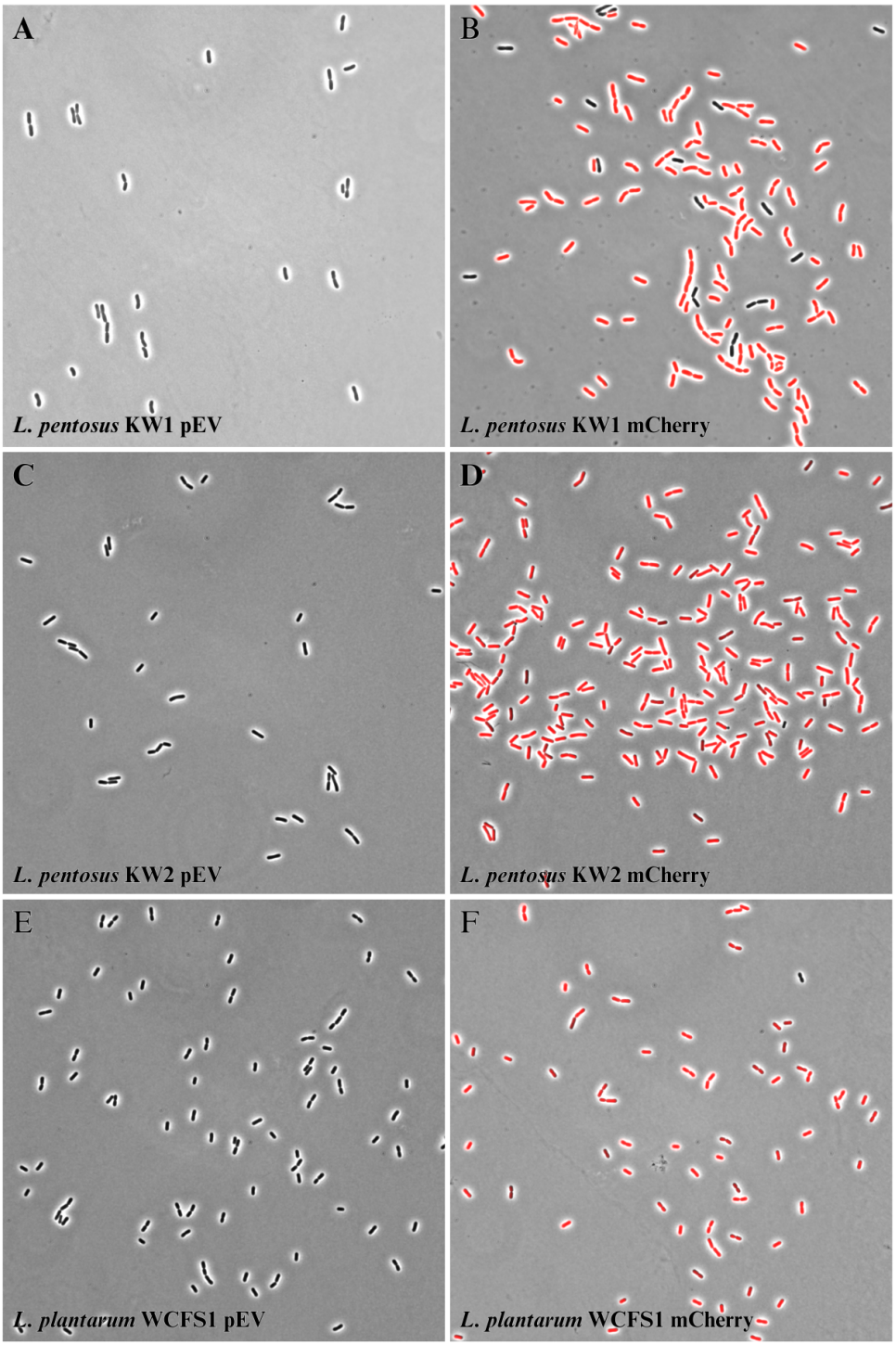

Figure 3.4: Fluoroscence microscopy of *L. pentosus* KW1 and KW2 and *L. plantarum* WCFS1. A) Microscope image of *L. pentosus* KW1 with pEV (negative control). B) Microscope image of induced *L. pentosus* KW1 with pSIP_mCherry (Wiull et al. (2022), table 3.2). C) Microscope image of *L. pentosus* KW2 with empty vector. D) Microscope image of induced *L. pentosus* KW2 with pSIP_mCherry. E) Microscope image of *L. plantarum* WCFS1 with pEV. F) Microscope image of induced *L. plantarum* WCFS1 with pSIP_mCherry.

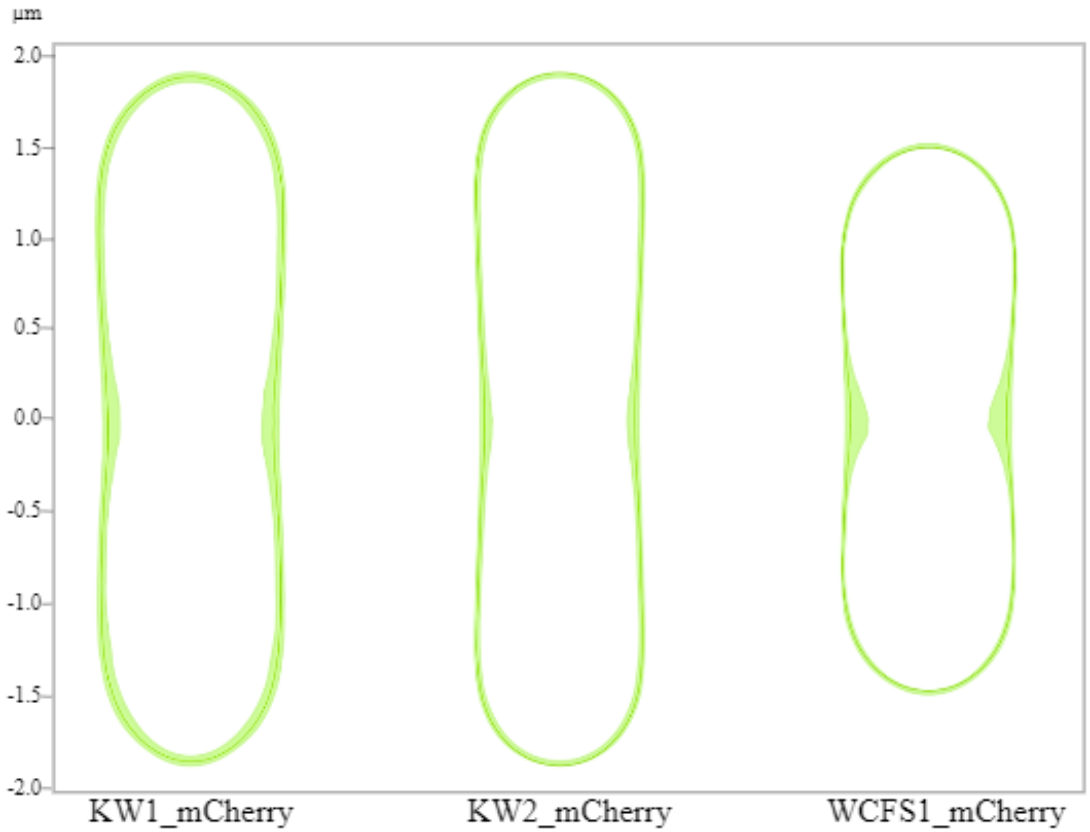

Figure 3.5: Morphology of *L. pentosus* KW1 and KW2 and *L. plantarum* WCFS1. Prediction of cell morphology analyzed by ImageJ based on fluorescence microscopy images shown in figure 3.4. The prediction of shape was analyzed based on 452 bacterial cells of KW1, 732 of KW2, and 395 of WCFS1.

3.4 Plasmid design

After confirming that the pSIP gene expression system is functional and strictly regulated *L. pentosus* KW1 and KW2 (section 3.2 and 3.3), it was investigated whether the KW1 and KW2 strains can be used for surface display of heterologous proteins. Both strains were examined for surface display of the hybrid TB antigen H56 (translational fusion of Ag85B, ESAT6, and Rv2660c) using the four main anchor domains: N- terminal transmembrane (NTTM) anchor, lipoprotein anchor, LysM anchor protein, and LPxTG anchor protein, described in more detail in section 1.4. Protein sequences of the anchor proteins used in this study were derived from the genome of *L. pentosus* KW1 and KW2, cloned into the pSIP plasmids already containing H56 antigen, and transformed into the respective bacteria. A total of eight plasmids were constructed for analysis in *L. pentosus* KW1 and KW2. The selected lipoprotein anchor was identical in both strains, therefore the same plasmid was used in both bacteria. In addition, one plasmid was constructed for intracellular localization of H56, as a negative control of secretion. This plasmid was also used in both KW1 and KW2. The rest of constructed plasmids were strain specific. All plasmids (listed in table 3.2) were checked with colony PCR and confirmed with sequencing before transforming into the *L. pentosus*.

3.4.1 Construction of anchor proteins

N-terminal transmembrane (NTTM) 0418 and 2724

Genes coding for NTTM proteins used in this study were the gene *KW1_0418* derived from *L. pentosus* KW1, and the gene *KW2_2724* from *L. pentosus* KW2. The total lengths of native proteins are 106 aa and 709 aa, respectively. SignalP was used to check for signal peptide cleavage sites, and none was predicted for either KW1_0418 or KW2_2724, which was as expected (see section 1.4 for more details). SignalP annotated KW1_0418 as a hypothetical protein, and KW2_2724 protein was annotated as a penicillin-binding protein. The Phobious database was used to predict the localization of the proteins across the membrane and cell wall. Results from analyses with SignalP and Phoboius, as well as protein sequences, are shown in the supplementary material of this thesis (table A1, figures A3 to A6). It was predicted that NTTM from *L. pentosus* KW1 has a transmembrane helix from the 22nd to the 34th amino acids. The N-terminal transmembrane helix of KW2_2724 was predicted to be located from the 44th to 62nd amino acids.

For the construction of NTTM anchors, it was chosen to select 52 aa from the end of the helix of the native proteins, resulting in lengths of 87 aa and 114 aa. Amino acid sequences of the native proteins with indicated anchor motifs are shown in the supplementary material (table A1). Restriction enzyme sites were added during the PCR amplification at the start (*Nde*I) and the end (*Sal*I) of the chosen sequences. During the PCR a linker sequence (GTI-AAVD) designed by Fredriksen et al. (2012) was also added between the anchor motif and *Sal*I restriction site. Fusion of the designed anchors to the backbone harboring H56 antigen sequence resulted in pSIP_KW1_NTTM-0418_H56 and pSIP_KW2_NTTM-2724_H56 plasmids (table 3.2). Figure 3.6 illustrates a standard recombinant protein consisting of NTTM anchor and antigen.

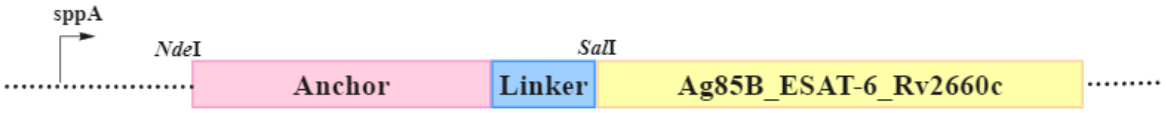

Figure 3.6: Schematic overview of the expression cassette for a typical recombinant protein. The standard recombinant protein constructed in this study is composed of an anchor motif (*pink*), derived from the genome of *L. pentosus* KW1 and KW2, fused to Ag85B, ESAT6, and Rv2660c (H56) antigens (*yellow*). Restriction sites for *Nde*I and *Sal*I were added right before the start of the anchor motif and right before the antigen. Also, a linker sequence (*blue*) was added between NTTM anchors and the antigens.

Lipoprotein 0478

Selected lipoproteins have identical sequences in both *L. pentosus* KW1 and KW2. Therefore only one gene coding for lipoprotein (*KW1_0478*) was selected for use in both *L. pentosus* KW1 and KW2. Based on a search with amino acids sequence in the BLAST database, it seems

like the KW1_0478 protein is common among *L. pentosus* and *L. plantarum* strains. However, sequence identity was between 50-60% for *L. plantarum* strains, while it was over 96% for *L. pentosus*. The signal peptide part of the protein showed an alignment with 100% identity in several strains., indicating a high level of conservation. The whole native protein is 308 amino acids long. Using the SignalP database, it was predicted that the signal peptide (SPaseII) cleavage site is between 17th and 18th amino acids in the sequence (figure A2 in supplementary).

To construct pSIP_KW1-2_Lipo-0478_H56 (table 3.2), the same strategy as for NTTM was used (figure 3.6). It was chosen to start from the start codon of the native protein and select a sequence of 52 amino acids, as indicated in table A1 in the supplementary material. A linker sequence (GTIAAVD) was added between the protein and antigens for increased flexibility (Fredriksen et al., 2012). Besides the linker sequence, restriction sites were also added to the sequences. *Nde*I restriction sites were added at the beginning of the anchor protein motifs, and *Sal*I restriction sites were added at the end.

LysM 1485 and 1392 proteins

The genes *KW1_1485* and *KW2_1392* coding for LysM proteins in *L. pentosus* KW1 (KW1_1485) and KW2 (KW2_1392) were chosen as anchors. Protein sequences were analyzed through BLAST and SignalP databases. KW1_1485 has a total length of 225 aa, and it was recognized as LysM domain-containing protein by BLAST. It is found among several *Lactiplantibacillus* species with an identity above 95%, indicating that the gene is conserved. SignalP predicted signal peptide (SPaseI) cleavage site between residue positions 28 and 29. KW2_1392 is 364 aa long, most commonly found in *L. plantarum* and *L. pentosus* with high sequence identity (over 92% for *L. plantarum* and over 97% identity with *L. pentosus*), indicating that the sequence is highly conserved. The BLAST database recognizes the KW2_1392 protein as LysM domain-containing protein. The signal peptide cleavage site was predicted to be between positions 26 and 27 in the amino acid sequence.

To construct plasmids harboring LysM anchors, the whole sequence of the native genes (*KW1_1485* and *KW2_1392*) were selected. The sequences and the results from SignalP are given in the supplementary material (table A1 and figures A7 and A8). *Nde*I and *Sal*I restriction sites were added at the beginning and the end of anchor proteins, respectively.

LPxTG 1420 and 1650 proteins

For constructing LPxTG peptidoglycan anchors, *KW1_1420* and *KW2_1650* genes were chosen from *L. pentosus* KW1 and KW2, respectively. The amino acid sequences were analyzed with SignalP and TMHMM software (analyses results shown in figures A9 to A12 in the supplementary material). KW1_LPxTG-1420 was 444 amino acids long and recognized as an LPxTG cell wall anchor domain-containing protein, common among *L. pentosus* strains with high identity. On the other hand, KW2_LPxTG-1650 was 815 amino acids long and was

classified as SpaA isopeptide-forming pilin-related protein by the BLAST database. SignalP predicted signal peptide cleavage sites after positions 27 and 28, respectively, for KW1_LPxTG-1420 and KW2_LPxTG-1650. LPxTG motifs were identified as LPQTD for KW1 and LPQTS for KW2.

To construct plasmids, the H56 antigen was placed between the signal peptide and the N-terminal part of the protein (figure 3.7). The *Nde*I restriction site was added at the start of the proteins, and 30 aa downstream were taken before *Sal*I restriction sites were added to the sequences of signal peptides. To construct the cell-wall anchor part of the LPxTG anchors, 235 aa and 317 aa counting from the stop codon upstream were selected from the native proteins. *Mlu*I and *Hind*III restriction sites were added at the start and end of the cell wall anchor sequences.

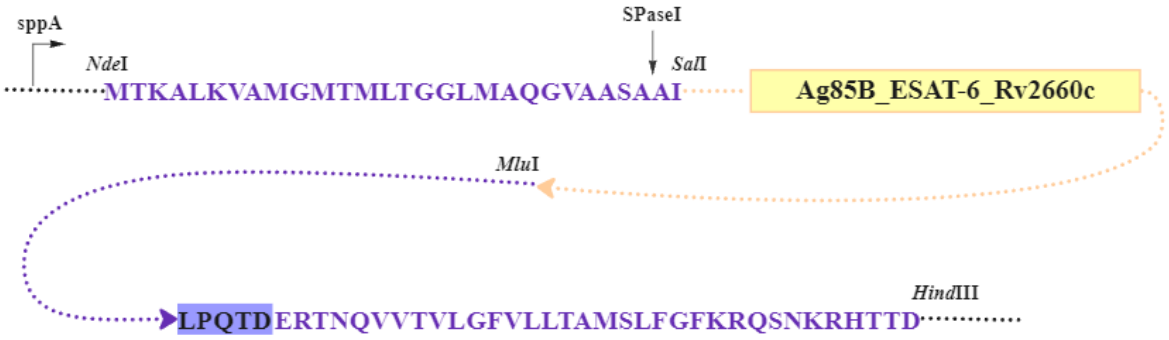

Figure 3.7: Strategy for the design of recombinant proteins harboring LPxTG anchors, shown on the example of KW1_1420. The figure illustrates the sequence of signal peptide (*purple*) with indicated cleavage site, fused to antigen (*yellow*), followed by cell wall anchor with LPQTD motif (*purple*). Restriction sites for *Nde*I and *Sal*I were added at the beginning and at the end of the signal peptide. *Mlu*I restriction site was added between the antigen and anchor sequence, while *Hind*III restriction site was added at the C-terminus of the cell wall anchor. The figure is designed inspired by Michon et al. (2016).

3.4.2 Construction of plasmids

Plasmids constructed in this study are derivatives of plasmids containing the H56 antigen, created by Trondsen (2021) and described in table 3.2. Plasmids containing NTTM, lipoprotein, and LysM protein sequences were constructed in one step. For the backbone of these plasmids, pLp1261_H56_DC (lipoprotein anchor) or pLp3014_H56_DC (LysM-motif anchor) were digested with the *Nde*I and *Sal*I restriction enzymes (figure 3.8).

NTTM, lipoprotein, and LysM protein anchors were amplified using specific primers (table 2.1, named with target gene) and the genome of *L. pentosus* KW1 and KW2 as templates. The primers have inserted restriction sites for *Nde*I and *Sal*I and 15 bp overhangs complementary to the backbone DNA for In-Fusion cloning. Amplified fragments were cloned into *Nde*I/*Sal*I digested pLp1261_H56_DC or pLp3014_H56_DC using In-Fusion cloning (section 2.13.1). Construction of the plasmids using the In-Fusion method went without challenges for KW1_NTTM, KW1-

2_Lipo, and KW2_LysM (table 3.2). For the rest of the plasmids, the In-Fusion method didn't give rise to any colonies on multiple tries. Optimization of the method was attempted by increasing the insert:vector ratio but without avail. However, when the cloning method was changed to ligation, the construction work went without major challenges. The amplified PCR fragments were digested with *Nde*I and *Sal*I and ligated into *Nde*I/*Sal*I digested plasmids. The ligation method was used for pSIP_Cyt_H56, KW1_LysM, and KW2_NTTM. A description of the plasmids and an overview of the method used for the construction is given in table 3.2.

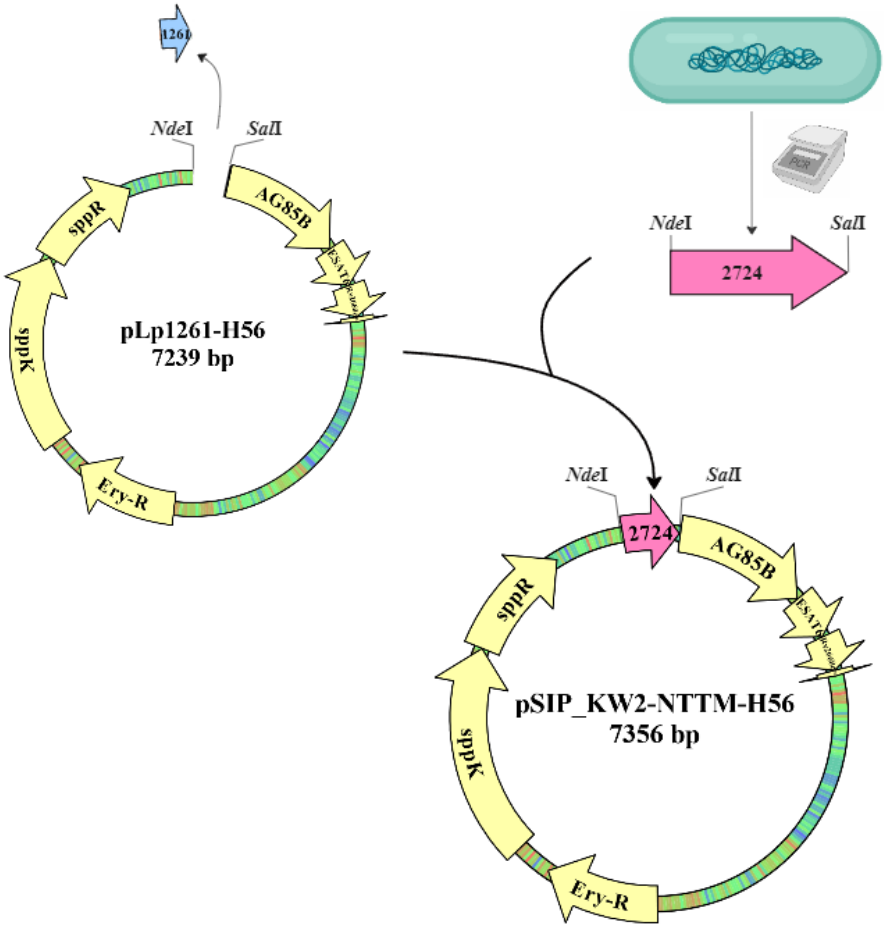

Figure 3.8: Strategy for plasmid construction of NTTM, lipoprotein, and LysM protein anchors, shown on the example of NTTM anchor. pLp1261_H56_DC (Trondsen, 2021) was used as the backbone of the plasmid and digested with *Nde*I and *Sal*I restriction enzymes. NTTM anchor protein was amplified from the genome of *L. pentosus* KW2 using In-Fusion primers. Either In-Fusion cloning protocol was followed, or alternatively, the fragment was digested with *Nde*I and *Sal*I enzymes and ligated with the digested backbone DNA. An equivalent procedure was used for the construction of NTTM, lipoprotein, and LysM-anchored proteins for use in *L. pentosus* KW1 and KW2.

Table 3.2: Plasmids used in this study.

Plasmid	Description	Source	Method
pEV	Empty vector. Derivate of pSIP401 without target genes.	Fredriksen et al., 2012	
pSIP_mCherry	mCherry protein expressed in pSIP vector.	Wiull et al., 2022	
pLp1261_H56_DC	Derivate of pSIP401 for production of Ag85B, ESAT6, and Rv2660c antigens with 1261 (lipoprotein) anchor.	Trondsen, 2021	
pLp3014_H56_DC	Derivate of pSIP401 for production of Ag85B, ESAT6, and Rv2660c antigens with 3014 (LysM) protein anchor.	Trondsen, 2021	
pLp3050_H56_cwa1643	Derivate of pSIP401 for production of Ag85B, ESAT6, and Rv2660c antigens with Lp_3050 signal peptide and Lp_1643 LPxTG anchor.	Trondsen 2021	
pSIP_Cyt_H56	Cytoplasmic localization of H56 antigen.	This work	Ligation
pSIP_KW1_NTTM-0418_H56	Derivate of pLp1261_H56_DC with 1261 gene replaced with a sequence from KW1 NTTM.	This work	In-Fusion
pSIP_KW1-2_Lipo-0478_H56	Derivate of pLp1261_H56_DC where the 1261 gene is replaced with 0478 (lipoprotein) from KW1 and KW2.	This work	In-Fusion
pSIP_KW1_LysM-1485_H56	Derivate of pLp3014_H56_DC where the 3014 gene is replaced with 1485 (LysM) from KW1.	This work	Ligation
pSIP_KW1_LPxTG-1420_H56	Derivate of pLp3050_H56_cwa1643 where signal peptide and 1643 gene are replaced with a signal peptide and LPxTG anchor from KW1.	This work	In-Fusion
pSIP_KW2_NTTM-2724_H56	Derivate of pLp3014_H56_DC with 3014 gene replaced with 2724 (NTTM) from KW2.	This work	Ligation

Table 3.2: Plasmids used in this study.

Plasmid	Description	Source	Method
pSIP_KW2_LysM-1392_H56	Derivate of pLp3014_H56_DC with 3014 gene replaced with LysM (1392) protein from KW2.	This work	In-Fusion
pSIP_KW2_LPxTG-1650_H56	Derivate of pLp3050_H56_cwa1643 where signal peptide and 1643 gene are replaced with a signal peptide and LPxTG anchor from KW2.	This work	Ligation

To construct LPxTG anchored H56 antigen, pLp3050_H56_cwa1643 (Trondsen, 2021) plasmid was used as backbone. Because of a *Sal*I restriction site within the Lp_1643 anchor, these plasmids must be constructed in two steps, as illustrated in figure 3.9. The first step was to replace the Lp_1643 anchor with cell-wall anchors derived from the genome of *L. pentosus* KW1 or KW2. The second step was to replace the original signal peptide with the signal peptide from KW1 or KW2. The cell wall anchors were PCR amplified from *L. pentosus* KW1 and KW2 using KW1_CWA-1420_F/ KW1_CWA-1420_R and KW2_CWA-1650_F / KW1_CWA-1650_R (table 2.1). The Lp_1643 anchor was removed from pLp3050_H56_cwa1643 using *Mlu*I and *Hind*III restriction enzymes. Subsequently, the two PCR-amplified anchor fragments (KW1_1420 & KW2_1650) were fused or ligated into the digested pLp3050_H56_cwa1643. This generated two intermediate plasmids consisting of the new cell wall anchors (KW1_1420 or KW2_1650) and original signal peptide (Lp_3050), illustrated on figure 3.9 (1). When these intermediate plasmids were checked and confirmed with sequencing, the signal peptides were replaced by digesting the plasmids with *Nde*I and *Sal*I and ligating new signal peptides. This yield pSIP_KW1_LPxTG-1420_H56 and pSIP_KW2_LPxTG-1650_H56.

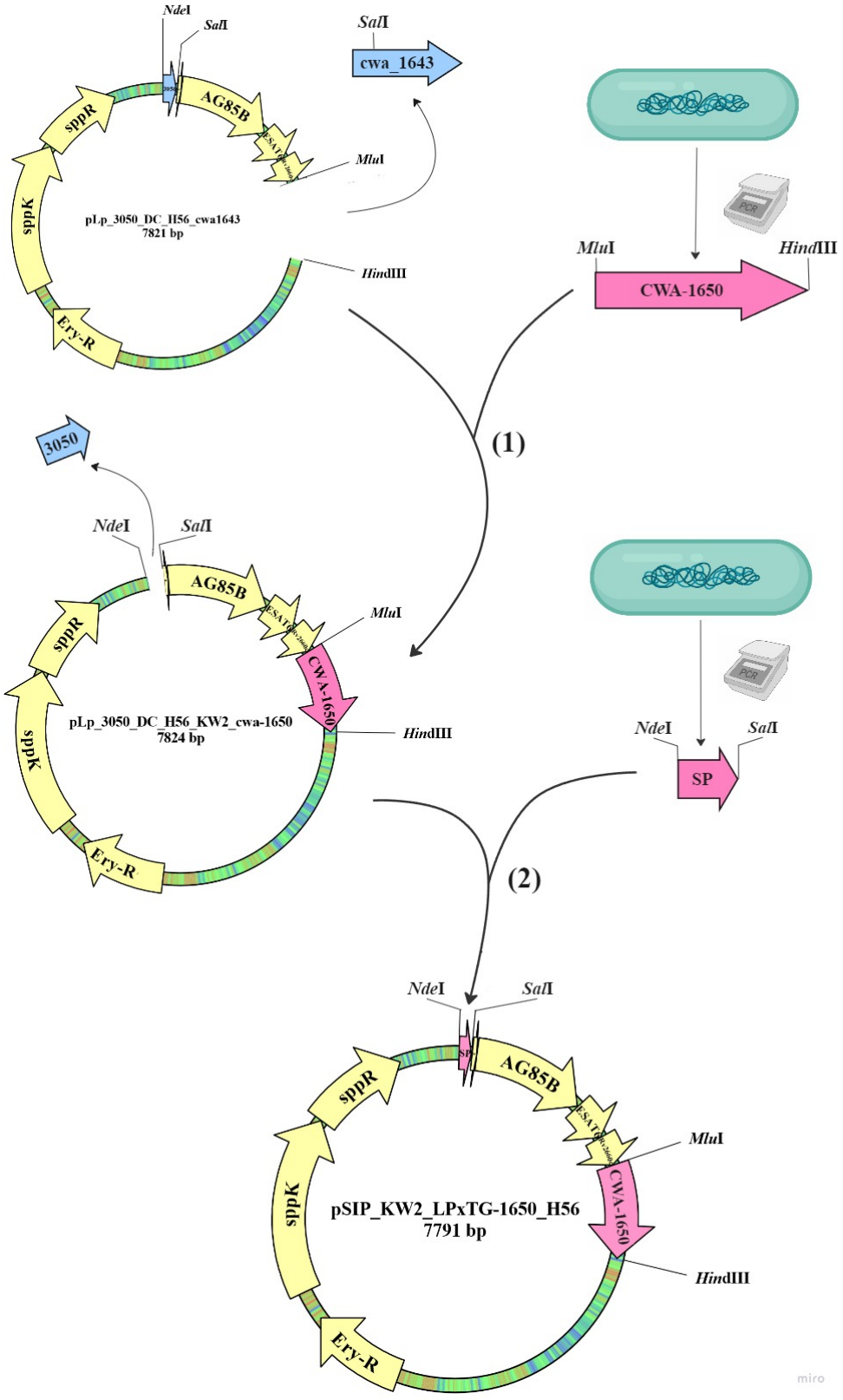

Figure 3.9: Strategy for plasmid construction of LPxTG anchor proteins, shown for *L. pentosus* KW2. The first step (1) includes digestion of the backbone plasmid with *Mlu*I and *Hind*III restriction enzymes and PCR amplification of cell wall anchors from the genome using In-Fusion primers. This results in an intermediate plasmid where only the cell wall anchor is replaced. The second step (2) is the replacement of the signal peptide with the fragment derived from the genome of *L. pentosus*. The *Nde*I/*Sal*I digested intermediate plasmid is ligated with *Nde*I/*Sal*I digested signal peptide, previously PCR amplified.

3.5 Growth curve analysis of recombinant *L. pentosus* KW1 and KW2

Growth curve analysis was used to examine the influence of H56 antigen production on the growth of recombinant *L. pentosus*. Growth rates of non-induced and induced *L. pentosus* strains harboring different anchor proteins were followed for 24 hours by measuring the absorbance (OD) at 595 nm. All samples were grown in triplicates, and the analysis was done in three parallels, giving rise to nine measurements per sample. Based on the mean value of all parallels, growth curves were plotted and visualized through figure 3.10. The growth rates of non-induced recombinant strains were similar to pEV. These growth curves were excluded from the figure 3.10, to declutter the figure. Figure 3.10 shows that growth of the NTTM anchored antigen (shown in red in the figure) was strongly reduced in both *L. pentosus* KW1 and KW2. Also, there is a noteworthy difference in the growth of KW1-LysM and KW2-LPxTG compared to empty vectors. Nevertheless, the growth curves of KW1-lipoprotein, KW1-LPxTG, KW2-lipoprotein, and KW2-LysM, seem similar to the growth of empty vectors. This analysis clearly points out that the growth rate can be influenced by the production of recombinant proteins.

The analysis compare the growth of non-induced and induced recombinant strains to the growth rate of an empty vector (pEV). The growth rates of non-induced strains were similar to pEV, and were therefore not included in the figure 3.10, but are shown in the supplementary material (figure A1).

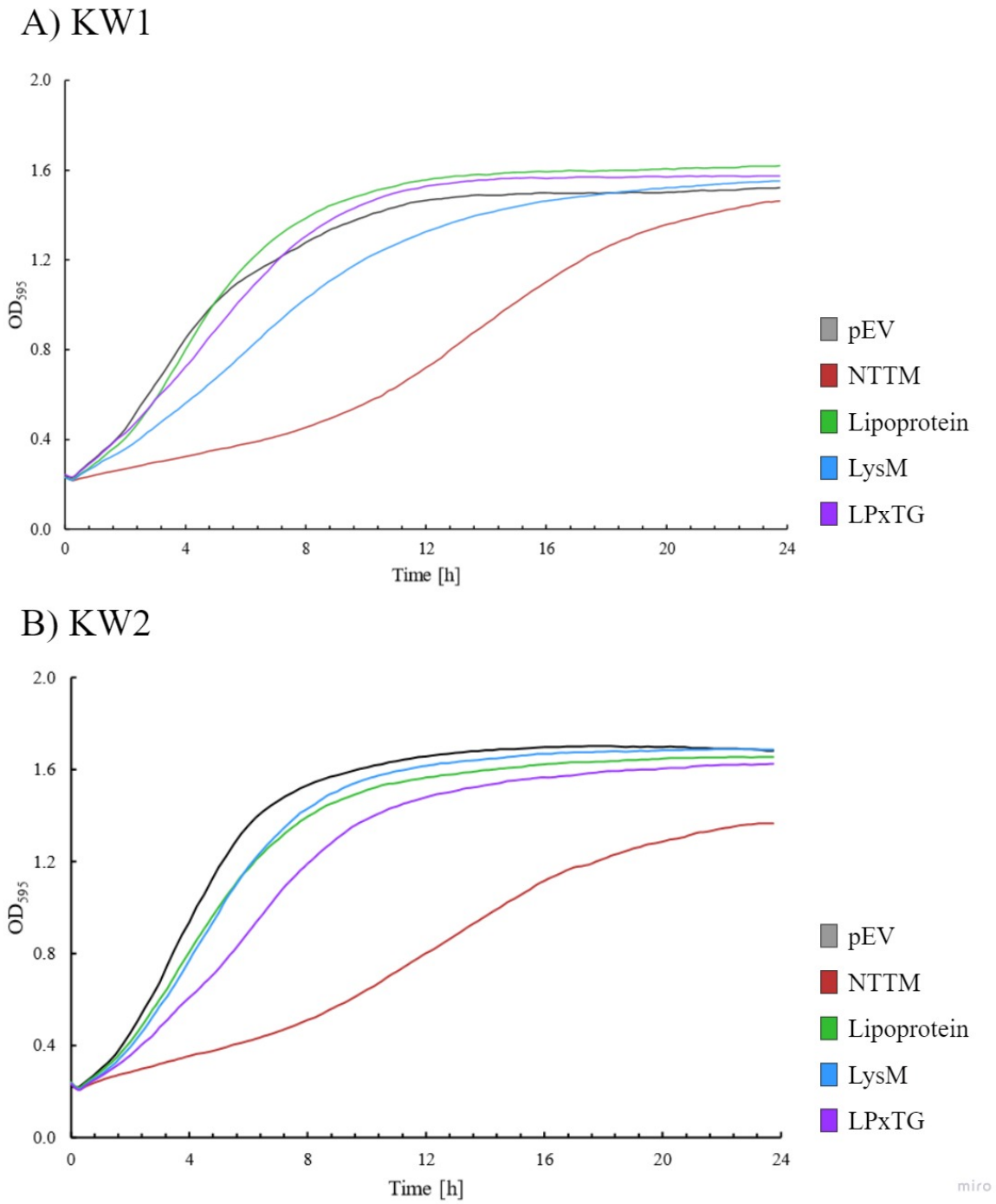

Figure 3.10: Growth curves of induced recombinant *L. pentosus* KW1 (A.) and KW2 (B.) harboring four different TB constructs and empty vector. For both KW1 and KW2, the same types of anchors are shown in the same color: NTTM (*red*), lipoprotein (*green*), LysM (*blue*), and LPxTG (*purple*). The growth curve of the induced pEV (negative control) is shown in *black* for both strains.

3.6 Detection of H56 antigen through western blot analysis

Reduction in growth for some TB constructs, analyzed in the previous section (3.5), indicates that antigen has been produced. To investigate this further, western blot analysis was utilized. The analysis was repeated three times, gaining similar results; therefore, only one parallel is presented in this thesis. *L. pentosus* KW1 and KW2 were prepared and harvested three hours after induction with SppIP inducer protein, as described in section 2.18. To analyze the heterologous protein production, a cell-free protein extract was made by lysing the bacteria (section 2.22), followed by separation of the proteins through SDS-PAGE gel electrophoresis (section 2.24.1). The concentration of the prepared protein extract was measured (sec), and the amount of all samples applied to SDS-PAGE gel (figure 3.11) was normalized to 4 µg. Although the protein concentration was normalized, the bands of KW1_NTTM anchored antigen were brighter than other bands on figure 3.11A, implying that a lower amount was applied. It was the opposite for KW2_NTTM anchored antigen, where it seems like the concentration was higher (figure 3.11B). It was possible to detect the recombinant proteins with KW1_LysM, KW1_LPxTG, and KW2_LPxTG anchored antigens on the SDS-PAGE gel (figure 3.11). This result implies that these proteins might be produced in high concentrations.

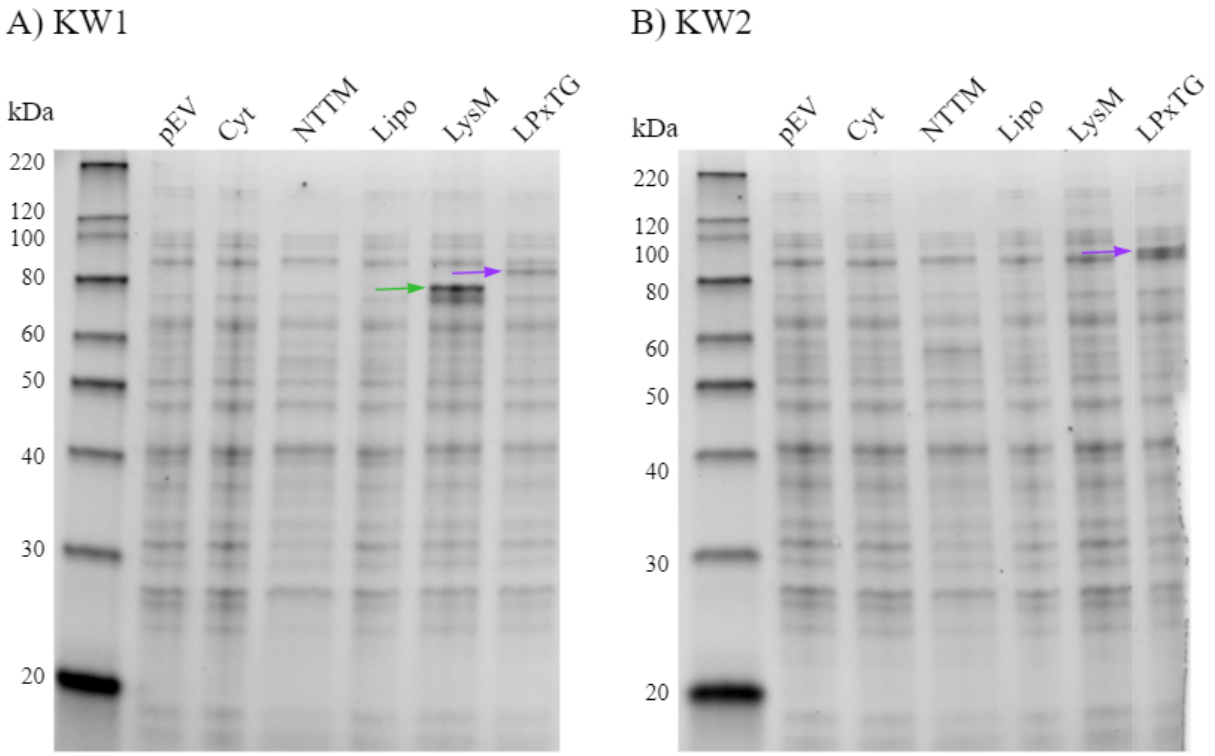

Figure 3.11: SDS-PAGE separation of recombinant proteins in *L. pentosus* KW1 (A) and KW2 (B). The amount of all samples was normalized to 2 µg. The order of samples applied on the gel is indicated in the figure. MagicMark™ XP Western Protein Standard was placed in the first wells. The detected recombinant proteins are marked with arrows.

For western blot analysis, the proteins were transferred from the SDS-PAGE gel to a nitrocellulose membrane (section 2.24.2), H56 antigens were hybridized with specific antibodies (section 2.24.3), and the proteins were detected with chemiluminescence (section 2.24.4). Figure 3.12 shows all detected bands of TB constructs except *L. pentosus* KW2 harboring LysM anchor. The expected band of KW2-LysM was exactly where the bobble was; thus, it is unclear if the band is there. Western blot analysis was repeated three times, but the quality of visualized proteins wasn't better than figure 3.12 shows. Hence, detecting KW2_LysM anchored antigen through western blotting was impossible. The weight (kDa) of all observed bands matches the theoretical weight even though the weight of KW2-LPxTG was approximately 90 kDa, which is higher than the calculated weight (77 kDa). As expected, the empty vector (pEV) showed no specific band.

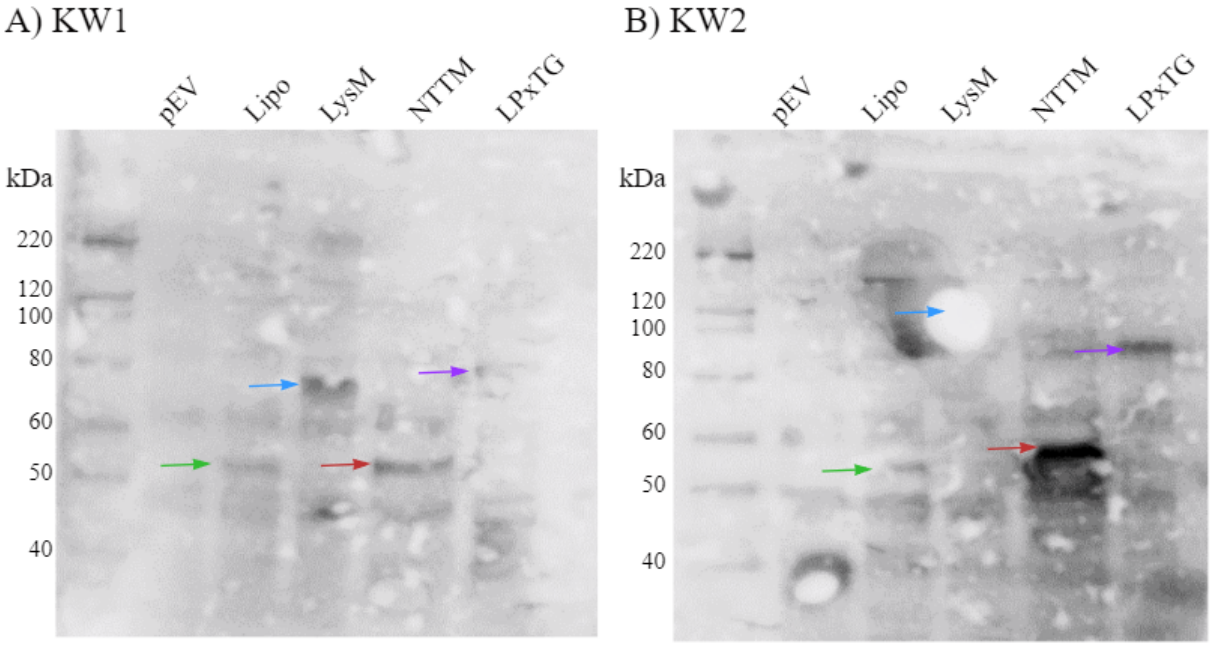

Figure 3.12: Western blot analysis of recombinant *L. pentosus* KW1 and KW2. Magic Mark XP Western Protein Standard is in the first wells of the gels (both A and B). (A) In well two is KW1 harboring empty vector, well three is KW1 carrying H56 anchored with lipoprotein, well 4 is KW1 with LysM anchored H56, well 5 is KW1 with NTTM anchored antigen, well 6 is KW1 with LPxTG anchor. (B) The order of the samples is respective to (A) only for anchors derived from KW2. Theoretical molecular weights for anchor proteins with fused H56 antigens are 57 kDa for lipoprotein in both KW1 and KW2 (identical protein), 74 kDa for KW1-LysM, 87 kDa for KW2-LysM, 60 kDa for KW1-NTTM, 50 kDa for KW2-NTTM, 78 kDa for KW1-LPxTG, and 77 kDa for KW2-LPxTG. 0.6µL(1:500-doblet) PA 0.3µL SA(1:20 000-som I protokoll)

3.7 Detection of TB antigens on the surface of recombinant *L. pentosus* KW1 and KW2

Flow cytometry analysis was used to investigate the surface display of H56 antigens on *L. pentosus* KW1 and KW2. Detection of the antigen is based on the primary antibody hybridization to

ESAT-6 antigen and attachment of secondary antibody to the primary. The secondary antibody conjugate to the FITC molecule and emits the fluorescent signal. Firstly the analysis was performed with the same primary antibody (ESAT6 Rabbit polyclonal (bs-13107R)) as for western blot analysis. The resulting chromatogram either did not show any or showed only slight shifts compared to empty vectors and cytoplasmically expressed antigens, used as negative controls (data not shown here). Optimization of analysis was attempted by increasing the concentrations of the antigens, doubling the incubation times, incubating at 25°C for hybridization instead on the laboratory bench, and changing the concentration of the BSA blocking solution. None of mentioned gave a noticeable change in the fluorescent signal. Nevertheless, it was decided to change the primary antibody to ESAT6 Mouse monoclonal (ab26246). The resulting plot gave evident shifts on the x-axis (figure 3.13), meaning there was a problem with the primary antibody. This leaves little doubt that the problem was in the three-dimensional binding of the antibody to the antigen since western blotting is based on denatured proteins, while flow cytometry analyzes live bacteria.

This study harvested and analyzed the recombinant *L. pentosus* constructs three hours after induction (see section 2.18). The protocol used for flow analysis (section 2.25) was earlier developed for use in *L. plantarum* and adapted for use in *L. pentosus*. Figure 3.13 shows flow cytometry analysis of recombinant *L. pentosus* KW1 and KW2 harboring four different constructs: NTTM, lipoprotein, LysM, and LPxTG. Empty vectors and cytoplasmically expressed antigens were used as negative controls and gave no signal (figure 3.13).

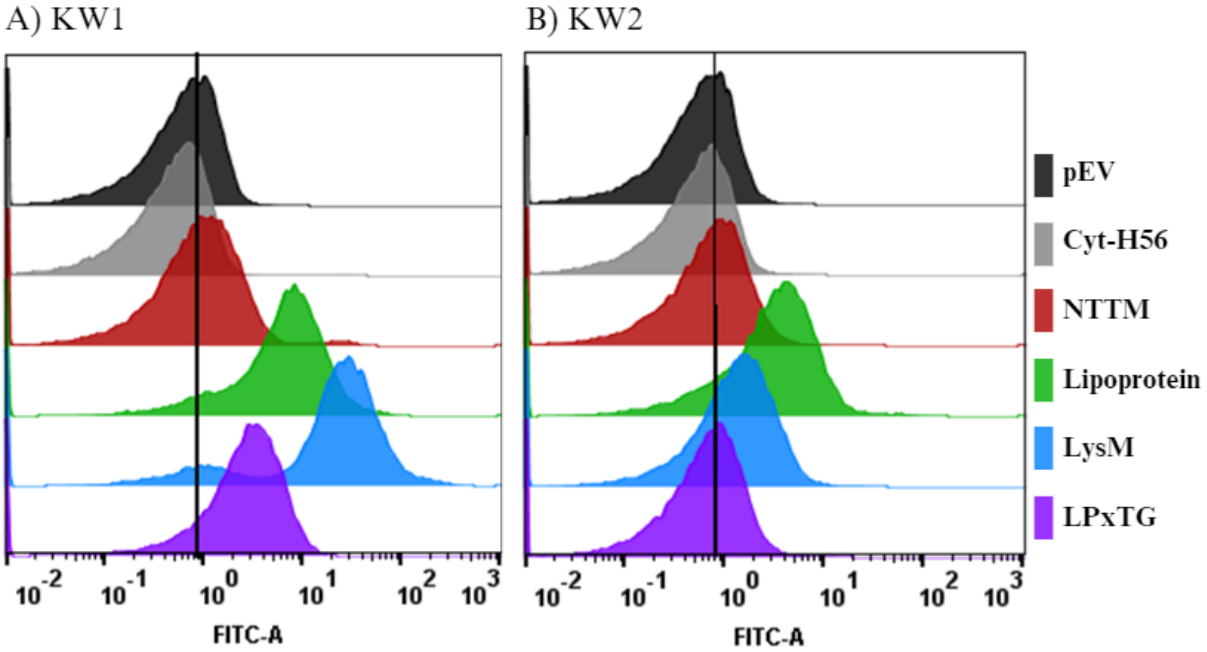

Figure 3.13: Flow cytometry analysis of recombinant *L. pentosus* KW1 and KW2 harboring different TB anchors. Analysis results for KW1 are shown on the left, and for KW2 on the right side of the figure. Empty vector (pEV) was included as a negative control. Along the x-axis fluorescence intensity (FITC) is shown.

The detected signals were generally stronger in *L. pentosus* KW1. The strongest signal of all eight recombinant strains was detected from KW1_LysM anchored H56 antigen, leaving no doubt that the antigen is exposed on the surface. Also, KW1_lipoprotein and KW1_LPxTG anchored antigens show clear shifts compared to the negative controls, implying that the surface display was successful. Somehow lower but still very clear shifts were detected from KW2_lipoprotein and KW2_LysM anchored H56, indicating surface display. The NTTM-anchored antigens show only weak fluorescent shifts in both KW1 and KW2. It could indicate that the antigens are less exposed on the surface and therefore more difficult to detect. The only recombinant strain that did not emit a detectable fluorescent signal was the strain harboring KW2_LPxTG. This firmly implies that the H56 antigen anchored with KW2_LPxTG is not exposed on the surface.

Flow cytometry proved that seven of eight antigens were located at the bacteria's surface and that novel *L. pentosus* strains can be used to expose heterologous proteins on the surface.

4 Discussion

4.1 Characterization of novel *L. pentosus* strains

In the present work, the characteristics of two novel *L. pentosus* strains, KW1 and KW2, have been studied through a series of analyses. The strains were isolated from table olives and regarded as food-grade bacteria. Previously, several *L. pentosus* strains have been isolated from various types of table olives (e.g. Romero-Gil et al., 2013; Hurtado et al., 2012; Blana et al., 2014; Montoro et al., 2016). *L. pentosus* has often been considered a potential probiotic bacteria, which is linked with positive health impact (Blana et al., 2016; Montoro et al., 2016).

During the work with *L. pentosus* KW1 and KW2, the cell pellet of KW1 was more difficult to separate from the supernatant than of KW2 due to its higher viscosity and the fact that it was not fastened to the tube. Negative staining done by a coworker at PEP (data not shown here) indicated that *L. pentosus* KW1 likely has an additional exopolysaccharide (EPS) layer around the cell. This can explain the viscosity and slime-like pellet formation of KW1 as EPS is related to biofilm and slime formation (Hidalgo-Cantabrana et al., 2012). Exopolysaccharides produced by lactic acid bacteria (LAB-EPS) play an important role in the attachment of LAB to the mucosal surfaces, enabling them to colonize the intestinal tract and preventing them from immediately being removed (Hidalgo-Cantabrana et al., 2012; Yang et al., 2023). Here, the potential of *L. pentosus* as a delivery vector of a mucosal vaccine was investigated. The vaccine must be in contact with the mucosa long enough in order to trigger an immune response. The desired immune response may not be elicited if the vaccine is quickly removed from the mucosa (REF). In addition, LAB-EPS have been associated with immunomodulatory activity, which might be positive for a vaccine candidate (Hidalgo-Cantabrana et al., 2012; Živković et al., 2016). In the *in vivo* study of Mansour et al. (2022), adding EPS to the vaccine against respiratory disease pneumonic mannheimiosis has boosted the immune response in goats (an adjuvant effect). Since tuberculosis is also a respiratory disease, an EPS-producing strain might have a booster effect for a TB mucosal vaccine. Additionally, EPS-producing microorganisms have potential applications in industry. They can be included in food products to facilitate the fermentation processes or increase the viscosity of the final product (Zannini et al., 2016). A more detailed study of EPS produced by *L. pentosus* KW1 and its role in biofilm formation is ongoing at NMBU (unpublished data).

Further, the optimal temperatures for the growth of *L. pentosus* strains were analyzed in figure 3.1. It was found that growth rates were highest in the range from 33 to 39°C, but 37°C being probably the most optimal temperature for the growth of both *L. pentosus* KW1 and KW2 (figure 3.1). However, KW2 showed slightly higher rates and lower standard deviation for all analyzed temperatures (figure 3.1). This is in line with the findings of a previous study on six *L. pentosus* strains, where the ideal growth temperatures were found to be between 34.7 and

37.1°C. The study examined cardinal temperatures and determined the optimum temperatures using a statistical model (Romero-Gil et al., 2013).

The growth curves of *L. pentosus* KW1 and KW2 were positioned on top of one another due to the strains' similar growth rates (figure 3.2). Given that the strains are closely related, this was expected. but it is a little unexpected because the traits of the strains that have been characterized vary between them.

In addition, the morphology of *L. pentosus* KW1 and KW2 was compared to *L. plantarum* WCFS1, which is one of the most extensively studied *Lactiplantibacilli* (van den Nieuwboer et al., 2016; Siezen & van Hylckama Vlieg, 2011). Based on fluorescence microscopy, it was found that *L. pentosus* KW1 and KW2 are morphologically identical to each other but about 20% more elongated compared to *L. plantarum* WCFS1 (figure 3.4 and figure 3.5). Because some of the *L. pentosus* KW1 cells were not red in color, microscopy images demonstrate that not all cells were induced (figure 3.4B). One explanation for this could be possible mutations in the PsppA promoter (see section 1.2.1 for details), which would inhibit the inducer protein from activating the system. Throughout the cell divisions of the mutant cell, a micro population of non-induced bacteria would be created. Additionally, the number of cells counted and analyzed by ImageJ for the KW1 and WCFS1 cultures was similar (452 and 395, respectively), whereas the KW2 culture had a higher number (732). As mentioned in section 3.3, the volumes of KW1 and KW2 cultures were doubled. Therefore, it seems like KW1 has a lower cell number at the same optical density than the other strains. To define the morphology of analyzed strains, the analysis should be repeated on a larger sample size. Furthermore, figure 3.5 visualizes the predictions of bacterial cell morphology. The thicker line displays an area that is more difficult to predict because of greater variation among analyzed bacteria. Since the predicted shape is the thickest for L. pentosus KW1, it indicates more variation between bacteria taken in analysis and, therefore, is more difficult to predict their morphology.

Interestingly, the protein production analysis (figure 3.3) showed that *L. pentosus* KW1 produced more protein per bacterial cell than KW2, though the induction factors were similar (table 3.1). The protein production of the non-induced pSIP system (leakage) was just slightly higher than the wild type. A possible explanation could be that the measured RFU of non-induced strains was a reflection of the wells harboring induced strains because the measurements were performed in the same microtiter plate. However, this was taken into account, and a gap was left between the non-induced and induced samples. Consequently, it indicates that the fluorescent signal observed in non-induced strains was caused by minimal real leakage. Table 3.1 shows that *L. pentosus* KW1 and KW2 produced about 22 and 21 times more mCherry protein per bacterial cell than non-induced. This was slightly lower than the induction factor of 25-fold observed in *L. plantarum* using the pSIP system for heterologous protein production Mathiesen et al. (2004). Also, the study by Sørvig et al. (2003) tested the pSIP system in several strains and compared it to the NICE system. The study found that induction factors for recombinant *L. plantarum* and

Latilactobacillus sakei ranged from 7 to 32, and high leakage was a problem for some strains. Compared to these studies and based on the results of the present study, it was concluded that the pSIP system works effectively and is strictly regulated in both *L. pentosus* KW1 and KW2, implying that it can be used for controlled heterologous protein production (figure 3.3, table 3.1). This was a very interesting finding because Karlskås et al. (2014) tested the pSIP system for use in several LAB species and concluded that the system did not work in *L. pentosus*.

Furthermore, based on figure 3.3 the optimum temperature for protein production was unclear. Both strains appear to produce the most at 37°C, however, with a higher standard deviation than for other temperatures (see error bars in figure 3.3). Although the optimum production temperature should be investigated further, for the purpose of this study and for practical reasons, it was concluded that 37°C is the best temperature for growth and production for KW1 and KW2.

4.2 Plasmid construction

The PEP group has studied *L. plantarum* for antigen delivery for several years with great promises for further vaccine development (e.g. Mathiesen et al., 2009, 2008; Kuczkowska et al., 2015, 2017). However, the goal for the group was to isolate their own strains and have no restrictions for further application (Parashar, 2017).

Therefore, in this study, the ability of strains to surface display recombinant proteins was investigated by comparing four main anchoring strategies. A review paper by Michon et al. (2016) highlighted that the type of anchor protein affects surface localization and the degree of exposure of the target protein on the bacterial surface. After it was confirmed that the pSIP system is functional in *L. pentosus* KW1 and KW2 (section 3.2), four different anchor sequences were chosen from the genomes of *L. pentosus* KW1 and KW2; thus, eight plasmids were constructed.

Prior to the plasmid construction, an *in silico* analysis of potential anchor proteins was performed, as described in section 3.4.1. These anchor proteins bind to the bacterial surface at different positions through either covalent (lipoprotein and LPxTG) or non-covalent (NTTM and LysM) interactions (Michon et al., 2016). A general strategy for designing recombinant proteins was to select part of the anchor sequence, which is important for the surface attachment, and translationally fuse it to a hybrid tuberculosis antigen. This resulted in eight recombinant proteins, each consisting of two parts: anchor and antigen. Based on *in silico* analysis, the transmembrane helixes of NTTM anchor proteins were predicted and selected. It was important to ensure that the transmembrane helixes were included in the anchor sequence because otherwise, the proteins would not be secreted out of the cell (Michon et al., 2016). For the construction of anchor proteins with signal peptides (lipoprotein, LysM, and LPxTG), it was essential to ensure that the whole signal peptide was selected in order for the protein to be secreted through the cell membrane (figure 1.4). Therefore, the strategy for the construction of a lipoprotein anchor

was to select the signal peptide and ensure that the protein has enough length to expose the antigen on the cell membrane. Based on previous studies (e.g. Michon et al., 2016; Zadravec et al., 2014), the sequence was shortened because shorter lipoprotein anchors may increase the exposure on the bacterial surface. Interestingly, the genomes of *L. pentosus* KW1 and KW2 contain lipoproteins with identical sequences. The lipoproteins with the same sequence were selected to compare whether and how the use of different strains influences protein production and secretion. Therefore only one plasmid with lipoprotein needed to be constructed for both strains. The fact that two bacteria strains share the same gene is not strange since *L. pentosus* KW1 and KW2 were isolated from a common source and were naturally living in the same environment, which gives them a possibility for horizontal gene transfer. Another possibility, of course, is that the gene evolved from a common ancestor since the strains belong to the same genus and are closely related. Further, for the construction of LysM anchors, the whole genes were selected. This was done because LysM proteins differ in the number of LysM motifs required for maximal binding to the cell wall; one protein can have several LysM motifs, and the motifs are not well conserved, making it difficult to predict them (Visweswaran et al., 2014; Buist et al., 2008). Here, the LysM proteins were predicted to have only one LysM motif. Lastly, the most important aspect of the peptidoglycan anchors construction was to include the transmembrane helix and, of course, the LPxTG motif (Michon et al., 2016). Since the distance from the transmembrane helix to the LPxTG motif differs in various proteins, it results in different anchor lengths for KW1_LPxTG and KW2_LPxTG.

All selected anchor protein motifs (sequences shown in table A1 in supplementary material) were cloned into pSIP vectors that already contained *M. tuberculosis*-derived antigens in order to achieve surface display (Trondsen, 2021). This way, the anchors were translationally fused to the H56 antigens (Ag85B, ESAT6, and Rv2660c). Seven plasmids, harboring different anchors and pSIP_Cyt_H56 (table 3.2), were constructed without major challenges. The only exception was the signal peptide part of the KW1_LPxTG plasmid. It took several attempts to clone the signal peptide into the plasmid. The reason for it might be that the fragment was very short (only about 90 bp), making it possible that the religation of the backbone vector could occur more easily.

4.3 Growth of recombinant *L. pentosus*

The growth of almost all recombinant *L. pentosus* KW1 and KW2 showed a slight to heavy reduction compared to pEV (figure 3.10). The growth of the strains harboring empty vectors (figure 3.10) was similar to the growth rates of wild type strains (figure 3.2) and to non-induced cultures (data shown in supplementary material). It was clearly shown that protein production affects growth since the reduction in growth occurred only when the SppIP inducer was added to the cultures. This is also supported by previous studies, especially for cultures harboring LPxTG anchors (e.g. Berggreen, 2020; Fredriksen et al., 2010; Kuczkowska et al., 2015; Lulko et al.,

2007). However, in this study, the growth of KW1_LPxTG was even better than KW1 harboring the empty vector. In contrast, figure 3.10 shows that the growth of KW2_LPxTG was just slightly reduced. Reduction in the growth of recombinant bacteria is caused by overexpression of the heterologous protein, which has been observed earlier (Mathiesen et al., 2020). One hypothesis is that when the pSIP system is activated, bacteria produce recombinant proteins in high amounts, which is achieved by slowing down cell division and other processes. Also, it could be possible that the Sec pathway is unable to translocate proteins as quickly as they are synthesized, which would accumulate protein inside the cell and repress the normal function of the cell. This would probably be possible to test by modifying bacteria to upregulate genes involved in the Sec pathway (Anné et al., 2017).

4.4 Detection of the H56 antigen through Western blot analysis

For further characterization of antigen production, Western blot and flow cytometry analyses were performed. It was possible to detect heterologous proteins from *L. pentosus* KW1 harboring LysM and LPxTG anchor and *L. pentosus* KW2 harboring LPxTG anchor already on the SDS-PAGE gel (figure 3.11). This is interesting because the proteins have to be produced in high amounts to be visible on SDS-PAGE gel. It is especially intriguing for KW1_LPxTG anchored antigen because of its growth rate, which is similar to KW1_pEV (figure 3.10). This suggests that the prediction of the signal peptide was correct, that the optimal combination of signal peptide and cell wall anchor was utilized, and that the pSIP system and secretion machinery work optimally. pSIP_KW1_LysM and pSIP_KW2_LPxTG were the second most reduced constructs in *L. pentosus* KW1 and KW2, respectively. It is not surprising that reduced bacterial growth can be influenced by high protein production. As discussed in section 4.3, growth reduction influenced by overexpression of the recombinant protein, especially for the strains with LPxTG anchors, has been reported in several studies (Berggreen, 2020; Fredriksen et al., 2010; Kuczkowska et al., 2015; Lulko et al., 2007). All proteins were detected by Western blot except KW2-LysM. The Western blot analysis was repeated several times in an attempt to optimize the method, but all blots were similar to the one presented in figure 3.12. The growth curve of pSIP_KW2_LysM was slightly reduced (section 3.5 and figure 3.10), hence it is expected that the antigen will be produced in a high amount.

4.5 Detection of the H56 antigen on the surface of *L. pentosus*

Although Western blotting confirmed that the recombinant proteins (except KW1_LysM) had been produced, it was still unknown if the antigens actually were displayed on the surface of *L. pentosus* KW1 and KW2. In contrast to Western blot, flow cytometry is based on the detection of surface-exposed antigens in live bacteria. During early flow cytometry analyses, none

or extremely weak signals were observed from recombinant *L. pentosus* KW1 and KW2 (figure A14 in supplementary material). For investigation of KW2, *L. plantarum* WCFS1 harboring pLp3014_H56_DC (Trondsen, 2021) was included as a positive control. The fluorescent shift of the positive control was lower than formerly observed by Trondsen (2021). The protocol for the current study was adopted from Trondsen (2021) (section 2.25), but a different primary antibody was used. Therefore and because denatured recombinant proteins were successfully detected (figure 3.12), it was assumed that there was an issue with the primary antibody's three-dimensional binding to the antigen. In addition, the producer of the ESAT6 Rabbit polyclonal (bs-13107R) antibody did not state that the antibody is compatible for use in flow cytometry analysis.

After changing the antibody, greater shifts in fluorescence signal were observed. Flow cytometry analysis (figure 3.13) showed detectable signals for antigens anchored with NTTM, lipoproteins, LysM, and LPxTG (last named only for *L. pentosus* KW1). The greater shifts seemed to be similar or even better than similar studies of *L. plantarum* WCFS1 observed (Wiull et al., 2022; Trondsen, 2021). Antigens anchored with N-terminal transmembrane (NTTM) anchors showed extremely weak shifts in fluorescence signals in *L. pentosus* KW1 and KW2. The reason might be that the location of the anchor protein can affect the strength of the signal. NTTM-anchored antigens are less exposed at the surface and more embedded in the cell membrane (Michon et al., 2016). This suggests that although it is difficult to detect these proteins, they might still be on the surface. There is no doubt that the antigens anchored with the NTTM proteins had been produced. The growth curve analyses showed strong growth reduction and the antigens were detected through Western blotting for both strains. The cells of NTTM-anchored strains could be treated with lysozyme, an enzyme that hydrolyses glycosidic bonds of peptidoglycan. By disrupting the cell wall formation, it would be possible to analyze the antigen exposure on the surface further. Since the long-term goal of this project was to develop a mucosal vaccine, it might be beneficial to have antigens less exposed to hydrolytic enzymes such as proteases and lysozymes. For a vaccine, the administration route is also important. If the vaccine should be given nasal, it might be better to have the antigen more exposed on the surface. However, if the vaccine is given orally, more embedded localization, resulting in less exposure would be favorable because of higher catalytic activity in the mouth and through the GIT. Otherwise, there is a risk the antigens would be degraded before they get a chance to interact with an immune system. Hence, *in vivo* studies are needed to investigate this hypothesis.

Although it is not completely clear if KW2_NTTM anchored antigens show very weak signals or no signal at all, it is evident that LPxTG anchored antigen in *L. pentosus* KW2 does not show any signal in flow cytometry analysis (figure 3.13). The recombinant protein with KW2_LPxTG anchor was detected through Western blot analysis (figure 3.12), and even on SDS-PAGE gel (figure 3.11). The growth of recombinant *L. pentosus* KW2 carrying the pSIP_KW2_LPxTG-1650_H56 was only slightly reduced (figure 3.10). Based on these analyses, it is evident that

recombinant protein has been produced in high concentrations. This implies that proteins have not been exported through the membrane, suggesting that the choice of signal peptide might be wrong. The choice of signal peptide was based on analysis through bioinformatical tools (SignalP) that are only a prediction and could be inaccurate. However, the same issue was not observed for *L. pentosus* KW1. In the study done by Mathiesen et al. (2009), several signal peptides were tested for use in *L. plantarum*, where 62 of 76 tested signal peptides successfully transported the target protein out of the cell. Tjåland (2011) tested 11 signal peptides using the same cell-wall anchor protein, resulting in the secretion of all recombinant proteins, but with differences in efficiency. On the other hand, the study by Berggreen (2020) compared the use of seven different cell-wall LPxTG anchors using the same signal peptide. The study showed strongly reduced growth of all recombinant *L. plantarum* with different cell wall anchors. This finding is supported by other studies (e.g. **?**Kuczkowska et al., 2017). It is assumed that there was a problem with the signal peptide. Therefore it is believed that changing the signal peptide will help in surface anchoring of the antigen. Interestingly, LPxTG anchored antigen expressed in *L. pentosus* KW1 did not reduce the growth (figure 3.10). Hence, it could be interesting to test if the signal peptide from KW1_1420 would work for expressing the KW2_1650 cell wall anchor in *L. pentosus* KW2. LPxTG anchored antigen expressed in *L. pentosus* KW1 shows a clear signal (figure 3.13), although it was weaker than for lipoprotein and LysM.

Both lipoprotein and LysM anchored proteins show strong signals in flow cytometry analysis (figure 3.13), confirming that antigens were displayed at the surface of both *L. pentosus* strains. However, the signals were stronger in *L. pentosus* KW1, and even stronger than what previously was observed in *L. plantatum* (Mathiesen et al., 2020; Wiull et al., 2022).

Further studies could test if the signal peptide from KW1_LPxTG would work in KW2 or replace the anchor protein with another LPxTG protein from the KW2 genome. However, it is strange if the signal peptide from KW1 would be better than that from KW2's own genome.

Although it was concluded that NTTM-anchored proteins were exposed on the surface, their fluorescent shifts in flow cytometry analysis were very weak. Thus, the strains with NTTM-anchored antigens should be further investigated to be completely sure that antigens are exposed on the surface. This could be achieved by disrupting cell wall synthesis with lysozymes and repeating the flow cytometry analysis. Such enzymatic treatment would, to some degree, mimic exposure to catalytic enzymes, like lysozymes and proteases, which occur naturally in humans.

4.6 Conclusions and future prospects

In conclusion, the two novel *L. pentosus* strains, KW1 and KW2, grew at similar rates and produced mCherry in high concentrations. The pSIP gene expression system was functional and strictly regulated in both strains. The capability of *L. pentosus* KW1 and KW2 to surface display hybrid tuberculosis antigen H56 (Ag85B, ESAT-6, and Rv2660c) was explored using

four anchor proteins selected from the genomes of KW1 and KW2. The analysis showed that the type of anchor affects the growth of the recombinant strain. Production of all recombinant proteins was confirmed, and seven of eight were exposed at the bacterial surface. The best fluorescent signals were obtained from antigens anchored with lipoproteins and LysM-anchors.

L. pentosus KW1 produced more mCherry protein, exhibited a higher induction factor, and gave stronger signals in flow cytometry than KW2. In addition, *L. pentosus* KW1 has an EPS layer, which could act as a vaccine adjuvant. The present study was part of a larger project with the long-term goal of developing a LAB-based mucosal vaccine. Because of its better performance throughout the whole study, *L. pentosus* KW1 seems to be a better choice as a production strain.

All protocols used in this study were adopted from *L. plantarum*. Thus, it should be tested to see if optimization of the protocols is needed. *In vivo* studies are needed to investigate the correlation between anchor type, acquired immune responses, and administration route. The hypothesis is that the oral administration route might generate better immune responses for less exposed antigens, such as NTTM-anchored ones, due to higher catalytic activity. More exposed antigens, like lipoprotein- and LysM-anchored ones, might be a better choice for nasal administration. Further, potential vaccine adjuvant effects, as well as possible probiotic properties of the *L. pentosus* strains, should be studied *in vivo*.

Furthermore, if one recombinant strain were to be used in vaccine development, a big issue would be the erythromycin resistance gene expressed in all plasmids. Because of the increasing global problem of antibiotic resistance, the use of antibiotics should be minimized. The erythromycin resistance gene was included in the plasmids to minimize the risk of culture contamination. Consequently, removing the erythromycin resistance gene would require strict protocols for vaccine manufacturing to prevent contamination. However, it has been shown that the removal of the erythromycin gene can even be beneficial for bacterial growth (Nguyen et al., 2011).

To sum up, it seems like the novel *L. pentosus* KW1 is a promising candidate to replace or supplement the more well-studied *L. plantarum* in the development of delivery vehicles for heterologous proteins.

References

Aagaard, C., Hoang, T., Dietrich, J., Cardona, P.-J., Izzo, A., Dolganov, G., Schoolnik, G. K., Cassidy, J. P., Billeskov, R., & Andersen, P. (2011). A multistage tuberculosis vaccine that confers efficient protection before and after exposure. Nature medicine, 17(2), 189–194. https://doi.org/10.1038/nm.2285

Anné, J., Economou, A., & Bernaerts, K. (2017). Protein secretion in gram-positive bacteria: from multiple pathways to biotechnology. Protein and sugar export and assembly in gram-positive bacteria, 267–308. https://doi.org/10.1007/82_2016_49

Aukrust, T. W., Brurberg, M. B., & Nes, I. F. (1995). Transformation of lactobacillus by electroporation. Electroporation protocols for microorganisms, 201–208. https://doi.org/10.1385/0-89603-310-4:201

Babu, M. M., Priya, M. L., Selvan, A. T., Madera, M., Gough, J., Aravind, L., & Sankaran, K. (2006). A database of bacterial lipoproteins (dolop) with functional assignments to predicted lipoproteins. Journal of bacteriology, 188(8), 2761–2773. https://doi.org/10.6026/97320630001130

Berggreen, H. (2020). Cell wall anchoring of *Mycobacterium tuberculosis* antigens to the surface of *Lactobacillus plantarum*. Norwegian University of Life Sciences. https://nmbu.brage.unit.no/nmbu-xmlui/handle/11250/2673171

Blana, V. A., Grounta, A., Tassou, C. C., Nychas, G.-J. E., & Panagou, E. Z. (2014). Inoculated fermentation of green olives with potential probiotic lactobacillus pentosus and lactobacillus plantarum starter cultures isolated from industrially fermented olives. Food microbiology, 38, 208–218. https://doi.org/10.1016/j.fm.2013.09.007

Blana, V. A., Polymeneas, N., Tassou, C. C., & Panagou, E. Z. (2016). Survival of potential probiotic lactic acid bacteria on fermented green table olives during packaging in polyethylene pouches at 4 and 20 c. Food microbiology, 53, 71–75. https://doi.org/10.1016/j.fm.2015.09.004

Buist, G., Steen, A., Kok, J., & Kuipers, O. P. (2008). Lysm, a widely distributed protein motif for binding to (peptido) glycans. Molecular microbiology, 68(4), 838–847. https://doi.org/10.1111/j.1365-2958.2008.06211.x

Charbit, A., Boulain, J. C., Ryter, A., & Hofnung, M. (1986). Probing the topology of a bacterial membrane protein by genetic insertion of a foreign epitope; expression at the cell surface. The EMBO journal, 5(11), 3029–3037. https://doi.org/10.1002/j.1460-2075.1986.tb04602.x

Daniel, C., Roussel, Y., Kleerebezem, M., & Pot, B. (2011). Recombinant lactic acid bacteria as mucosal biotherapeutic agents. Trends in Biotechnology, 29(10), 499–508. https://doi.org/https://doi.org/10.1016/j.tibtech.2011.05.002

Driessen, A. J. & Nouwen, N. (2008). Protein translocation across the bacterial cytoplasmic membrane. Annu. Rev. Biochem., 77, 643–667. https://doi.org/10.1146/annurev.biochem.77.061606.160747

FAO/WHO (2001). Health and nutritional properties of probiotics in food including powder milk with live lactic acid bacteria.

Fogel, N. (2015). Tuberculosis: a disease without boundaries. Tuberculosis, 95(5), 527–531. https://doi.org/10.1016/j.tube.2015.05.017

Foley, J. (2015). Mini-review: strategies for variation and evolution of bacterial antigens. Computational and structural biotechnology journal, 13, 407–416. https://doi.org/10.1016/j.csbj.2015.07.002

Fredriksen, L., Kleiveland, C. R., Hult, L. T. O., Lea, T., Nygaard, C. S., Eijsink, V. G. H., & Mathiesen, G. (2012). Surface display of n-terminally anchored invasin by lactobacillus plantarum activates NF-κb in monocytes. Applied and Environmental Microbiology, 78(16), 5864–5871. https://doi.org/10.1128/aem.01227-12

Fredriksen, L., Mathiesen, G., Sioud, M., & Eijsink, V. G. (2010). Cell wall anchoring of the 37-kilodalton oncofetal antigen by lactobacillus plantarum for mucosal cancer vaccine delivery. Applied and environmental microbiology, 76(21), 7359–7362. https://doi.org/10.1128/AEM.01031-10

Gu, M., Cho, J.-H., Suh, J.-W., & Cheng, J. (2023). Potential oral probiotic lactobacillus pentosus mjm60383 inhibits streptococcus mutans biofilm formation by inhibiting sucrose decomposition. Journal of Oral Microbiology, 15(1), 2161179. https://doi.org/10.1080/20002297.2022.2161179

Hidalgo-Cantabrana, C., López, P., Gueimonde, M., de Los Reyes-Gavilán, C. G., Suárez, A., Margolles, A., & Ruas-Madiedo, P. (2012). Immune modulation capability of exopolysaccharides synthesised by lactic acid bacteria and bifidobacteria. Probiotics and Antimicrobial Proteins, 4, 227–237. https://doi.org/10.1007/s12602-012-9110-2

Hurtado, A., Reguant, C., Bordons, A., & Rozès, N. (2012). Lactic acid bacteria from fermented table olives. Food microbiology, 31(1), 1–8.

Hurtado, A., Reguant, C., Esteve-Zarzoso, B., Bordons, A., & Rozès, N. (2008). Microbial population dynamics during the processing of arbequina table olives. Food Research International, 41(7), 738–744. https://doi.org/10.1016/j.foodres.2008.05.007

Kanabalan, R. D., Lee, L. J., Lee, T. Y., Chong, P. P., Hassan, L., Ismail, R., & Chin, V. K. (2021). Human tuberculosis and mycobacterium tuberculosis complex: A review on genetic diversity, pathogenesis and omics approaches in host biomarkers discovery. Microbiological Research, 246, 126674. https://doi.org/https://doi.org/10.1016/j.micres.2020.126674

Karlskås, I. L., Maudal, K., Axelsson, L., Rud, I., Eijsink, V. G., & Mathiesen, G. (2014). Heterologous protein secretion in lactobacilli with modified psip vectors. PLOS one, 9(3), e91125. https://doi.org/10.1371/journal.pone.0091125

Kiousi, D. E., Efstathiou, C., Tzampazlis, V., Plessas, S., Panopoulou, M., Koffa, M., & Galanis, A. (2023). Genetic and phenotypic assessment of the antimicrobial activity of three potential probiotic lactobacilli against human enteropathogenic bacteria. Frontiers in Cellular and Infection Microbiology, 13, 115. https://doi.org/10.3389/fcimb.2023.1127256

Kleerebezem, M., Boekhorst, J., van Kranenburg, R., Molenaar, D., Kuipers, O., Leer, R., Tarchini, R., Peters, S., Sandbrink, H., Fiers, M., et al. (2003). Complete genome sequence of lactobacillus plantarum wcfs1. Proceedings of the National Academy of Sciences of the United States of America, 100(4), 1990–1995.

Kleerebezem, M., Hols, P., Bernard, E., Rolain, T., Zhou, M., Siezen, R. J., & Bron, P. A. (2010). The extracellular biology of the lactobacilli. FEMS microbiology reviews, 34(2), 199–230. https://doi.org/10.1111/j.1574-6976.2009.00208.x

Kuczkowska, K., Copland, A., Øverland, L., Mathiesen, G., Tran, A. C., Paul, M. J., Eijsink, V. G. H., & Reljic, R. (2019a). Inactivated lactobacillus plantarum carrying a surface-displayed ag85b-esat-6 fusion antigen as a booster vaccine against mycobacterium tuberculosis infection. Frontiers in Immunology, 10. https://doi.org/10.3389/fimmu.2019.01588

Kuczkowska, K., Kleiveland, C. R., Minic, R., Moen, L. F., Øverland, L., Tjåland, R., Carlsen, H., Lea, T., Mathiesen, G., & Eijsink, V. G. (2017). Immunogenic properties of lactobacillus plantarum producing surface-displayed mycobacterium tuberculosis antigens. Applied and environmental microbiology, 83(2), e02782–16. https://doi.org/10.1128/AEM.02782-16

Kuczkowska, K., Mathiesen, G., Eijsink, V. G., & Øynebråten, I. (2015). Lactobacillus plantarum displaying ccl3 chemokine in fusion with hiv-1 gag derived antigen causes increased recruitment of t cells. Microbial Cell Factories, 14(1), 1–12. https://doi.org/10.1186/s12934-015-0360-z

Kuczkowska, K., Øverland, L., Rocha, S. D., Eijsink, V. G., & Mathiesen, G. (2019b). Comparison of eight lactobacillus species for delivery of surface-displayed mycobacterial antigen. Vaccine, 37(43), 6371–6379. https://doi.org/10.1016/j.vaccine.2019.09.012

Kurien, B. T. & Scofield, R. H. (2015). Western blotting: an introduction. Western Blotting: Methods and Protocols, 17–30. https://doi.org/10.1007/978-1-4939-2694-7_5

Liu, Y., Liu, Q., Jiang, Y., Yang, W., Huang, H., Shi, C., Yang, G., & Wang, C. (2020). Surface-displayed porcine ifn-λ3 in lactobacillus plantarum inhibits porcine enteric coronavirus infection of porcine intestinal epithelial cells. https://doi.org/10.4014/jmb.1909.09041

Lulko, A. T., Veening, J.-W., Buist, G., Smits, W. K., Blom, E. J., Beekman, A. C., Bron, S., & Kuipers, O. P. (2007). Production and secretion stress caused by overexpression of

heterologous α-amylase leads to inhibition of sporulation and a prolonged motile phase in bacillus subtilis. Applied and environmental microbiology, 73(16), 5354–5362. https://doi.org/10.1128/AEM.00472-07

Mansour, G. H., Razzak, L. A., Suvik, A., & Wahid, M. E. A. (2022). Stimulating immunoglobulin response by intramuscular delivery of exopolysaccharides-adjuvanted mannheimiosis vaccine in goats. Veterinary World, 15(12). https://doi.org/10.14202/vetworld.2022.2945-2952

Mathiesen, G., Øverland, L., Kuczkowska, K., & Eijsink, V. G. (2020). Anchoring of heterologous proteins in multiple lactobacillus species using anchors derived from lactobacillus plantarum. Scientific Reports, 10(1), 9640. https://doi.org/10.1038/s41598-020-66531-7

Mathiesen, G., Sørvig, E., Blatny, J., Naterstad, K., Axelsson, L., & Eijsink, V. (2004). High-level gene expression in lactobacillus plantarum using a pheromone-regulated bacteriocin promoter. Letters in applied microbiology, 39(2), 137–143. https://doi.org/10.1111/j.1472-765X.2004.01551.x

Mathiesen, G., Sveen, A., Brurberg, M. B., Fredriksen, L., Axelsson, L., & Eijsink, V. G. (2009). Genome-wide analysis of signal peptide functionality in lactobacillus plantarum wcfs1. BMC genomics, 10, 1–13. https://doi.org/10.1186/1471-2164-10-425

Mathiesen, G., Sveen, A., Piard, J., Axelsson, L., & Eijsink, V. (2008). Heterologous protein secretion by Lactobacillus plantarum using homologous signal peptides. Journal of Applied Microbiology, 105(1), 215–226. https://doi.org/10.1111/j.1365-2672.2008.03734.x

McKinnon, K. M. (2018). Flow cytometry: an overview. Current protocols in immunology, 120(1), 5–1. https://doi.org/10.1002/cpim.40

Meier, N. R., Jacobsen, M., Ottenhoff, T. H., & Ritz, N. (2018). A systematic review on novel mycobacterium tuberculosis antigens and their discriminatory potential for the diagnosis of latent and active tuberculosis. Frontiers in immunology, 9, 2476. https://doi.org/10.3389/fimmu.2018.02476

Michon, C., Langella, P., Eijsink, V. G., Mathiesen, G., & Chatel, J. M. (2016). Display of recombinant proteins at the surface of lactic acid bacteria: Strategies and applications. Microbial Cell Factories, 15(1). https://doi.org/10.1186/s12934-016-0468-9

Montoro, B. P., Benomar, N., Lavilla Lerma, L., Castillo Gutiérrez, S., Gálvez, A., & Abriouel, H. (2016). Fermented aloreña table olives as a source of potential probiotic lactobacillus pentosus strains. Frontiers in microbiology, 7, 1583. https://doi.org/10.3389/fmicb.2016.01583

Moraïs, S., Shterzer, N., Grinberg, I. R., Mathiesen, G., Eijsink, V. G., Axelsson, L., Lamed, R., Bayer, E. A., & Mizrahi, I. (2013). Establishment of a simple lactobacillus plantarum cell consortium for cellulase-xylanase synergistic interactions. Applied and environmental microbiology, 79(17), 5242–5249. https://doi.org/10.1128/AEM.01211-13

Nguyen, T.-T., Mathiesen, G., Fredriksen, L., Kittl, R., Nguyen, T.-H., Eijsink, V. G., Haltrich, D., & Peterbauer, C. K. (2011). A food-grade system for inducible gene expression in lactobacillus plantarum using an alanine racemase-encoding selection marker. Journal of agricultural and food chemistry, 59(10), 5617–5624. https://doi.org/10.1021/jf104755r

Nielsen, H. (2017). Predicting secretory proteins with signalp. Protein function prediction: methods and protocols, 59–73. https://doi.org/10.1007/978-1-4939-7015-5_6

Parashar, A. (2017). International depository authority and its role in microorganism's deposition. Journal of Clinical and Diagnostic Research: JCDR, 11(8), DE01. https://doi.org/10.7860/JCDR/2017/29077.10408

Ramirez, J. E. V., Sharpe, L. A., & Peppas, N. A. (2017). Current state and challenges in developing oral vaccines. Advanced drug delivery reviews, 114, 116–131. https://doi.org/10.1016/j.addr.2017.04.008

Ravimohan, S., Kornfeld, H., Weissman, D., & Bisson, G. P. (2018). Tuberculosis and lung damage: from epidemiology to pathophysiology. European respiratory review, 27(147). https://doi.org/10.1183/16000617.0077-2017

Romero-Gil, V., Bautista-Gallego, J., Rodríguez-Gómez, F., García-García, P., Jiménez-Díaz, R., Garrido-Fernández, A., & Arroyo-López, F. (2013). Evaluating the individual effects of temperature and salt on table olive related microorganisms. Food microbiology, 33(2), 178–184. https://doi.org/https://doi.org/10.1016/j.fm.2012.09.015

Sak-Ubol, S., Namvijitr, P., Pechsrichuang, P., Haltrich, D., Nguyen, T.-H., Mathiesen, G., Eijsink, V. G., & Yamabhai, M. (2016). Secretory production of a beta-mannanase and a chitosanase using a lactobacillus plantarum expression system. Microbial Cell Factories, 15(1), 1–12. https://doi.org/10.1186/s12934-016-0481-z

Seegers, J. F. (2002). Lactobacilli as live vaccine delivery vectors: progress and prospects. Trends in biotechnology, 20(12), 508–515. https://doi.org/10.1016/s0167-7799(02)02075-9

Sia, J. K. & Rengarajan, J. (2019). Immunology of mycobacterium tuberculosis infections. Microbiology spectrum, 7(4), 7–4. https://doi.org/10.1128/microbiolspec.GPP3-0022-2018

Siezen, R. J. & van Hylckama Vlieg, J. E. (2011). Genomic diversity and versatility of lactobacillus plantarum, a natural metabolic engineer. Microbial cell factories, 10(1), 1–13. https://doi.org/10.1186/1475-2859-10-S1-S3

Silhavy, T. J., Kahne, D., & Walker, S. (2010). The bacterial cell envelope. Cold Spring Harbor perspectives in biology, 2(5), a000414. https://doi.org/10.1101/cshperspect.a000414

Sørvig, E., Grönqvist, S., Naterstad, K., Mathiesen, G., Eijsink, V. G., & Axelsson, L. (2003). Construction of vectors for inducible gene expression in Lactobacillus sakei and L. plantarum. FEMS Microbiology Letters, 229(1), 119–126. https://doi.org/10.1016/S0378-1097(03)

00798-5

Sørvig, E., Mathiesen, G., Naterstad, K., Eijsink, V. G. H., & Axelsson, L. (2005). High-level, inducible gene expression in lactobacillus sakei and lactobacillus plantarum using versatile expression vectors. Microbiology, 151(7), 2439–2449. https://doi.org/https://doi.org/10.1099/mic.0.28084-0

Tjåland, R. (2011). Secretion and anchorig of *Mycobacterium tuberculosis* antigens in*Lactobacillus plantarum*. Norwegian University of Life Sciences.

Trondsen, L. (2021). Production and surface anchoring of mycobacterium tuberculosis and sars-cov-2 antigens in *Lactobacillus plantarum*. Norwegian University of Life Sciences.

Tsirigotaki, A., De Geyter, J., Šoštaric´, N., Economou, A., & Karamanou, S. (2017). Protein export through the bacterial sec pathway. Nature Reviews Microbiology, 15(1), 21–36. https://doi.org/10.1038/nrmicro.2016.161

van den Nieuwboer, M., van Hemert, S., Claassen, E., & de Vos, W. M. (2016). Lactobacillus plantarum wcfs 1 and its host interaction: a dozen years after the genome. Microbial biotechnology, 9(4), 452–465. https://doi.org/10.1111/1751-7915.12368

Visweswaran, G. R. R., Leenhouts, K., van Roosmalen, M., Kok, J., & Buist, G. (2014). Exploiting the peptidoglycan-binding motif, lysm, for medical and industrial applications. Applied microbiology and biotechnology, 98, 4331–4345. https://doi.org/10.1007/s00253-014-5633-7

WHO (2022). Global tuberculosis report 2022. https://www.who.int/teams/global-tuberculosis-programme/tb-reports/global-tuberculosis-report-2022. Last accessed 21.04.2023

Wiull, K., Boysen, P., Kuczkowska, K., Moen, L. F., Carlsen, H., Eijsink, V. G., & Mathiesen, G. (2022). Comparison of the immunogenic properties of lactiplantibacillus plantarum carrying the mycobacterial ag85b-esat-6 antigen at various cellular localizations. Frontiers in Microbiology, 13. https://doi.org/https://doi.org/10.3389/fmicb.2022.900922

Xu, M., Li, Z., Zhao, X., & Li, W. (2022). Prebiotic properties of exopolysaccharides from lactobacillus helveticus lz-r-5 and l. pentosus lz-r-17 evaluated by in vitro simulated digestion and fermentation. Foods, 11(16), 2501. https://doi.org/10.3390/foods11162501

Yang, S., Xu, X., Peng, Q., Ma, L., Qiao, Y., & Shi, B. (2023). Exopolysaccharides from lactic acid bacteria, as an alternative to antibiotics, on regulation of intestinal health and the immune system. Animal Nutrition. https://doi.org/10.1016/j.aninu.2023.02.004

Zadravec, P., Mavrič, A., Bogovič Matijašić, B., Štrukelj, B., & Berlec, A. (2014). Engineering bmpa as a carrier for surface display of igg-binding domain on lactococcus lactis. Protein Engineering, Design & Selection, 27(1), 21–27. https://doi.org/10.1093/protein/gzt059

Zannini, E., Waters, D. M., Coffey, A., & Arendt, E. K. (2016). Production, properties, and industrial food application of lactic acid bacteria-derived exopolysaccharides. Applied microbiology and biotechnology, 100, 1121–1135. https://doi.org/10.1007/s00253-015-7172-2

Zanoni, P., Farrow, J. A., Phillips, B. A., & Collins, M. D. (1987). Lactobacillus pentosus (fred, peterson, and anderson) sp. nov., nom. rev. International Journal of Systematic and Evolutionary Microbiology, 37(4), 339–341. https://doi.org/10.1099/00207713-37-4-339

Zheng, J., Wittouck, S., Salvetti, E., Franz, C. M., Harris, H. M., Mattarelli, P., O'toole, P. W., Pot, B., Vandamme, P., Walter, J., et al. (2020). A taxonomic note on the genus lactobacillus: Description of 23 novel genera, emended description of the genus lactobacillus beijerinck 1901, and union of lactobacillaceae and leuconostocaceae. International journal of systematic and evolutionary microbiology, 70(4), 2782–2858. https://doi.org/10.1099/ijsem.0.004107

Živković, M., Miljković, M. S., Ruas-Madiedo, P., Markelić, M. B., Veljović, K., Tolinački, M., Soković, S., Korać, A., & Golić, N. (2016). Eps-sj exopolisaccharide produced by the strain lactobacillus paracasei subsp. paracasei bgsj2-8 is involved in adhesion to epithelial intestinal cells and decrease on e. coli association to caco-2 cells. Frontiers in microbiology, 7, 286. https://doi.org/10.3389/fmicb.2016.00286

Supplementary material

A Growth curve analysis

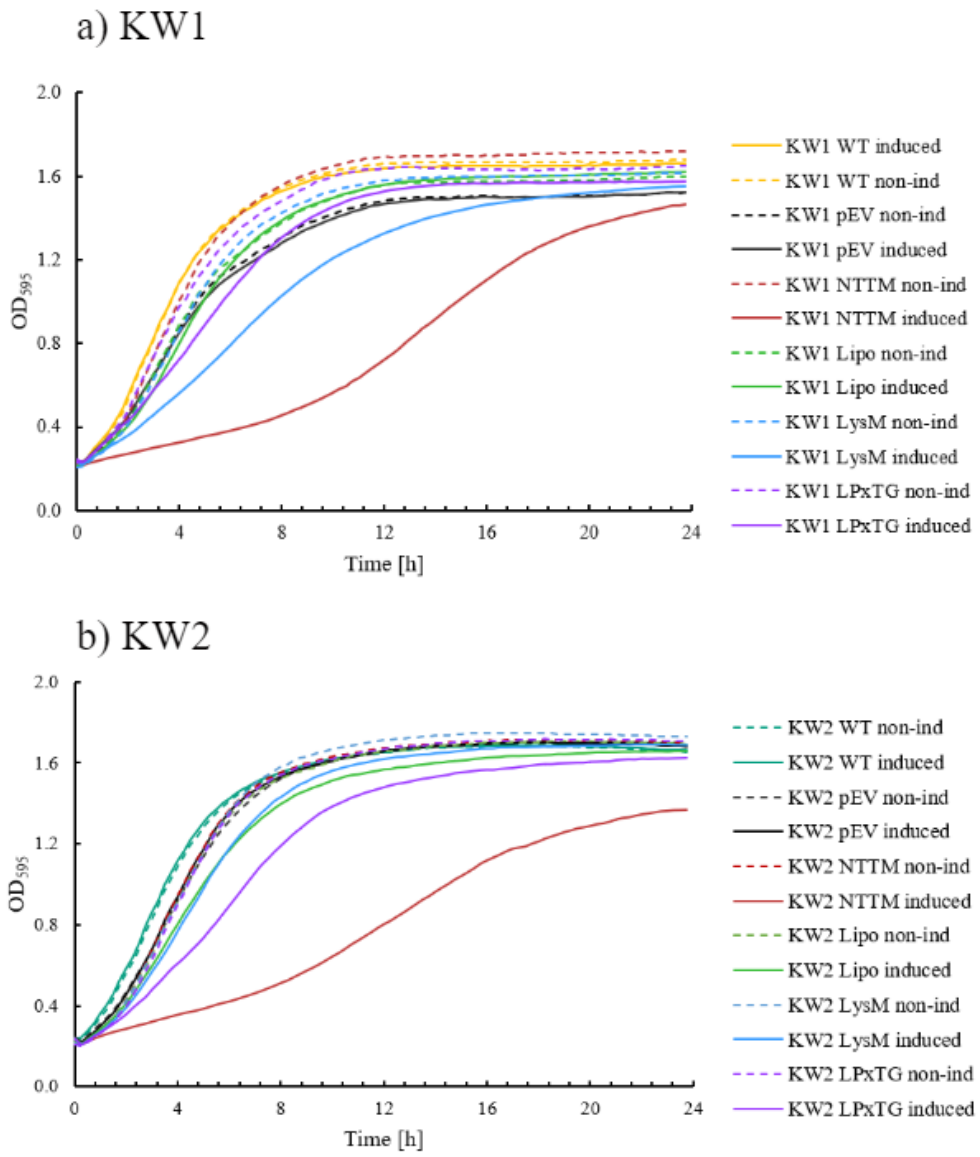

Figure A1: Growth curve analysis of the wild type and recombinant *L. pentosus* KW1 and KW2. The same figure as shown in the results (figure 3.10), included curves of non-induced and wild type strains.

B Anchor proteins

Table A1: Amino acid sequences of native proteins where bolded parts were selected for the construction of recombinant proteins. For LPxTG proteins, LPQTx motifs are shown in highlighted yellow.

Protein	Amino acid sequence
KW1-2_Lipo-0418	**MRFKSLFILPLALLLVGCSTSQSTTKSDASSSSARKTTTVSKKASVKQSKKAA AKSKSKAAATSTSQAAK**QTTSSSKQSSTAKASSSASTQSSTKATTTTNGTTRLAT LNQQLTKALGNVLLPQTDGLTSGSQQLNVRYQGSQANYTVSYSVGQTAQAFNS KAVAKETPYATVNKKTYASNQAAAQAIGHRNASDAKGLPTVDLGHQITGYLDS GAGQRYILWNEGQWSLQVHTYTTQNDLGVALAKQTVNTLESYYLPAPKSVGSI QLEAISTDGLRQVIQWQAGRVVYKVSAHDATTAIKLAASMQ
KW1_NTTM-0418	**MRVQRRRRPERLIMIILVVILAIIVAVYGTLWAAQRPMHQAQKTAYSLAVSK GKLKTTTAFSQYNGTSSYYVVTGTNSKNVPVYALI**NTNKHHKTTVVKQSAGI SRTKALKKVWSKRNPSKVIKATLGEYDGTTVWEITYLNQKKNLCYEILQYSNGN QLKSIINI
KW2_NTTM-2724	**MQNNGFWATIKDGLRVIGHWLAPYWRRFAAVVGYQWHRRQVTRWLIVLV LSVILVGSAYLTYEAKTAKVGNLQAELEKTTVIYDQDNKKAGSLYSQKGTY VHLSSISKNLQNAV**ISTEDRNFYKEHGFSIKGIGRAFVLYAMNKILGRDYISGGG STLTQQLVKNAYLTQQQTFSRKFREIFLAIETENVYSKKQILTMYLNNAYFGHGV WGAEDASERYFGVHASELSVDQAATLAGMLSSPSGYDPISHPKASTARRNVVLN NMVENGKLTKSEYNVYSKKTMALTNNYHYESGYNYPYYFDAVIDEAINKYGLS ESDIMNRGYKIYTSLNQDDQTQMQDSFKNSALFPANADDGTKVQGASIAVDPST GGVLAVVGGRGKHVFRGFNRATQIKRQPGSTIKPLAVYTPALQNGYTYDSKLSN KKQTFGANKYAPKNYDNVYSKSVPMYTALAQSMNIPAVWLLNKIGVNKGYQS VKKFGLPVTKSDDNLALALGGLTTGVSPEQMASAYTAFANNGKKTTAHFITKIV DASGNVIVDNTKTKTKRLMSASVAKEMTSMMLGTYNSGTGATAKPYGYSVAG KTGSTQADYSTGSGTKDQWMIAYTPDIVMTTWIGFDTTNSTHYLKSLSENQLSS LVKNELQNILPNTANTSFGTKDAATLATENDNNDSDSSDSGSSVWENVEKGANA VKNKAKDWFSKAKSLLGN
KW1_LysM-1485	**MKKLLTTILTTSAATVGLLMAGTLSANADATYTVKKGDCVWAISQEYKTTI ESIETANNIHGHLILPGQQLRIPGATAPVTATQTPAAPVTSAPVQTAPVQQAP ATTPAQPAETPAVTAPAAPVETAPAQTSEPAATTPAPETYTGGNLQSYVLGQ MQSRTGVSASTWDHIINRESNWQPHVVNGASGAYGLFQNIHISGGSVQQQID AAVNLYHAQGMQAWALY**

Table A1: Amino acid sequences of native proteins where bolded parts were selected for the construction of recombinant proteins. For LPxTG proteins, LPQTx motifs are shown in highlighted yellow.

Protein	Amino acid sequence
KW2_LysM-1392	**MKIKHLLLSSLATTGAIALGATAAKADTVTVKAGDTVSEIADTHKTTVAAV QKLNHLKNVNLIYVGDKLKVNKHQSVKVVRPTTTTTTQATTTNTTSNATSA SAASSTTTASQASVSSVSNAASQSSTSQVSASSVSNATSQSSTSQASASSVSDAT SQSSASQASASSVTSASSQSSTSQASASSVTSATSQSSTSQASASSVSNATSQSST SQASASSVSNATSQSSTTTTHAVATSAATSQSATSSAASSSTASSSAASSSSSAA TTASSSSTATTSSTSTSTSTSSTAEAAAKAWIAARESGGSYTATNGIYYGKYQ LGKSMLNGDYSAANQEATADAYVAARYGSWVAAKAFWQANGWY**
KW1_LPxTG-1420	**MTKALKVAMGMTMLTGGLMAQGVAASAAI**TTKPVVYTAKSTQTPDSIAAQ VDRHSAVQAAQARVDVADQTYTNAKQALTAAKSAAQAAQDELVAADGVLAK NQQIQDAMAALHDTAVARQTKAKQAVNTATANQATAQTAVTTAQATVDQLT ANVKTAQMAVDKDNSAANQAALDAAKGKLTTAQTALTAAQAKLTKATTALT AAKEER**ANADIEVSGTAVDYRVAKKEHDTVKPRAAVEKAEATVKAARNHV DSAKAEVRAAEKERTAAQSDLTALLNEAKQPARPDDGKGGQTPAKPTTDH GNDKGGQAPIDQSTGHGNNSNGQTPANPTGHHNNHTDGPVGGAPQPTVTH STDQPQVKGTANPHVKSALRTTTSPVVTKPVATHPIATHPTSTAKTTTRTAT LPQTDERTNQVVTVLGFVLLTAMSLFGFKRQSNKRHTTD**
KW2_LPxTG-1650	**MRKKRIGFLLSVLMAILTLFVLGSTAHAKE**ISVSGLDANSAQVYDKNGQLMP PSSLLNTTTSYQVTYNWQIPDSEVLNAGDTVTVGIPANVKVQNNVSFPVVDADG ATIGTFTYKAGDPTGTITFNDRISGLQNRHGTLTINANGNSTISGDERSIAKSGSIFT SDEAGSPTTLFWHITVQPGNNPTIVITDTLGPNQTFLPDTVQAYLVNVVNGMEVP GRTVTPTVAVDGNIITFSFTNVTSKLVLNYRTKPENVDPAAGNVWHNTASLNGL DVAADADIVFGGNGSAQQDYSVRLTKHDADTQAVLAGATYDLQDSTGKVLQS GLTTDANGQLIVEKLAAGNYQFVETKAPEGYELNTKPLTFTLGTPKTLLSIEVSQ DDQKMPVVPATGDVTLTKTDATTKKVLAGAVYELRDANGKVLQSNLKTDAAG QLTVTGLTAGDYQFVETAAPTGYELNATPLPFTIKAGQTAAVTVYATDEPVTNP SQPGEPGQPEEP**GKPSEPGTTEPGQPEEPGKPSEPGTTEPGQPEEPGKPSEPG TTEPGQPEEPGKPSEPGTTEPGQPEEPGKPSEPGTTEPGQPEEPGKPSEPGTT EPGQPEEPGKPSEPGTTEPGQPEEPGKPSEPGTTEPGQPEEPGKPSKPGTTEP GQPGKPSKPGTTEPGQPGQPSKPGTTEPSQPSKPGTTEPGQPSQPGTTGPST PSQPSVPGTTTPSTPSQPSGTLPTNPSQPGVPAPSLPVAGNPSASQGVTTSNGS GTLASGTGLNGTTAGTGTTGAGAGHGAGLPQTSETPTSLLMMLAGLLGLL MAGTGVVYLRRRHG**

C *In silico* analysis of anchor proteins

KW1_00478 hypothetical protein
Prediction: Lipoprotein signal peptide (Sec/SPII)

Cleavage site between pos. 17 and 18.
Probability 0.996666

Protein type	Other	Signal Peptide (Sec/SPI)	Lipoprotein signal peptide (Sec/SPII)	TAT signal peptide (Tat/SPI)	TAT Lipoprotein signal peptide (Tat/SPII)	Pilin-like signal peptide (Sec/SPIII)
Likelihood	0	0	1.0001	0	0	0

Download: PNG / EPS / Tabular

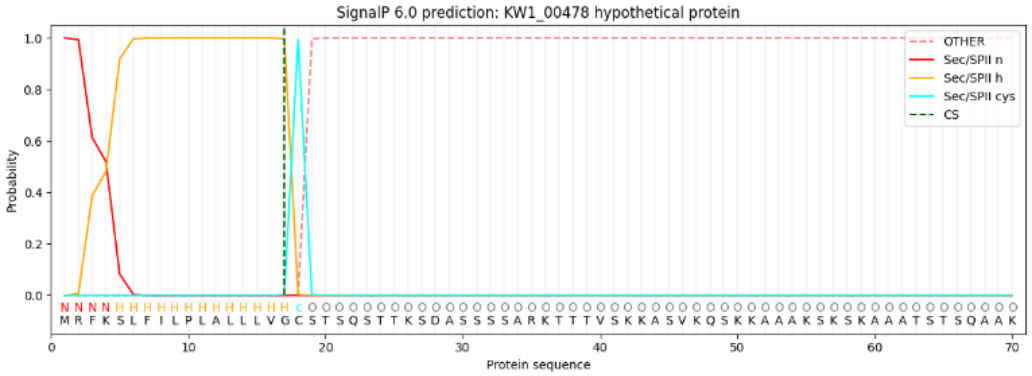

Figure A2: SignalP analysis of KW1_0478 lipoprotein. The signal peptide was predicted to be of type SPaseI, with cleavage site between aa residue positions 17 and 18.

KW1_00418 hypothetical protein
Prediction: Other

Protein type	Other	Signal Peptide (Sec/SPI)	Lipoprotein signal peptide (Sec/SPII)	TAT signal peptide (Tat/SPI)	TAT Lipoprotein signal peptide (Tat/SPII)	Pilin-like signal peptide (Sec/SPIII)
Likelihood	0.9666	0.0259	0.0006	0.0002	0.0001	0.0066

Download: PNG / EPS / Tabular

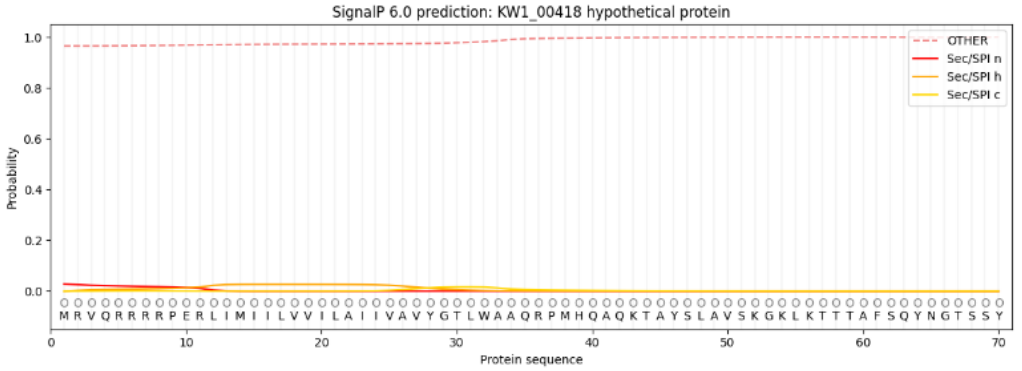

Figure A3: SignalP analysis of KW1_NTTM-0418. No signal peptide was predicted in the analysis.

Prediction of KW1_00418

```
ID   KW1_00418
FT   TOPO_DOM      1     11       CYTOPLASMIC.
FT   TRANSMEM     12     34
FT   TOPO_DOM     35    166       NON CYTOPLASMIC.
//
```

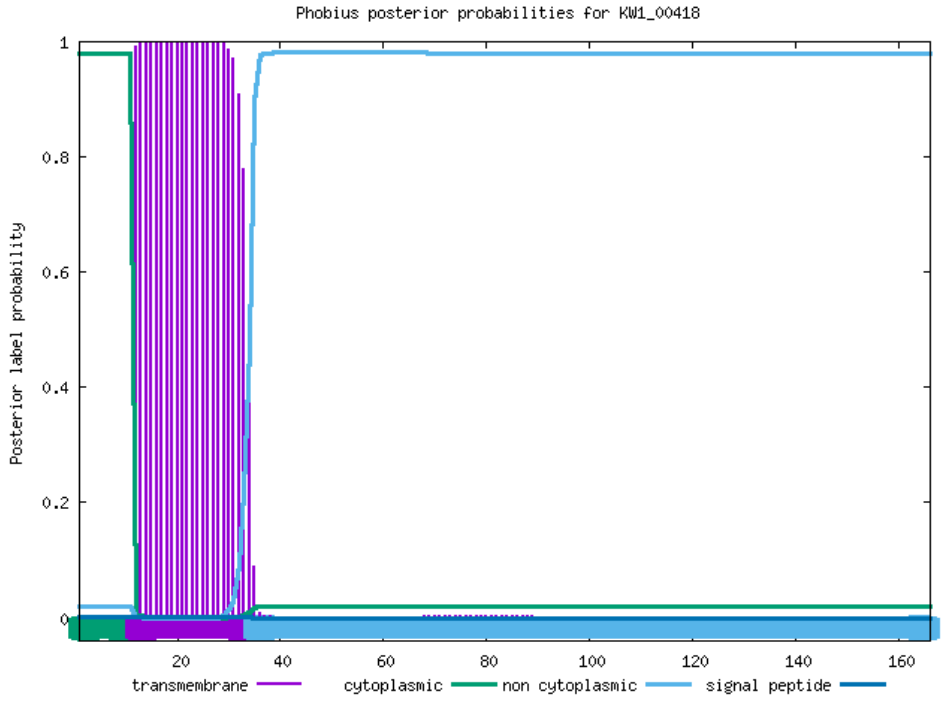

Figure A4: Phobius analysis of KW1_NTTM-0418. Transmembrane helix was predicted to be located between residue positions 12 and 34.

KW2_02724 Penicillin-binding protein 1F
Prediction: Other

Protein type	Other	Signal Peptide (Sec/SPI)	Lipoprotein signal peptide (Sec/SPII)	TAT signal peptide (Tat/SPI)	TAT Lipoprotein signal peptide (Tat/SPII)	Pilin-like signal peptide (Sec/SPIII)
Likelihood	0.9998	0.0002	0	0	0	0

Download: PNG / EPS / Tabular

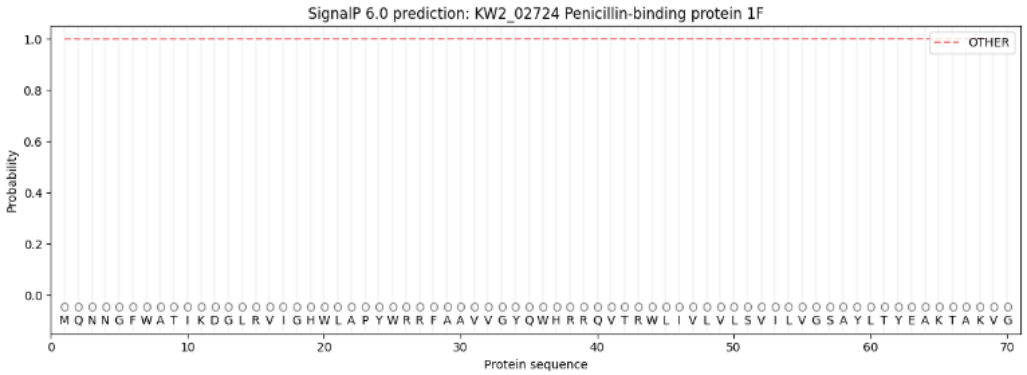

Figure A5: SignalP analysis of KW2_NTTM-2724. No signal peptide was predicted. The protein was recognized as a penicillin-binding protein.

Prediction of KW2_02724

```
ID   KW2_02724
FT   TOPO_DOM      1     43       CYTOPLASMIC.
FT   TRANSMEM     44     62
FT   TOPO_DOM     63    709       NON CYTOPLASMIC.
//
```

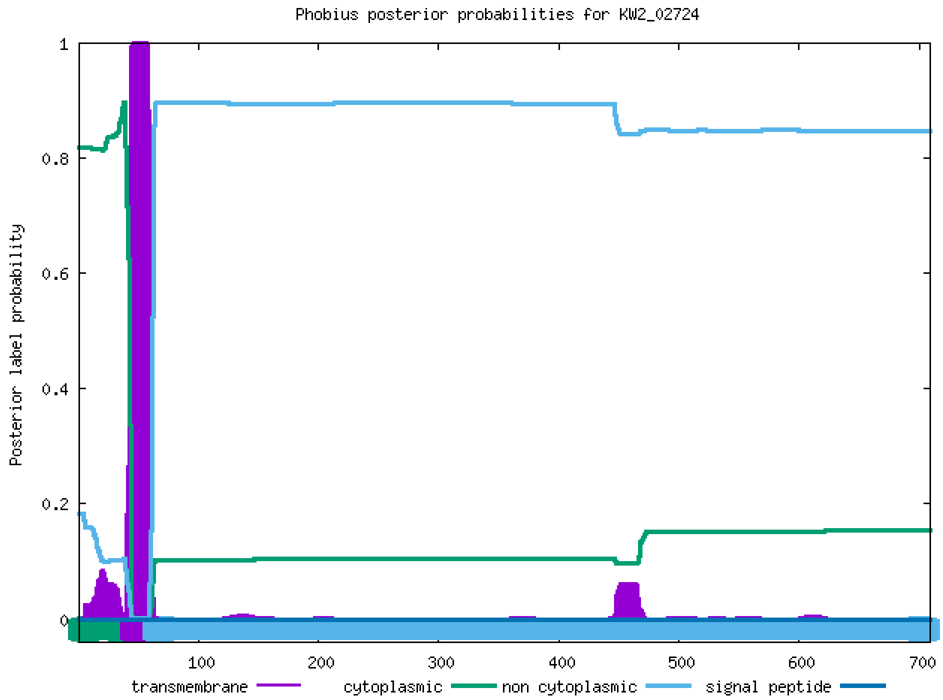

Figure A6: Phobius analysis of KW2_NTTM-2724. The predicted transmembrane helix was localized between the 44th and 62nd residue position.

KW1_01485 hypothetical protein
Prediction: Signal Peptide (Sec/SPI)

Cleavage site between pos. 28 and 29.
Probability 0.968679

Protein type	Other	Signal Peptide (Sec/SPI)	Lipoprotein signal peptide (Sec/SPII)	TAT signal peptide (Tat/SPI)	TAT Lipoprotein signal peptide (Tat/SPII)	Pilin-like signal peptide (Sec/SPIII)
Likelihood	0.0002	0.9991	0.0002	0.0002	0.0002	0.0001

Download: PNG / EPS / Tabular

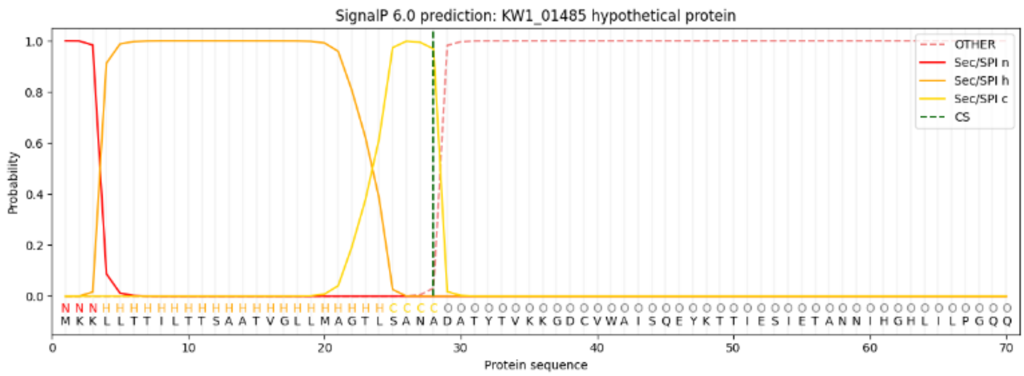

Figure A7: SignalP analysis of KW1_LysM-1485. The analysis predicted signal peptide cleavage site between residue positions 28 and 29. The SPase was predicted as type I.

KW2_01392_hypothetical_protein
Prediction: Signal Peptide (Sec/SPI)

Cleavage site between pos. 26 and 27.
Probability 0.964637

Protein type	Other	Signal Peptide (Sec/SPI)	Lipoprotein signal peptide (Sec/SPII)	TAT signal peptide (Tat/SPI)	TAT Lipoprotein signal peptide (Tat/SPII)	Pilin-like signal peptide (Sec/SPIII)
Likelihood	0.0003	0.9989	0.0002	0.0002	0.0002	0.0002

Download: PNG / EPS / Tabular

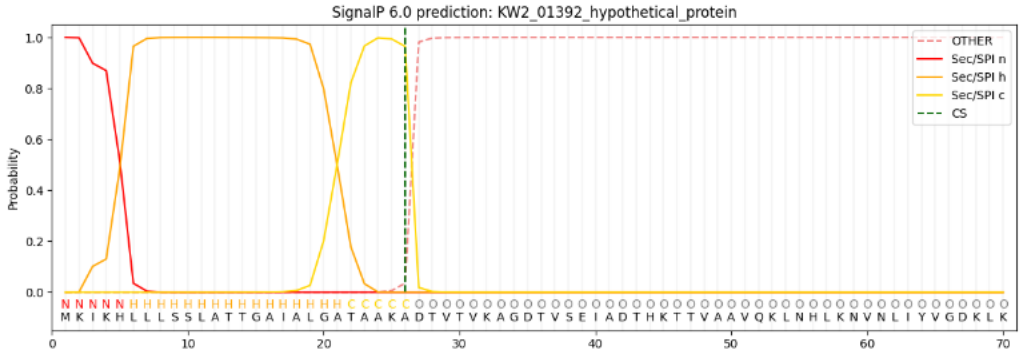

Figure A8: SignalP analysis of KW2_LysM-1392. Cleavage site of this signal peptide was predicted to be positioned between position 26 and 27, with SPaseI as the catalysator.

KW1_01420 hypothetical protein
Prediction: Signal Peptide (Sec/SPI)

Cleavage site between pos. 27 and 28.
Probability 0.855332

Protein type	Other	Signal Peptide (Sec/SPI)	Lipoprotein signal peptide (Sec/SPII)	TAT signal peptide (Tat/SPI)	TAT Lipoprotein signal peptide (Tat/SPII)	Pilin-like signal peptide (Sec/SPIII)
Likelihood	0.0003	0.9991	0.0001	0.0002	0.0001	0.0001

Download: PNG / EPS / Tabular

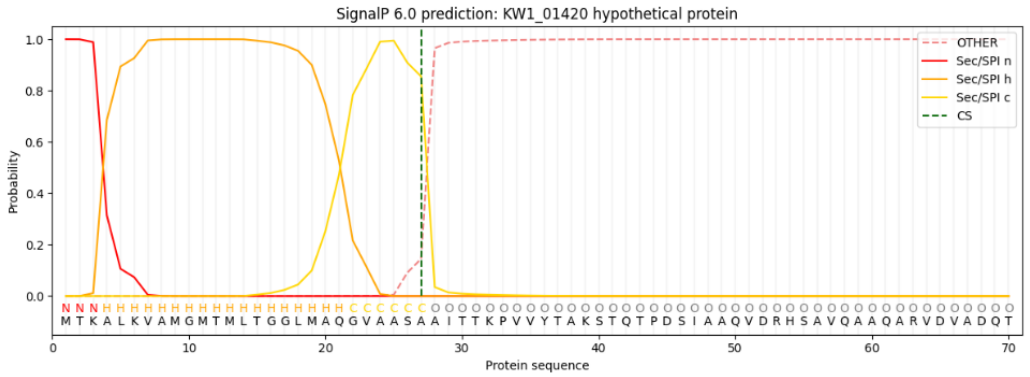

Figure A9: SignalP analysis of KW1_LPxTG-1420. The analysis predicted signal peptide with cleavage site between residue 27 and 28, and SPase type I was predicted.

```
# KW2_01650 Length: 815
# KW2_01650 Number of predicted TMHs:  2
# KW2_01650 Exp number of AAs in TMHs: 42.54167
# KW2_01650 Exp number, first 60 AAs:  20.41718
# KW2_01650 Total prob of N-in:        0.99565
# KW2_01650 POSSIBLE N-term signal sequence
KW2_01650       TMHMM2.0        inside        1     6
KW2_01650       TMHMM2.0        TMhelix       7    26
KW2_01650       TMHMM2.0        outside      27   787
KW2_01650       TMHMM2.0        TMhelix     788   810
KW2_01650       TMHMM2.0        inside      811   815
```

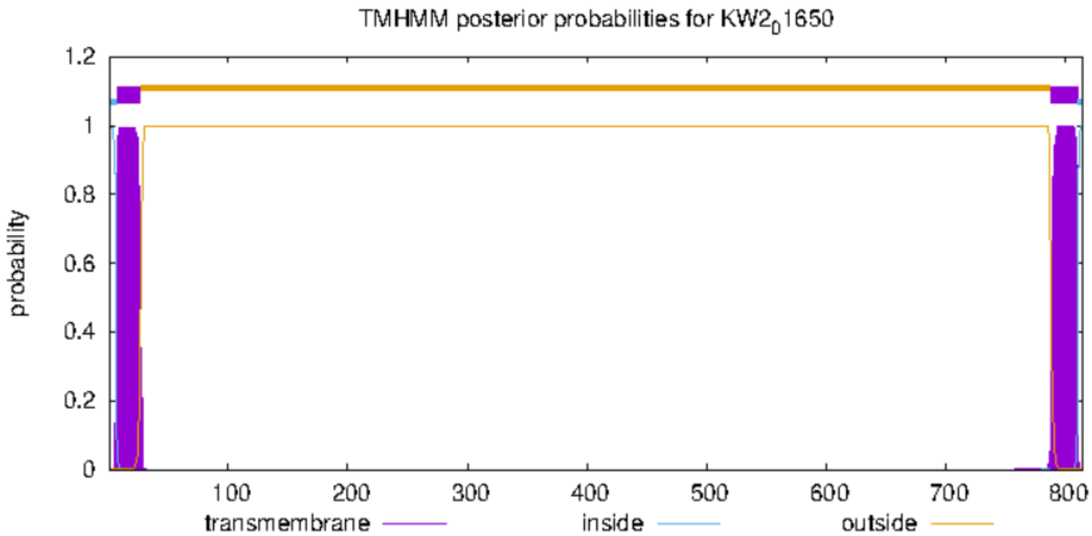

Figure A10: TMHMM analysis of KW2_LPxTG_1650. This analysis predicted that the protein is located as follows: inside the cell from first to sixth position in the amino acid sequence, as transmembrane helix from position seven to 26, outside the cell from 27 to 787, as transmembrane helix between position 788 and 810, and finally inside the cell for last four residues.

KW2_01650 hypothetical protein
Prediction: Signal Peptide (Sec/SPI)

Cleavage site between pos. 28 and 29.
Probability 0.975286

Protein type	Other	Signal Peptide (Sec/SPI)	Lipoprotein signal peptide (Sec/SPII)	TAT signal peptide (Tat/SPI)	TAT Lipoprotein signal peptide (Tat/SPII)	Pilin-like signal peptide (Sec/SPIII)
Likelihood	0.0005	0.9985	0.0002	0.0003	0.0002	0.0002

Download: PNG / EPS / Tabular

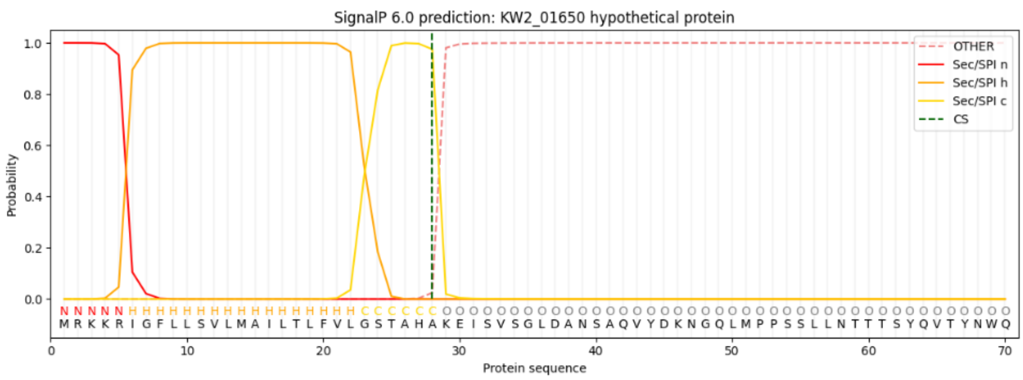

Figure A11: SignalP analysis of KW2_LPxTG-1650. The cleavage site of signal peptide was predicted to be between positions 28 and 29 in the amino acid sequence, with SPaseI as a functional enzyme.

```
# KW1_01420 Length: 444
# KW1_01420 Number of predicted TMHs:  2
# KW1_01420 Exp number of AAs in TMHs: 31.9382
# KW1_01420 Exp number, first 60 AAs:  14.154
# KW1_01420 Total prob of N-in:        0.62748
# KW1_01420 POSSIBLE N-term signal sequence
KW1_01420       TMHMM2.0        inside       1     6
KW1_01420       TMHMM2.0        TMhelix      7    29
KW1_01420       TMHMM2.0        outside     30   415
KW1_01420       TMHMM2.0        TMhelix    416   433
KW1_01420       TMHMM2.0        inside     434   444
```

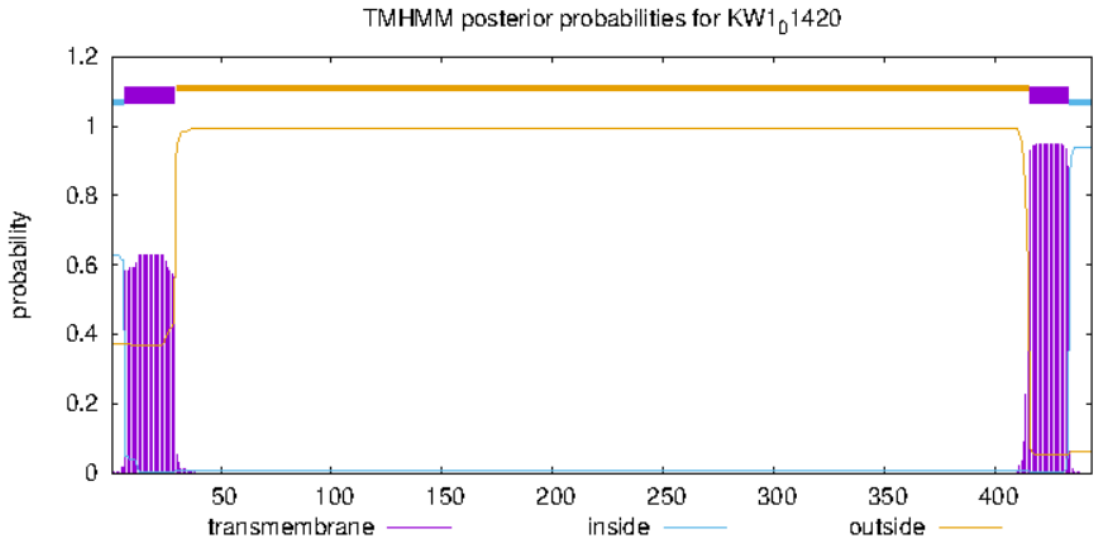

Figure A12: TMHMM analysis of KW1_LPxTG-1420. The performed analysis predicted that this protein is located inside the cell from position one to six, has a transmembrane helix from position seven to 29, then stretches outside of the membrane between position 30 and 415, goes back through the membrane as a transmembrane helix from position 416 and 433, and ends with C-terminal part inside the membrane from position 434 to 444.

D Western blot

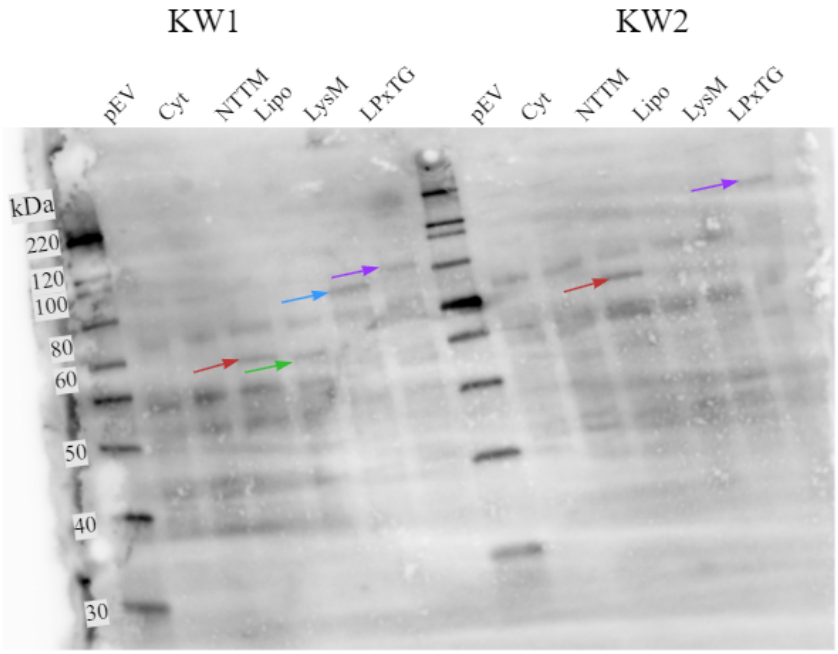

Figure A13: Additional western blot analysis. pEV and Cyt-H56 were included as controls. Four recombinant proteins for each of *L. pentosus* strains were analyzed. Detected proteins are indicated with arrows.

E Flow cytometry

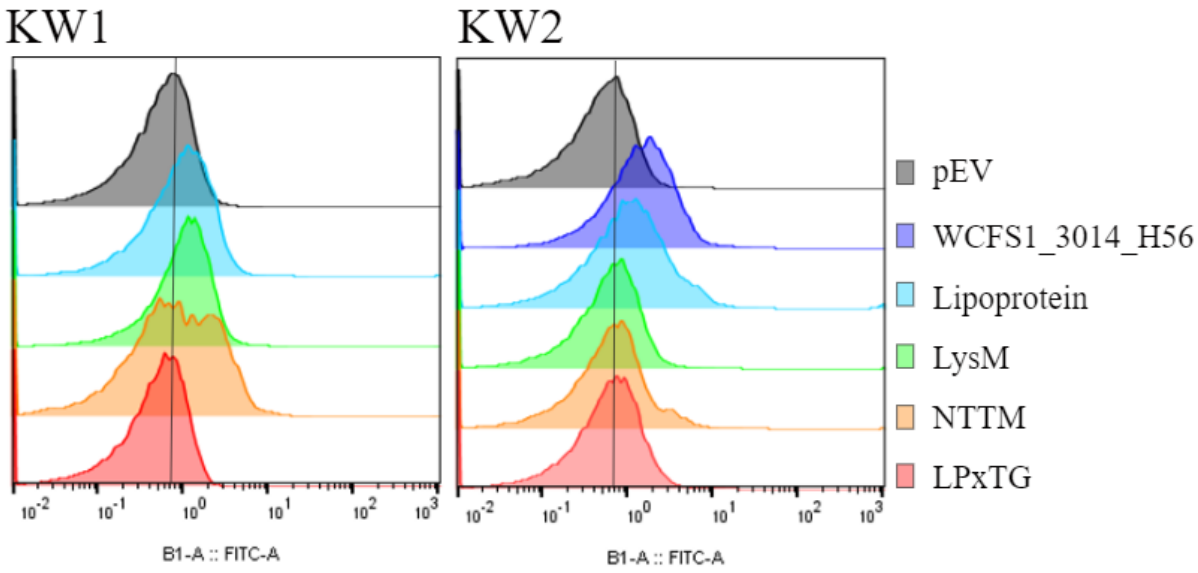

Figure A14: Flow cytometry analysis performed with ESAT6 Rabbit polyclonal (bs-13107R) as the primary antibody (same as used in Western blot). The signals are marked with the same colors in both strains, as follows: gray for pEV (negative control), dark blue *for L. plantarum* WCFS1 harboring pLp3014_H56_DC (Trondsen, 2021) (positive control), light blue for lipoprotein anchors, green for LysM anchors, orange for NTTM, and red for LPxTG.

Norges miljø- og biovitenskapelige universitet
Noregs miljø- og biovitskapelege universitet
Norwegian University of Life Sciences

Postboks 5003
NO-1432 Ås
Norway